NTNU

Norwegian University of
Science and Technology

Simulation of Wells with Fishbones using ECLIPSE

Carl-Ivar Klovning

Petroleum Geoscience and Engineering
Submission date: June 2016
Supervisor: Per Arne Slotte, IPT
Co-supervisor: Jon Kleppe, IPT

Norwegian University of Science and Technology
Department of Petroleum Engineering and Applied Geophysics

Abstract

Fishbones is a new stimulation technology that aims to provide hydraulic fracturing like stimulation while also leaving the operator in full control of the stimulation process. The technology creates up to several hundred thin, 12 meter long laterals that extend orthogonally out from the wellbore. This increases the effective wellbore radius and improves well to reservoir communication. Three full scale tests of Fishbones have previously been conducted and found successful.

This thesis considers fine scale simulation of a well with Fishbones in ECLIPSE. Two different ways of modeling the Fishbones laterals, as fractures and as laterals, are compared. Modeling the Fishbones laterals as fractures was found to give a more accurate solution than defining them as laterals, but with an increased run time.

Several cases that investigated the effect of Fishbones in a well producing under steady state conditions were run. Fishbones was found to increase production by up to 60% compared to an unstimulated well, depending on spacing between the Fishbones laterals. The increase in production from a well with Fishbones also depend on the Fishbones lateral length. Doubling the Fishbones lateral length increased production rate by 80% compared to an unstimulated. Long needles with long spacing was found to give a higher increase in production compared to an unstimulated well than short needles with short spacing.

Cases with Fishbones in a well that had severe damage in the near wellbore area showed that Fishbones was able to remove the effect of the damage and in some cases even increase the production above that of an unstimulated and undamaged well. Fishbones also increased production in formations with a low k_v/k_h compared to an unstimulated well. Fishbones was also capable of penetrating impermeable layers close to the well and improving communication throughout the reservoir.

Upscaling using an apparent wellbore radius was also investigated. An apparent wellbore radius was found to be able to match the production rate and flowing bottom hole pressure (depending on well control) from a well with Fishbones in all flow conditions.

Sammendrag

Fishbones er en ny teknologi for å stimulere brønner der målet er å oppnå stimuleringseffekt på linje med hydraulisk oppsprekking, men med langt mer kontroll på stimuleringsprosessen. Fishbones lager opp til flere hundre tynne, 12 m lange lateraler ortogonalt til brønnen, Dette øker bade den effektive brønnradiusen samtidig som kommunikasjon mellom brønn og reservoir kan økes. Tre fullskala tester av Fishbones er tidligere utført med stor suksess.

Denne oppgaven tar for seg finskala simulering av en brønn med Fishbones i ECLIPSE. To forskjellige måter å modellere lateralene som lages av Fishbones blir sammenlignet, modelering som sprekker og som lateraler. Å modellere lateralene som lages av Fishbones som sprekker var mer nøyaktig enn å modellere dem som lateraler.

Flere forskjellige simuleringer hvor en brønn med Fishbones ble produsert under stasjonære produksjonsforhold ble kjørt. Fishbones kan øke prouduksjonen med opp til 60% i forhold til en ustimulert brønn avhengig av hvor lang avstand det er mellom lateralene. Økningen i produksjon er også avhengig av lengden på nålene. Dersom lengden av lateralene ble doblet økte produksjonen med 80% i forhold til en ustimullert brønn. Lange lateraler med lang avstand var mer effektivt enn korte lateraler med kort avstand.

I brønner med alvorlig skade i nærbrønnsområdet kunne Fishbones trenge igjennom området og fjerne den negative effekten av skaden og til og med øke produksjonen i forhold til en ustimulert og ustimulert brønn. Fishbones økte også produksjonen i en brønn i et reservoar med lav k_v/k_h i forhold til en uskadet brønn. En brønn med Fishbones ble likevel stertk påvirket av lav k_v/k_h. I et tilfelle med et impermeabelt lag som lå over eller under brønnen trengte nålene igjennom og økte kommunikasjonen i reservoaret.

Oppskalering ved å bruke en effektiv brønnradius ble også vurdert. En effektiv brønnradius klarer å duplisere produksjonsraten eller det strømmende bunnhullstrykket (avhengig av brønnkontroll) fra en brønn med Fishbones for alle strømningsforhold.

Preface

This thesis is written as a complete fulfillment in the subject "TPG4915 Petroleum Engineering – Reservoir Engineering and Petrophysics, Master's Thesis", which completes my Master study in Petroleum Engineering at the Norwegian University of Science and Technology (NTNU).

During my five years at NTNU I have met a lot of smart people and they all deserve to be thanked. There are however some that deserve a special mention. First of all I would like to thank my supervisor, Associate Professor Per Arne Slotte and co-supervisor, Professor Jon Kleppe for their inputs and advices on my thesis. This thesis certainly would not have been possible without it. Anne-Mette R. Engedal (Statoil), Justin Nash (BP) and Torgrim T. Thingvoll (BP Norge AS) also deserves to be thanked for taking good care of me during my summer internships.

Lastly, and perhaps most importantly, I would like to thank my family and girlfriend for the support they have always provided throughout the five years.

Klovning, out!

Trondheim, 10.06.2015

Table of Content

List of Figures

List of Tables

Nomenclature

$A_{drainage}$ = Drainage area, m^2

B_0 = Formation volume factor, Sm^3/Sm^3

cP = centipoise

C_{GR} = Constant in logarithmic gridding

d = Diameter, m

d_i = Inner diameter, m

d_o = outer diameter, m

f = Friction factor

ft = feet

h = Height, m

k = Permeability, m^2 (mD)

k_f = Fracture block permeability, m^2 (mD)

k_h = Horizontal Permeability, m^2 (mD)

k_s = Permeability in damaged/stimulated zone, m^2 (mD)

k_v = Vertical Permeability, m^2 (mD)

k_w = Well block permeability, m^2 (mD)

ΔL = Grid block length, m

mD = Millidarcy

m = Meter

mm = Millimetre

n_{GR} = Number of grid blocks an interval is divided into

p_e = Edge pressure, Pa (bara)

p_{wf} = Flowing well pressure, Pa (bara)

Δp_s = Pressure difference due to skin, Pa (bara)

r_{ea} = Apparent outer radius, m

r_e = Edge radius, m

r_s = Radius of damaged/stimulated zone, m

r_{wa} = Apparent wellbore radius, m

r_{wac} = Calculated apparent wellbore radius, m

r_{wag} = Graphical apparent wellbore radius, m

r_{was} = Simulated apparent wellbore radius, m

r_w = Well radius, m

R^2 = Quality of curve fit in excel

Re = Reynold's number

s = Skin factor

t = time, s (days)

v = Flow velocity, m/s

q_{ideal} = Flow rate from an undamaged/unstimulated well, Sm^3/D

q = Flow rate, Sm^3/D

Q_{90} = Cumulative production after 90 days, Sm^3

μ = Fluid viscosity, Pa•s (cP)

ρ = Fluid density, kg/m^3

Abbreviations

CFD = Computational fluid dynamics

FBHP = Flowing bottomhole pressure

FBL = Fishbones lateral

HCPV = Hydrocarbon pore volume

IAF = Infinite acting flow

NTNU = Norwegian University of Science and Technology

LGR = Local grid refinement

PSS = Pseudo steady state

1. Introduction

Well stimulation is the process of improving the productivity of a well by physically altering the formation in the area near the well. This can be done in many different ways and has enabled operators world wide to exploit new resources that have previously been considered non-profitable. The most recent, and perhaps best example is that of massive hydraulic fracturing in shale. This has enabled production from liquid rich shales and has taken USA from being the third largest oil producer in 2012 (Bjørsvik, 2013) to the largest in 2014 (Qvale, 2015). Many analysts considers this to be one of the main events that caused the unexpected drop in oil prices from the middle of 2014 to early 2016, which had a huge impact on the market.

Stimulating a well brings with it many challenges and the most important one is perhaps the lack of control over the stimulation job. When a well is hydraulically fractured the only parameters the operator controls are fluid pressure and pumping rate along with viscosity modifications to the fracturing fluids. The operator has no control over fracture propagation, which can lead to fracture growth into unwanted reservoir sections. This has become a major area of concern in the U.S. because hydraulic fractures are believed to propagate into ground water resources leaving them heavily polluted.

The Norwegian company Fishbones AS has developed a new stimulation technique with the goal to achieve hydraulic fracturing like stimulation, but with complete control over the stimulation job and less resource consumption. Fishbones stimulates a well by creating up to several hundred 12 m long, thin laterals extending orthogonally out from the well. The Fishbones laterals (FBL) can increase the apparent wellbore radius as well as improving well to reservoir communication.

In order to investigate the effect of a stimulation job in a well, reservoir simulation is often used. This is done to determine which stimulation that will work best in a well and also to design the stimulation so that it maximizes the stimulation effect. Because Fishbones is a new technology there has not been published much work on how to model it in reservoir simulators. The challenges are to model the complex geometry created by the laterals accurately. This can of course be modeled by introducing a very detailed grid around the well, but with detailed grids comes large run times. Another approach is to define an apparent wellbore radius that will be able to capture the stimulating effect of Fishbones. This will sacrifice some detailed information on flow around the FBLs, but run time will be reduced.

This thesis will focus on modeling wells stimulated with Fishbones on a fine scale using the commercial reservoir simulator ECLIPSE, which is developed by Schlumberger. ECLIPSE was chosen because it is a dedicated reservoir simulation software that is easy to use and is used extensively within the oil and gas industry. It is also developed to be run on super computers, which makes the run time per simulation significantly shorter. Super computers also enables several simulations to be run simultaneously thus making the work more efficient. The model will then be used to investigate the stimulating effect of Fishbones.

This thesis contains six chapters. The second chapter discusses how to model a well with Fishbones on a fine scale in ECLIPSE. Two different models are created and compared. The best method is used to investigate how Fishbones affects productivity in a well in chapter three. Chapter three also discuss' upscaling of a well with Fishbones laterals using an apparent wellbore radius. A discussion about the results and limitations are given in chapter four and the work is concluded in chapter five. Chapter six contains recommendations for further work based on the discussion. There are also two appendixes. Appendix A shows calculation for frictional pressure drop within the well and FBLs and discuss how they affect the simulations. Appendix B contains tables with the PVT and relative permeability data that are used in the simulation models.

1.1 Fishbones

Parts of the following sections have been taken from the autumn project written by the author (Klovning, 2015) and have been modified where appropriate.

1.1.1 Technical Description

The Norwegian company Fishbones AS has developed a new technology called Fishbones. The technology is based on the traditional fishbone well where several laterals are drilled out from a main well so that the well ends up looking like the rib cage of a fish (Schlumberger, 2016). Fishbones creates up to several hundred small laterals by jetting small needles perpendicularly out from the wellbore in a chalk or coal bed formation. The needles have a maximum length of 12 m and create a lateral with a diameter of 10-20 mm (Fishbones AS, 2016). A well with Fishbones is illustrated in Figure 1.1.

Figure 1.1 – Illustration of a well stimulated with Fishbones (HORN International AS, 2015).

Fishbones is a liner completion. It is run in an open hole by connecting several Fishbones liner subs together into a long string in the same way that a normal reservoir liner is made up. Each liner sub can contain up to four needles being spaced with equal distance around the liner sub (i.e. four needles have a 90 degrees phasing). A Fishbones sub is shown in Figure 1.2. When the Fishbones string has reached the reservoir section and is secured in place by the liner hanger and a set of backbone anchors[1], the Fishbones liner is connected to the rig pumps

[1] Expansion based stabilizers in the reservoir section to prevent axial movement of the liner.

and pumping begins. Water or acid[2] is pumped through the Fishbones string and out in the formation through the needles. The end of the needle is equipped with a nozzle causing a differential pressure over the nozzle that jets away the formation and drives the needles outward. In addition to jetting, acid will also dissolve carbonates. Some needles can be attached with a pressure indicator that creates a spike in the measured pumping pressure when the needle is fully extended. When the needles are fully extended, pumping is stopped and the rest of the completion string is run and attached to the Fishbones liner.

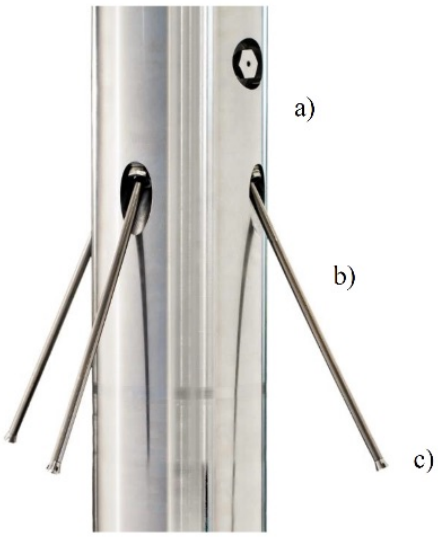

Figure 1.2 – A Fishbones sub. Different elements of the sub are shown; a) Liner port, b) Fishbones needle, c) jet nozzle. The needles are only partially extended and will be oriented orthogonally to the sub at full extension. (Rice et al., 2014)

Production can begin without an extensive cleanout. Fluid will then be produced in the annulus between the needle and the FBL wall into the well annulus. Fluid may also flow inside the needle if it flows into the tip of the needle. As Figure 1.2 shows each sub contains two (only one is shown in the figure) one-way production valves with a 7 mm diameter that allows fluid to flow from the annulus of the well into the liner. This also enables fluid close to the well in between FBLs to be produced directly into the annulus of the well (Rice et al., 2014).

Fishbones AS has also developed a stimulating method to be used in formations where the FBLs cannot be jetted, called Dreamliner[3]. The technology is essentially equal to the Fishbones stimulation method, but instead of the jet nozzle that is found at the tip of the needles, a small drill bit is used on the Dreamliner needles. The maximum needle length is

[2] Water in coal beds, acid in carbonates.
[3] Laterals created by the Dreamliner will also be referred to as "FBLs" for simplicity.

10.8 m and the number of needles per sub is three. This means that the needles will have a 120 degrees phasing. Several videos describing Fishbones and Dreamliner can be found on Fishbones' web page (Fishbones AS, 2016).

One of the main benefits with Fishbones is that operational time and resource consumption are reduced. While a hydraulic fracturing job requires special high-pressure fracture pumps and large fluid volumes, Fishbones can be installed using ordinary rig pumps and small fluid volumes are consumed. Because the FBLs are all jetted simultaneously, the pumping time is also short. A hydraulic fracturing job usually requires the operator to zone of small parts of the well with packers, perforate the liner, run a pumping cycle to create the fractures and then repeat for as many times as necessary to stimulate the entire well. The reduced operation time and fluid volumes greatly reduces the health, safety and environment exposure and may also reduce operation costs compared to other stimulation methods (Freyer and Shaoul, 2011).

Fishbones may stimulate the well in two ways. First of all the FBLs will improve the productivity because they will increase the apparent wellbore radius of the well. Secondly the FBLs will be able to penetrate impermeable layers and damage in the near wellbore region. This will improve well to reservoir communication (Fishbones AS, 2016) and may also improve the inflow conformity along a well (Shaoul, 2013).

1.1.2 Previous Work

Because Fishbones is a new technology there has not been published very much work on it. This section presents the material currently available.

1.1.2.1 Field Tests

Three field tests have been conducted and documented. This involved one test with Fishbones in a coal bed methane (Fishbones AS, 2016), one test with Fishbones in a chalk oil reservoir (Rice et al., 2014) and one test with Dreamliner in a tight sand stone (Torvund et al., 2016). The well in the coal bed was completed with a slotted liner and two Fishbones subs and the needles were jetted to full extension using water. The initial flow rate was four times higher compared to a similar well that had been completed with a cemented liner.

The carbonate test was installed in a well in the Austin Chalk formation in Texas that had been producing for 20 years. A total of 60 Fishbones needles were successfully jetted to full extension after five hours of pumping. A positive pressure spike from needles that had been equipped with the pressure spike mechanism confirmed the full extension. Productivity index after stimulation was 30 times higher than before stimulation and cumulative production over 30 days was increased by a factor of 8.3. The stimulation job was considered to be a great success, both operationally and in terms of the stimulation it provided.

The tight sand stone test was installed in one of the laterals in a duo-lateral well in the Åsgard field in Norway. The other lateral was completed with a pre-drilled liner. 144 Fishbones laterals were created in the lateral containing the Dreamliner subs after six hours of pumping. Computational fluid dynamics (CFD) simulations had indicated that the lateral containing Dreamliner could have up to a 20% higher flow rate compared to the lateral with the pre drilled liner. The current production results indicate that the production from the lateral containing Dreamliner is higher than the production from the lateral containing the pre drilled liner. Sufficient information to accurately determine the difference in production between the laterals is unfortunately not yet available. The operator found that the downside risk of running a Dreamliner stimulation was similar to the risk of running a pre drilled liner, but the upside potential of the Dreamliner was much greater.

1.1.2.2 Experimental Work

The Fishbones laterals can essentially be considered as very long perforations. (McDowell and Muskat, 1950) investigated the effect that perforations would have on the productivity of a cased and perforated well compared to an open hole well. They conducted experiments

where perforation density and length were varied using an electrical analogue model. Results are presented in Figure 1.3 and Figure 1.4.

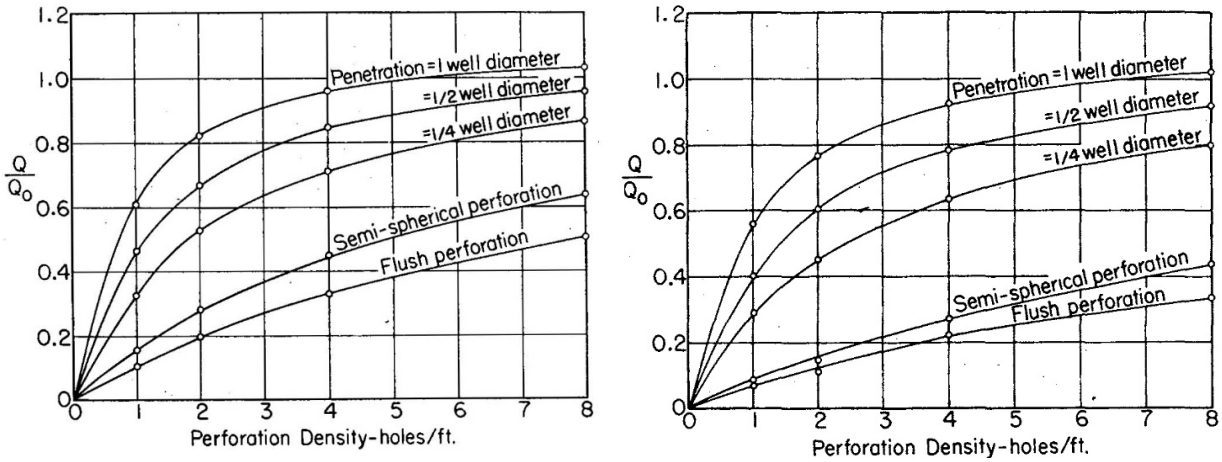

Figure 1.3 – Relative productivity as a function of perforation density for various perforation depths. Left: perforation diameter 0.5 in, right: perforation diameter 0.25 in. (McDowell and Muskat, 1950).

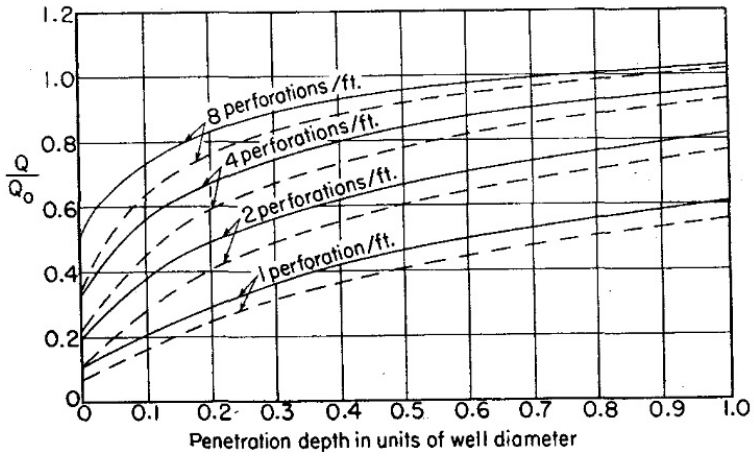

Figure 1.4 – Relative productivity as a function of perforation depth for various perforation densities. Solid line: Perforation diameter 0.5 in, dashed line: perforation diameter 0.25 in. (McDowell and Muskat, 1950).

1.1.2.3 Simulation Studies

(Shaoul, 2013)[4] describes how a well with Fishbones can be modelled in common reservoir simulators as a multilateral well. A grid geometry that resembles the Fishbones well can be made either through the main gridding or by using local grid refinement (LGR) in the grid blocks containing the well. Figure 1.5 shows an illustration of a Fishbones grid where the surrounding reservoir blocks have been removed. The blocks can then be given lateral properties using completion keywords to define laterals with a diameter corresponding to the jetted diameter.

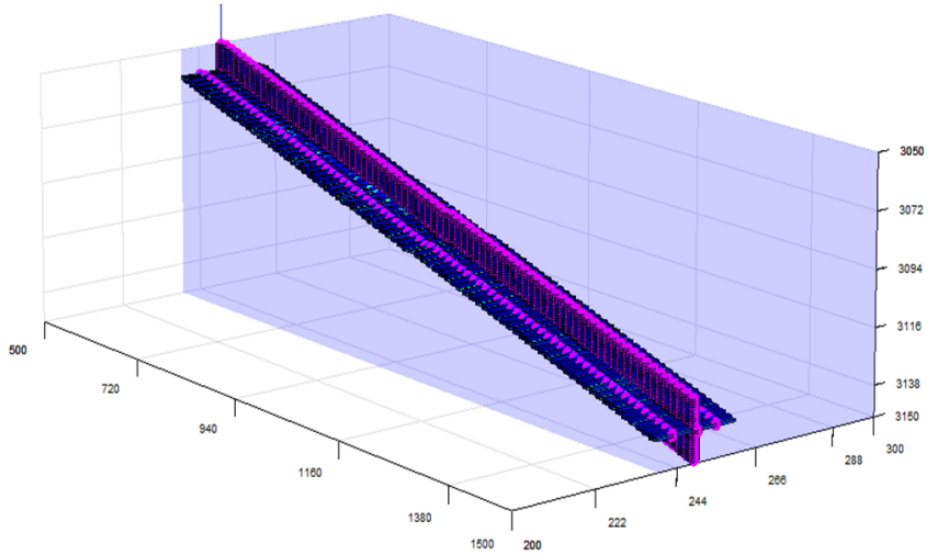

Figure 1.5 – Illustration of a grid used to model Fishbones in conventional reservoir simulators according to (Shaoul, 2013). Only the blocks containing the needles are shown.

In order to capture the effect of Fishbones it is important to make the grid near the well detailed enough. This is especially important in the vertical direction because of the vertical heterogeneity that exists in many reservoirs. A common method to model vertical heterogeneity in a simulation model is to use large grid blocks with a low k_v/k_h value. However, one of the main features about Fishbones is that it will completely penetrate impermeable layers close to the well and enabling production from more layers. It is therefore important that the reservoir grid 12 m above and below the well contains a detailed gridding in the z-direction to fully explore the effect of Fishbones (Shaoul, 2013).

Three different simulation cases of reservoirs containing wells with Fishbones were investigated by (Freyer & Shaoul, 2011). The first case was a gas condensate reservoir just below the high-pressure threshold. Test production had been disappointing, despite promising

[4] The paper is unfortunately not published an was aquired from Fishbones AS.

log interpretations. Poor well placement due to low seismic resolution was thought to be the reason. A well with 160, 12 m long FBLs was introduced and compared to a well without stimulation. Both wells were placed in what was considered the reservoir sweet spot. Well productivity was found to increase by 20-30%. Placing the unstimulated well outside of the sweet spot resulted in dramatically reduced rates, but adding Fishbones re-connect the well back to the sweet spot and production increased to that of the unstimulated well being placed in the sweet spot.

The second case investigated a layered, low permeability, layered sandstone gas reservoir. Horizontal permeability varied between 0.05 mD and 0.08 mD and k_v/k_h varied between 0.001 and 0.01. The effect of Fishbones was investigated by comparing an open hole well to a well with Fishbones and a well with propped fractures. A well with 160, 12 m long FBLs was found to give equal rates as a well with two propped fractures.

The final case is a mature chalk reservoir with permeability of 3.5 mD and k_v/k_h of 0.1. A well with Fishbones was found to give a significantly higher rate than six propped fractures over a period of five years. The fractures were modelled to be degrading with time based on observations from field data, but an open hole stability analysis showed that the FBLs could also be expected to experience instabilities.

(Freyer and Shaoul, 2011) also did CFD simulations to investigate pressure drop due to the small diameter of the FBLs in a high flow rate gas condensate well. No simulations showed a larger pressure drop than a 0.7 bara pressure drop in the FBLs and this was considered to be insignificant compared to the draw down in the reservoir.

(Priskila, 2014) compared simulations from Eclipse and Brilliant (a multi-physics CFD simulator) of a well with 12 m long FBLs and 20 m sub spacing. Brilliant was assumed to represent the "true" solution because of the ability to simulate several different flow models[5] and the ability to generate a more flexible grid. Eclipse was found to give a cumulative production after 90 days (Q_{90}) that was roughly 25% higher than the cumulative production from Brilliant.

(Priskila, 2014) also did simulation studies on sensitivity of different FBL parameters in a declining reservoir. The reservoir was homogeneous and isotropic and contained a vertical well with 12 m long FBLs and 20 m sub spacing. Cumulative production after 90 days was

[5] i.e. pipe flow in the well and FBLs and flow in porous media in the reservoir.

found to be 35% higher compared to an open hole well. Varying the number of FBLs per sub between zero, one and two gave a 34%, 14% and 6% reduction in Q_{90} compared to a well with four FBLs per sub. Increasing or decreasing the jetted diameter of the FBLs by 25% only resulted in a 5% change in Q_{90}. Reducing the needle length to 10 m and eight m reduced Q_{90} by 10% and 13%. The FBLs were also found to be able to penetrate vertical barriers close to the well and improve reservoir communication.

1.2 Skin Factor and Apparent Wellbore Radius

Darcy's law describes the relationship between the fluid production rate and the drawdown in the formation for ideal[6] wells.

$$q = \frac{2\pi kh}{\mu} \times \frac{p_e - p_{wf}}{\ln(\frac{r_e}{r_w})} \quad , \qquad (1)$$

Eq. (1) shows the Darcy equation for a cylindrical well that completely penetrates a cylindrical drainage area. Very few wells behave ideally however. Usually a well is either damaged during the drilling of the well or it is stimulated after drilling. These effects mainly affect the permeability in the near wellbore area and thus pressure profile close to the well is different than in an ideal well. Figure 1.6 shows the pressure profile for Eq. (1) on a semi-log plot along with the deviations due to damage and stimulation.

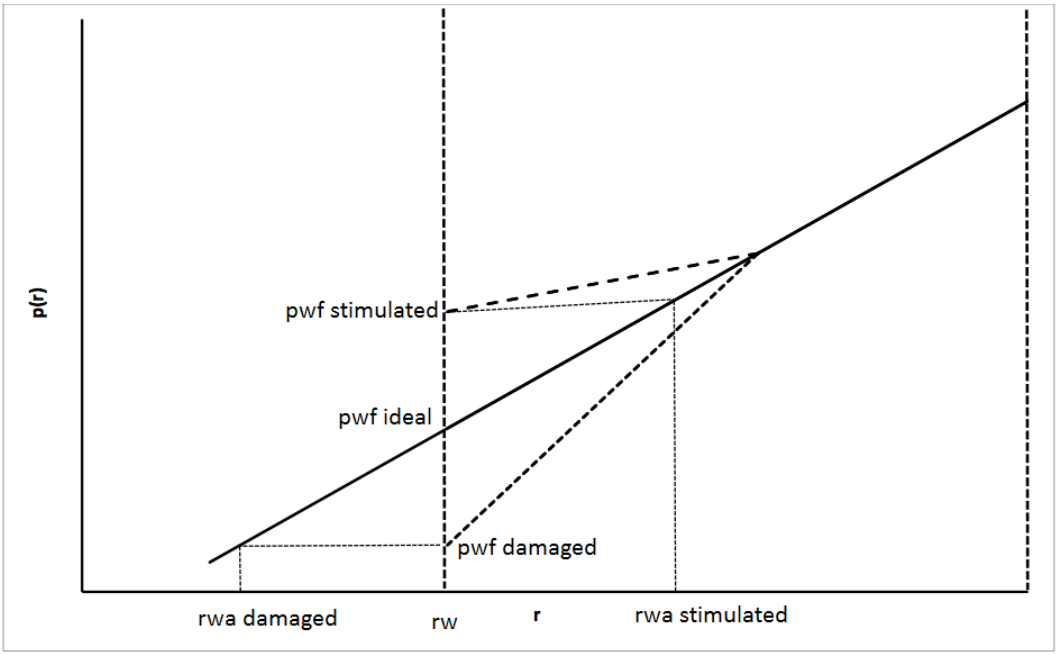

Figure 1.6 – Illustration of an ideal radial pressure profile (continuous line) in a radial drainage area. The x-axis is logarithmic. Pressure deviations due to damage (short dashed line) and stimulation (long dashed line) with the corresponding apparent wellbore radius are also shown.

In order to calculate the effects that damage and stimulation have on production, two approaches can be made. The first is to use Eq. (1) twice, once for the interval between the edge and the outer, unaffected zone with the formation permeability and once for the affected zone with the damage/stimulation permeability. The total reservoir behavior is then found by summing the two equations together. This approach is quite unpractical however as it requires

[6] Ideal means neither damaged nor stimulated and without turbulent flow.

solving two equations. It is also unlikely that the permeability and extension of the damaged/stimulated zones are known.

Another and simpler method is to modify Eq. (1) by including a skin factor according to **Eqs. (2)** and **(3)** to account for the increased or reduced draw down. If the radius of the damaged/stimulated area and the permeability in the area is known then the skin factor can be calculated according to **Eq. (4)**.

$$q = \frac{2\pi kh}{\mu} \times \frac{p_e - p_{wf}}{\ln \frac{r_e}{r_{wf}} + s}, \quad (2)$$

$$s = \frac{2\pi kh}{q\mu} \Delta p_s, \quad (3)$$

$$s = (\frac{k}{k_s} - 1) \ln(\frac{r_s}{r_w}), \quad (4)$$

Eq. (5) can be used to calculate the skin factor in a well if the flow rate from the damaged/stimulated and the unstimulated well and the size of outer drainage radius are known.

$$\frac{q}{q_{ideal}} = \frac{\ln(\frac{r_e}{r_{wf}})}{\ln(\frac{r_e}{r_{wf}}) + s}, \quad (5)$$

Eq. (5) is derived using Eqs. (1) and (2), which are based on a radial drainage area. (Golan and Whitson, 1996) do however suggest that Eq. (5) can be used with negligible error for all drainage areas if one uses an equivalent r_e according to **Eq. (6).**

$$r_{ea} = \sqrt{\frac{A_{drainage}}{\pi}}, \quad (6)$$

The concept of skin also introduces the apparent wellbore radius seen in Figure 1.6. The apparent wellbore radius can be considered as the imaginary wellbore radius in a well due to the damage (smaller apparent radius) or stimulation (higher apparent radius). **Eq. (7)** shows the definition of the apparent wellbore radius.

$$r_{wa} = r_w e^{-s}, \quad (7)$$

1.3 Well Modeling in ECLIPSE

The foundation for fluid flow simulation in ECLIPSE are the solution of the material balance equations for each fluid phase given by (Kleppe, 2016). This is done by discretizing the reservoir into a model consisting of a finite number of grid blocks and using numerical approximations for the differential equations to solve for phase saturations and pressures in each grid block.

In a typical model of a full field reservoir in ECLIPSE the size of the grid blocks are usually around 50 m long in each direction. Most of the draw down in a radial flow regime happens within a few meters of the well however. When the size of the grid block containing the well is much larger than the radius of the well the average pressure of the block is much higher than the well pressure. The draw down is therefore not accurately modeled. To calculate a flowing bottom hole pressure (FBHP) based on the average pressure in the block ECLIPSE therefore uses a connection factor. The default connection factor in ECLIPSE is the peaceman equation, which was introduced by (Peaceman, 1978). The peaceman equation relates the average pressure within a grid block containing a well to an equivalent outer radius in Eq. (1). This equivalent outer radius can then be used in Eq. (1) to calculate a connection factor that relates the average pressure to the FBHP. The FBHP or the flow rate (depending on well control) in a well can then be calculated.

Eq. (1) assumes that the flow into the well is completely radial, but there are many situations where the flow towards the well is in fact not radial at all. Two examples are wells that are not completed along the entire reservoir height/length, i.e. that experience spherical flow into the tips, and wells that are so closely spaced that they affect each other's flow. Thus there will be an error when using a connection factor that assumes radial flow.

(Shu, 2005) compared three different definitions of the connection factor used in numerical simulations to an analytical solution. He found that using the peaceman formula to compute a connection factor gave significant errors for a horizontal well with a length shorter than the reservoir section, i.e. where one would expect to find spherical like flow into the tips. Simulated flow rates from a horizontal well that had a vertical well placed close by also deviated from the analytical solution. The reason for this was that the closely spaced completions created a non-radial flow pattern in between the two wells. (Shu, 2005) also showed that an alternative way of determining the well index, know as the semi-analytical well index (Wolfsteiner et al., 2003), was able to match the analytical solution for all cases.

1.4 Grid Refinement

The process of discretizing a continuous partial differential equation into a grid with a finite number of grid blocks brings with it an inaccuracy. This happens because the parameters calculated in each grid block are applied over a distance equal to the length of the grid block. Thus if a parameter changes rapidly over a large interval discretized into few grid blocks the system will not be able to capture the real change in the parameter happening in the interval. This typically happens near a well because this is where the pressure drop is greatest.

A way to improve the accuracy is to use a more refined grid with smaller blocks around the well, as this will better capture the changes close to the well. Because the flow towards well is usually radial, a popular grid refinement to use is logarithmic gridding. Eq. (8) shows the definition of logarithmic gridding.

$$\Delta L_{i+1} = C_{GR} \times \Delta L_i , \quad (8)$$

Technically true logarithmic gridding is only possible in circular grids modeled using cylindrical coordinates where it ensures equal pressure drop in all the grid blocks. However, logarithmic gridding will still improve accuracy in a Cartesian grid.

2 Modeling Wells with Fishbones on a fine Scale in ECLIPSE

There is no doubt that Fishbones creates a complex inflow geometry around the well. In fact the sole purpose of Fishbones is to alter the inflow to a well[7] so that it becomes more efficient than a radial flow. As discussed by (Shu, 2005) and (Priskila, 2014) this new flow profile can therefore lead to serious errors in the simulations if care is not taken when the model is made. This section focuses on creating a model with a grid that is able to capture the details of the flow near the well as good as possible.

There are two ways of creating a grid that can be used to model the well and FBLs; local grid refinement and through the main grid. The advantage with local grid refinement is that it limits the refinement to the grid block(s) where the refinement is needed. This reduces the number of grid blocks in the model and thus the run time. By defining the needles using the main grid every grid block in a direction will be affected by the refinement. This results in significantly more grid blocks in the model and run time will be increased. The models considered in this thesis will be so small that run time is not a problem and because it is more convenient to only work with the main grid this is the method that will be used.

All the simulations in this section use mostly the same reservoir model, but with some differences. The FBLs were placed in the xz-plane, which measured 104 m x 104 m. The length and gridding in the y-direction varied in the different sections. The reservoir was homogeneous and isotropic with a permeability of 1 mD and 30% porosity. An illustration of the gridding used in xz-plane is shown in Figure 2.1. The grid model can be divided into to areas. The inner area (inside the green square) contains the FBLs and is 24 m x 24 m. The outer area is all the grid blocks outside the inner area with a 10 m length (width varies due to the refinements in the green area as Figure 2.1 shows). The inner area is refined using an n_{GR} = 2 (defined in section 2.1.1). The block inside the white square has dimensions 10 m x 10 m x 10 m.

Reservoir pressure was 350 bara and the well was run on a 310 bara constant FBHP constraint. The FBHP was set above the bubble point pressure to assure single-phase flow in the reservoir. PVT and relative permeability tables used in the model can be found in Appendix B. The flow inside the FBLs, annulus between the liner and wellbore wall and flow through the liner ports were all assumed to have a negligible pressure drop based on the results of (Freyer and Shaoul, 2011). Appendix B confirmed this.

[7] From here on the term well refers to the mother bore that Fishbones is run in.

Cases that are run on a constant FBHP constraint, but produce different rates due to different skin factors will have different declines in reservoir pressure. This causes the rates to decline accordingly and the cases are therefore not comparable any more. In order to make the cases comparable they should be simulated under steady state conditions, which ensures that the cases have equal FBHP and reservoir pressure. In order to make a steady state regime the pore volume in the outer grid shell was multiplied by 1000. This does not create a true steady state, but the change in reservoir pressure during the simulation was in the fourth decimal so the error was negligible.

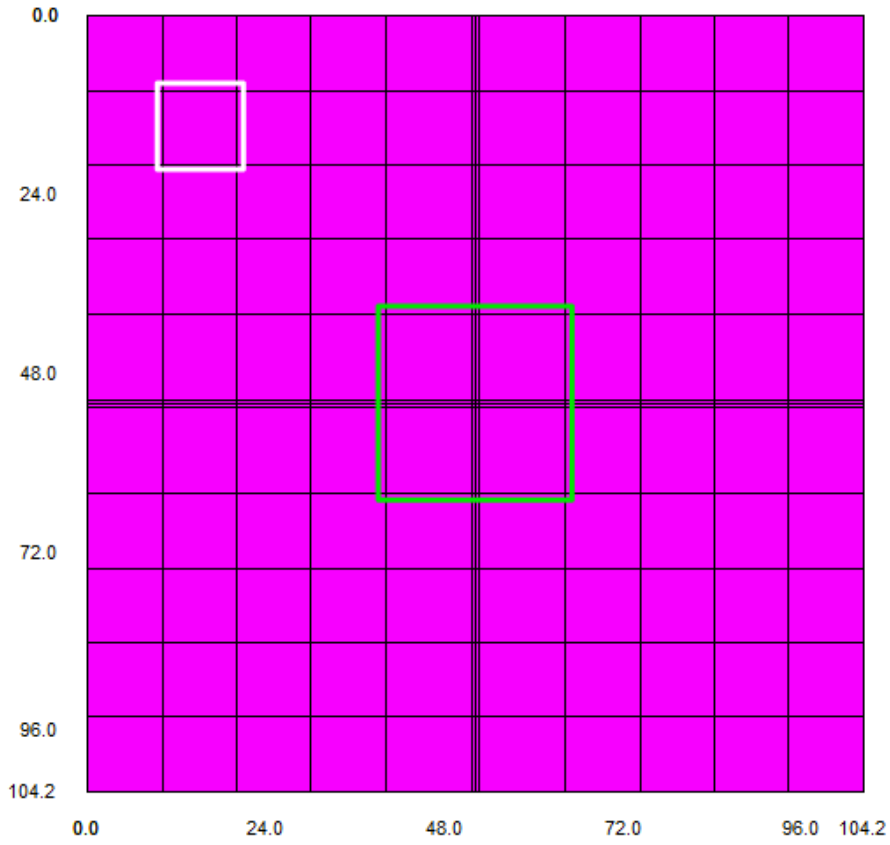

Figure 2.1 – Illustration of the main grid in the xz-plane. The inner area has been refined using an n_{GR} that is defined in section 0.

Modeling the FBLs as laterals is done by using completion keywords with a diameter of the FBL. There are two potential problems with this. First of all there will be an area within the grid that have a lot of completions in close vicinity and thus they will affect the flow area in different ways creating a non-radial inflow. In addition the FBLs will behave as partially penetrating wells because they do not penetrate the entire reservoir section. These are exactly the cases that (Shu, 2005) found to give significant errors when the peaceman connection factor was used. Increasing grid refinement around the laterals will bring more grid blocks inbetween the completions however and this may reduce the error.

To model the FBLs as fractures, small grid blocks with very high permeability and the same cross sectional area (CSA) as a FBL are used. This will remove the need for completions inside the FBL blocks leaving only the main completions along the well. This should eliminate the errors associated with the lateral model.

Section 2.1 discuss' how the FBLs can be modeled as fractures and section 2.2 discuss' how they can be modeled as laterals. Section 2.3 compares the two methods.

2.1 Fishbones Laterals Modeled as Fractures

As the previous section discussed, FBLs can be modeled as fractures by using long and thin grid blocks with a very high permeability (fracture blocks). The square CSA of the fracture blocks was equal to the circular CSA created by the jetting. Based on this the Fishbones lateral blocks were given a square CSA with 0.012 m sides, which equaled a 0.014 m circular diameter. The fracture blocks were 12 m long and the permeability in the fracture blocks, k_f, was set to 10^7 mD. Section 2.1.2 discusses the magnitude of k_f in the fracture blocks in order to ensure a negligible pressure drop.

Modeling the FBLs as fractures also requires the well to be modeled as a fracture (hereby referred to as a modified well). By adding four extra, 0.0179 m wide blocks on each side of the fracture blocks a square area in the middle of needles that had the same CSA as a circular well with 0.175 m diameter was created. A well completion was placed in the center, with a small wellbore diameter, and the permeability in the well blocks, k_w, was set to 10^5 mD. This created an area within the reservoir with zero pressure drop and with the same CSA as the well. An illustration of the modified well with the Fishbones laterals can be seen in Figure 2.2. Section 2.1.3 compares the modified well to a conventional well in ECLIPSE. Because of the small blocks close to the fracture blocks a grid refinement will be needed to ensure accurate simulations. This is discussed in section 2.1.1. Section 2.1.4 combines the results from sections 2.1.1 to 2.1.3 into a horizontal well with four FBLs.

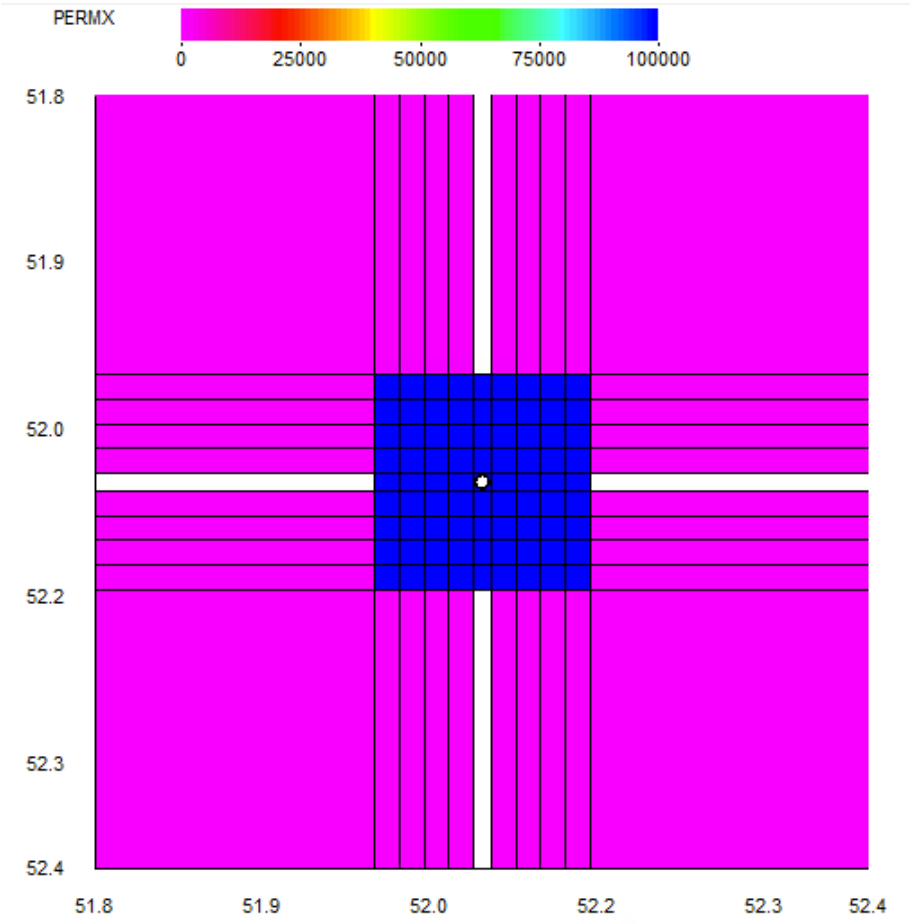

Figure 2.2 – Close up illustration of the modified well (blue squares) and fracture blocks (white). The completion is the white dot in the middle block. The full length of the fracture blocks is not shown.

2.1.1 The Effect of Grid Refinement around the Fracture Blocks

To see how the grid refinement around the fracture blocks affected the simulations, four different cases were run. The grid in the inner area inside the green square in figure Figure 2.1 was refined by dividing the 12 m fracture block length into two, four, eight and 12 segments using logarithmic gridding. The number of segments a fracture block is divided into is hereby referred to as n_{GR}. This corresponded to a C_{GR} from Eq. (8) of 25.4, 4.8, 2.1 and 1.6 where the ΔL_1 was 0.0179 m. Logarithmic gridding was found to have no effect in the outer area so a constant length of 10 m was used, but the width of the blocks varied according due to the refinement around the fracture blocks. This can be seen in Figure 2.1.

The length and gridding in the y-direction was the same as in the x- and z-direction. The resulting grid with $n_{GR} = 2$ and $n_{GR} = 12$ is shown in Figure 2.3. Because this section focuses on determining the effect of grid refinement around the needles no well was included, but a

single well “slice” with a completion had to be placed in the xz-plane where the needles were located to allow production.

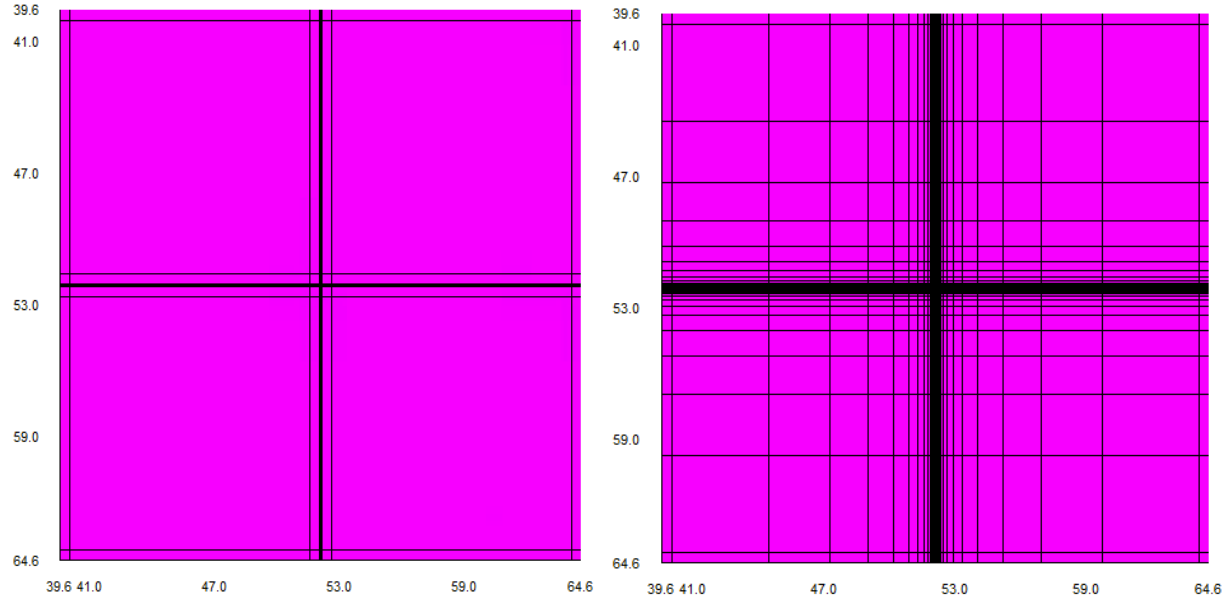

Figure 2.3 – Illustration of a grid refinement in the inner area around the fracture blocks with n_{GR} = 2 (left) and n_{GR} = 12 (right).

Figure 2.4 shows the simulated oil rate during the first 50 days for the four grid refinement cases. The rates show that steady state flow starts after roughly seven days. The curve for n_{GR} = 2 has a slightly different transient period than the three other curves as it seems to start at t = 1 day instead of t = 0 days as the other curves. This is because the simulator is run with a one day time step, but the simulator is unable to achieve convergence with such large time steps for the cases with $n_{GR} > 2$ during the early infinite acting flow (IAF) period. The time steps are therefore chopped until convergence is achieved thus resulting in a more detailed output during the early transient. For n_{GR} = 2 there are no convergence problems and the simulator jumps straight to t = 1 day. The model is able to converge without chopping the time step for all the simulation after approximately two simulation days.

Figure 2.4 also shows that grid refinement around the fracture blocks has a big impact on the simulated rates. The difference in steady state rate for a simulation with n_{GR} = 2 and a simulation with n_{GR} = 12 is 72%. Increasing n_{GR} does have a very positive effect and Figure 2.4 clearly shows that the steady state rate converges towards a final value for large values of n_{GR}. The difference in steady state rate for a simulation with n_{GR} = 8 and a simulation with n_{GR} = 12 is less than 2%.

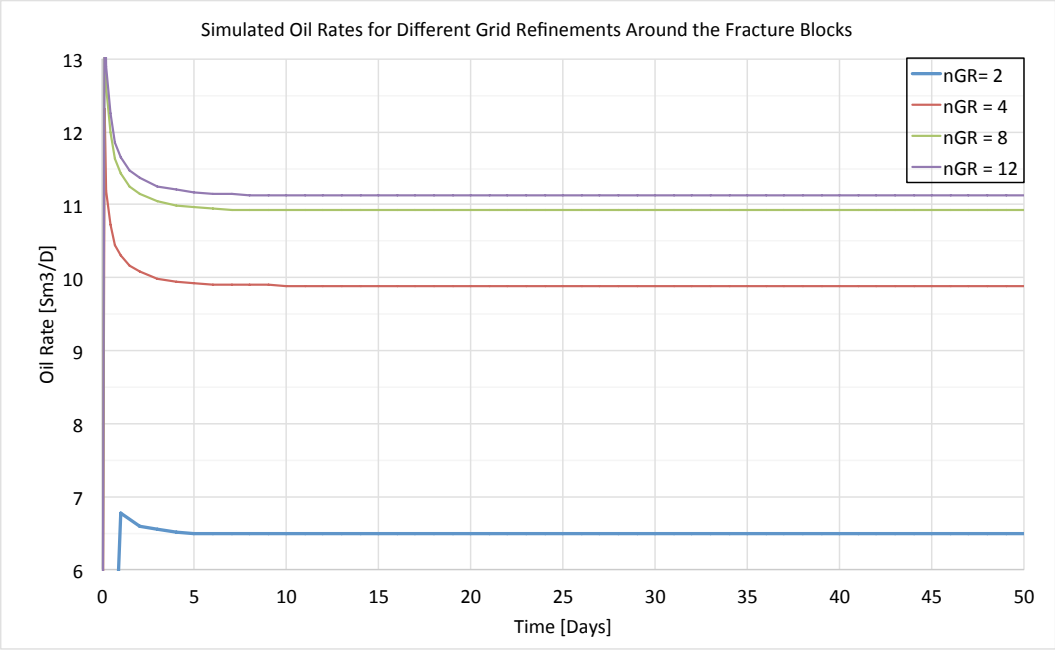

Figure 2.4 – Simulated oil rates for four different grid refinements around the fracture blocks.

Figure 2.5 shows the steady state oil rates plotted against the inverse square of n_{GR}, which gave the most linear trend. An exponential curve fit matches the points very well and extrapolation to $1/n_{GR}^2 = 0$ gave a 11.33 Sm^3/D state rate. This is less than a 2% increase over the steady state rate with $n_{GR} = 12$.

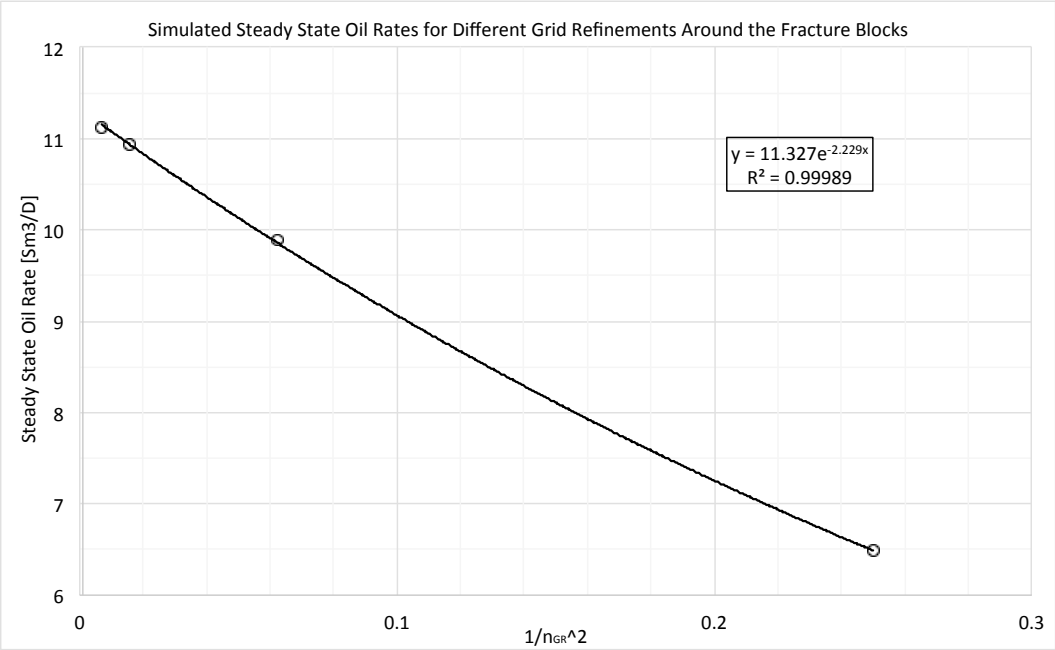

Figure 2.5 – Simulated steady state oil rates plotted against $1/n_{GR}^2$. An exponential curve fit is included for extrapolation to $1/n_{GR}^2 = 0$.

Figure 2.6 shows the pressure profile from the well to the edge of the reservoir. The pressure was recorded along a up sloping diagonal between the fracture blocks out to the corner of the

reservoir. This gives an additional hydrostatic pressure change and the points have been corrected for this. Three different flow regimes are seen. Between three and 11 meters from the well the flow is radial, as recognized by the straight line on a semi-logarithmic plot of pressure against distance from the well. Closer to the well the stimulation effect of the fracture blocks is seen as pressure deviates upwards from the straight line. The effects of the boundaries cause the deviation seen in the four outermost grid blocks. The well is also clearly seen as the four points where pressure does not change with distance.

Figure 2.6 shows that the pressure profile for $n_{GR} = 2$ clearly deviates from the other cases. For $n_{GR} = 4$ there is a slight deviation compared to $n_{GR} = 8$ and $n_{GR} = 12$, which are essentially equal. Based on this together with the results from Figure 2.4 and Figure 2.5 a $n_{GR} = 12$ were found to give sufficient accuracy in the simulations. The grid could have been refined even more, but that would lead to longer run times and more grid blocks to manage without really improving accuracy much.

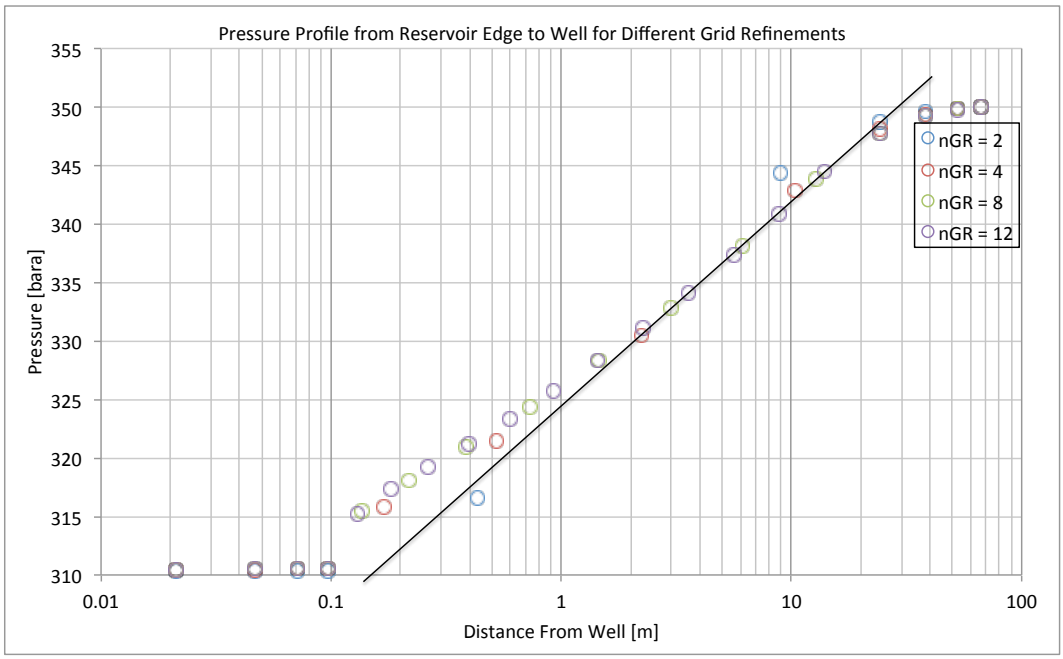

Figure 2.6 – Pressure profiles for different grid refinements around the fracture blocks. A hydrostatic correction has been made. The pressure in the block containing the well completion is not included. The distance is measured from the center of the well.

2.1.2 The Effect of Permeability in the Fracture Blocks

Four cases were run to investigate the effect that k_f has on the simulations. k_f was isotropic and varied between 10^5 mD, 10^6 mD, 10^7 mD and 10^8 mD. The same reservoir as in section 2.1.1 and a grid refinement with $n_{GR} = 12$ was used.

Figure 2.7 shows the simulated oil rates for the four cases. There is a big difference in the steady state rate for the two cases with low permeability compared to the two cases with high permeability. The difference in steady state rate between the case with $k_f = 10^5$ mD and the case with $k_f = 10^8$ mD is 112%. The differences are caused by pressure drop in the needles. The pressure drop in the fracture blocks for the different cases was 20.8 bara, 10.1 bara, 1.3 bara and 0.1 bara. As expected the simulated steady state rate approach a final rate when permeability is increased because the pressure drop within the fracture block approaches zero. The difference in steady state rate between the case with $k_f = 10^7$ mD and the case with $k_f = 10^8$ mD is only 2%.

Figure 2.8 shows the simulated steady state rate plotted against the inverse square root of k_f, as this gave the most linear trend. A linear trend line shows a decent fit. The extrapolation shows that the steady state production rate for fracture blocks without any pressure drop is 11.7 Sm^3/D, which is 3% higher than the rate with $k_f = 10^8$ mD. The points do not follow the linear exactly however and seems to have a downward curving trend towards $1/\sqrt{k_f} = 0$ indicating that the extrapolated rate is slightly too high. The downward curving trend can probably be explained by the permeability in the well being kept constant for all the cases.

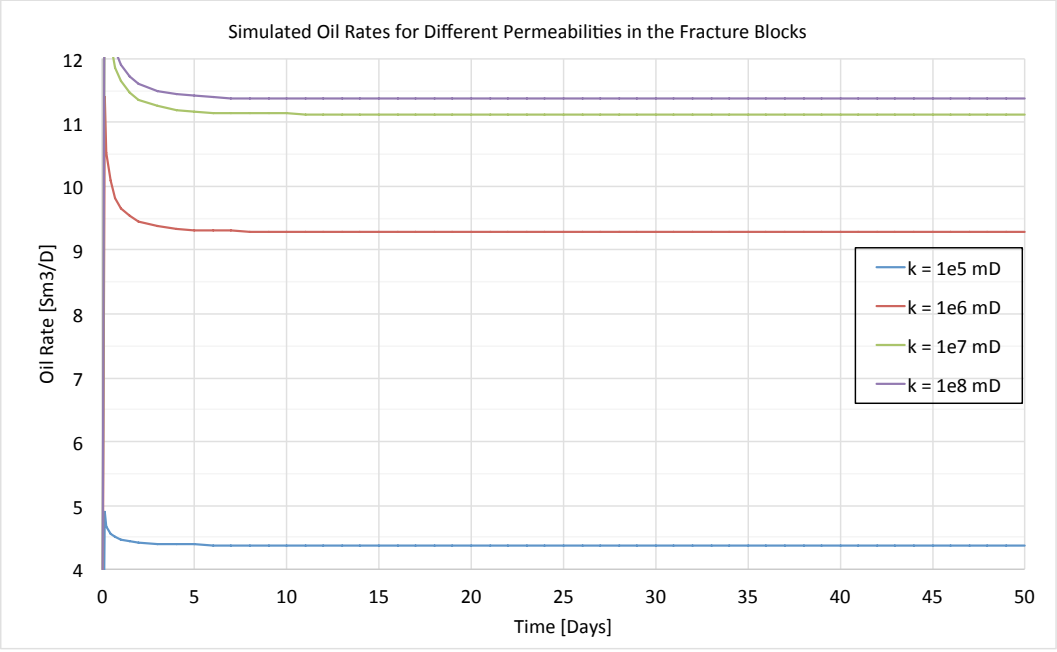

Figure 2.7 – Simulated oil rates for varying k_f.

Figure 2.9 shows the pressure profile from the well out to the reservoir edge for the four cases. It clearly shows that the cases with $k_f = 10^5$ mD and $k_f = 10^6$ mD have reduced stimulation effect. The cases with $k_f = 10^7$ mD and $k_f = 10^8$ mD have identical profiles and show a clear

deviation from the radial flow straight line indicating a good stimulation effect. They also have a pressure drop in the fracture blocks on the same order of magnitude as found by (Freyer and Shaoul, 2011). Appendix A suggested a $k_f = 10^9$ mD, but increasing k_f resulted in increasing run time. Based on this, together with the results from Figure 2.7 and Figure 2.8, a $k_f = 10^8$ mD needle permeability was found sufficient.

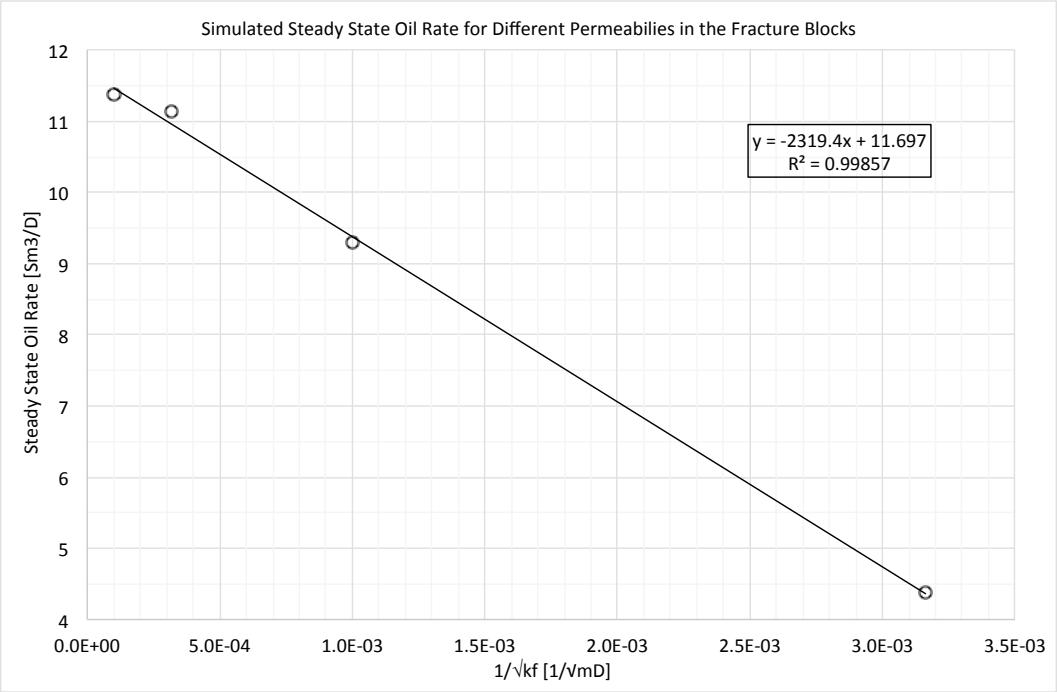

Figure 2.8 – Simulated steady state oil rate plotted against $1/\sqrt{k_f}$. A linear trend line is added for extrapolation to $1/\sqrt{k_f} = 0$.

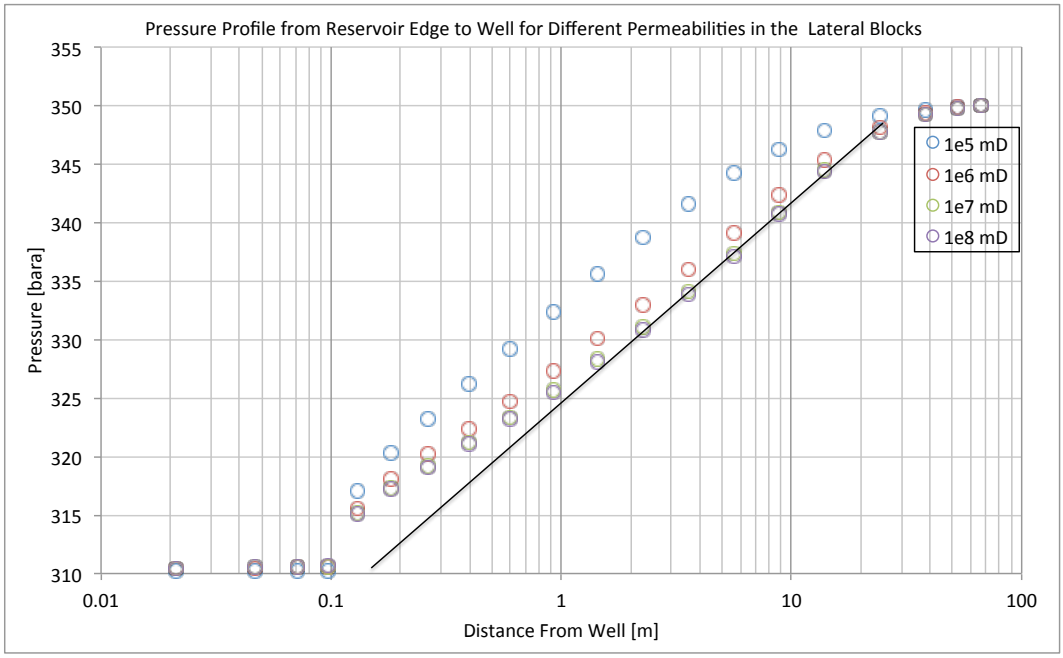

Figure 2.9 – Pressure profiles for varying k_f. A hydrostatic correction has been made. The pressure in the block containing the well completion is not included. The distance is measured from the center of the well.

2.1.3 Comparing the Modified Well to a Conventional Well

In order to see how the modified well performed, three cases were run with k_w varying between 10^4 mD, 10^5 mD and 10^6 mD. These were compared to a conventional well, which was modeled using completion keywords with the actual well diameter. None of the wells had any FBLs and same reservoir dimensions as in section 2.1.1 was used. Both wells were placed in the y-direction and spanned the entire reservoir length. The modified well was run with a grid refined using n_{GR} = 12 from section 2.1.1 in the x- and z-direction, while the conventional well had a logarithmic grid refinement in the x- and z-direction with C_{GR} = 1.3 and ΔL_1 = 0.5. Because there is only flow perpendicular to the well there was no need for refinement in the y-direction.

Figure 2.10 shows the simulated oil rates for a modified well with the two different permeabilities within the well blocks compared to the simulate oil rate from the conventional well. There is no significant difference in simulated steady state rate between the three cases with different k_w. The difference in steady state rate between the conventional well and the modified well is less than 1% for all three k_w. There was a large difference in simulation time between the the two cases with $k_w = 10^4$ mD and $k_w = 10^5$ mD the case with $k_w = 10^6$ mD however. The case with $k_w = 10^6$ mD had a three times longer simulation time.

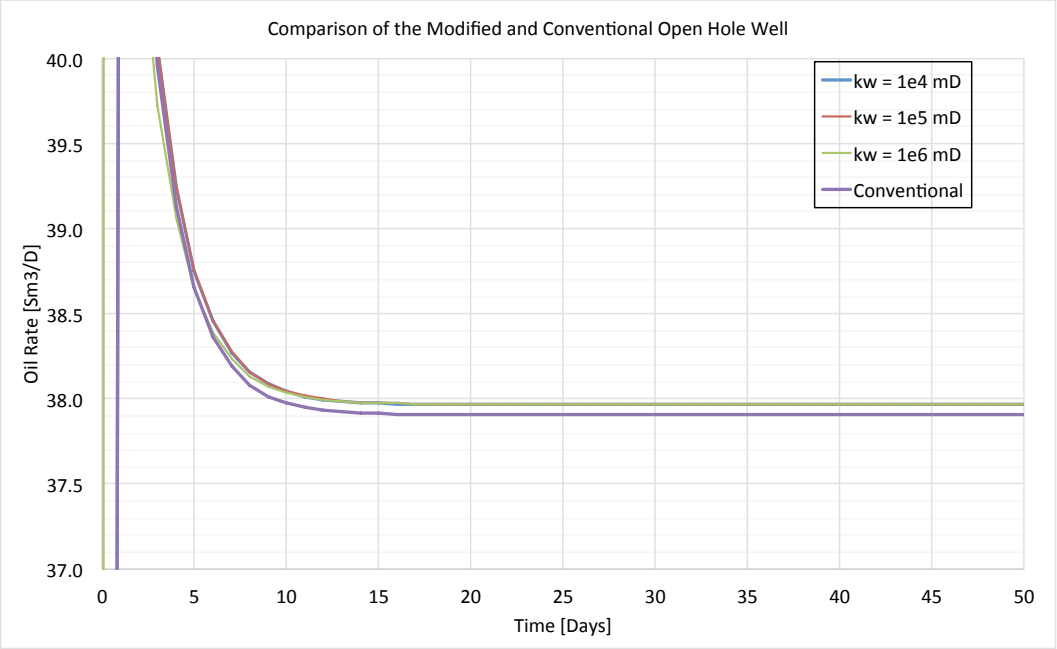

Figure 2.10 – Simulated oil rates for a modified well compared to a conventional well.

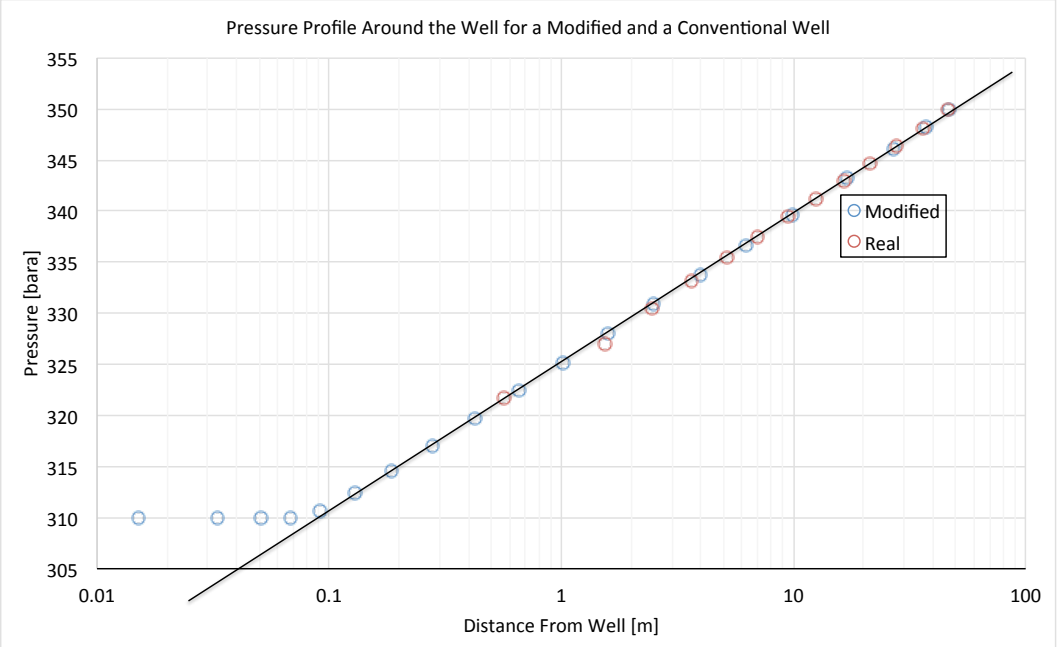

Figure 2.11 – Pressure profiles for the modified and conventional well. The pressures are recorded in the x-direction at the same height as the well is located. $k_w = 10^5$ mD. The distance is measured from the center of the well.

Figure 2.11 compare the pressure profile from a modified well with $k_w = 10^5$ mD and the conventional well. Because the wells do not have any FBLs the pressure could be recorded horizontally out from the well. There are therefore no boundary effects. Both wells follow a radial straight line along the entire reservoir section. The figure also shows that there is no

significant pressure drop within the well. An interesting observation is that the modified well have a more detailed pressure profile very close to the well. This is because the small blocks that make up the well creates a very fine grid close to the well due to the logarithmic grid refinement. For the conventional well the block the size of the block containing the well needs to be much larger than the well diameter according to the peaceman formula. The extrapolated radial straight line indicate that both wells have a well radius close to 0.085 m, which is the actual radius used in both cases.

Based on the results from Figure 2.10 and Figure 2.11 ECLIPSE is able to simulate flow into a horizontal well just as good with a modified well with $k_w = 10^5$ mD as with a conventional well.

2.1.4 Combining Well and Fishbones Laterals

This section combines the results from sections 2.1.1 to 2.1.3 into a horizontal well with four FBLs. The reservoir length in the y-direction is reduced to 40 m and the well spans the entire length. A $n_{GR} = 12$, a $k_f = 10^8$ mD and a $k_w = 10^5$ mD were used to model the well and FBLs.

In sections 2.1.1 and 2.1.2 the same gridding that was used in the x- and z-direction was also used in the y-direction, despite this direction not having any extending FBLs. As there was no well included in those sections this did not pose a big problem. However when a well is added, employing the same gridding in all three directions results in an unnecessary amount of well completions because of the many grid blocks in the y-direction.

In order to find the optimal grid that minimizes the number of required completions, but also ensures that the simulation results are accurate, four cases with different grid refinement in the y-direction were run. The total number of grid blocks in the y-direction, n_y, was varied between nine, 13, 17 and 25. The Δy in the center xz-plane was 0.5 m long for all cases, resulting in a C_{GR} of 6.1, 3.2, 2.4 and 1.7. Figure 2.12 show the effect on the grid in the y-direction for $n_y = 9$ and $n_y = 25$.

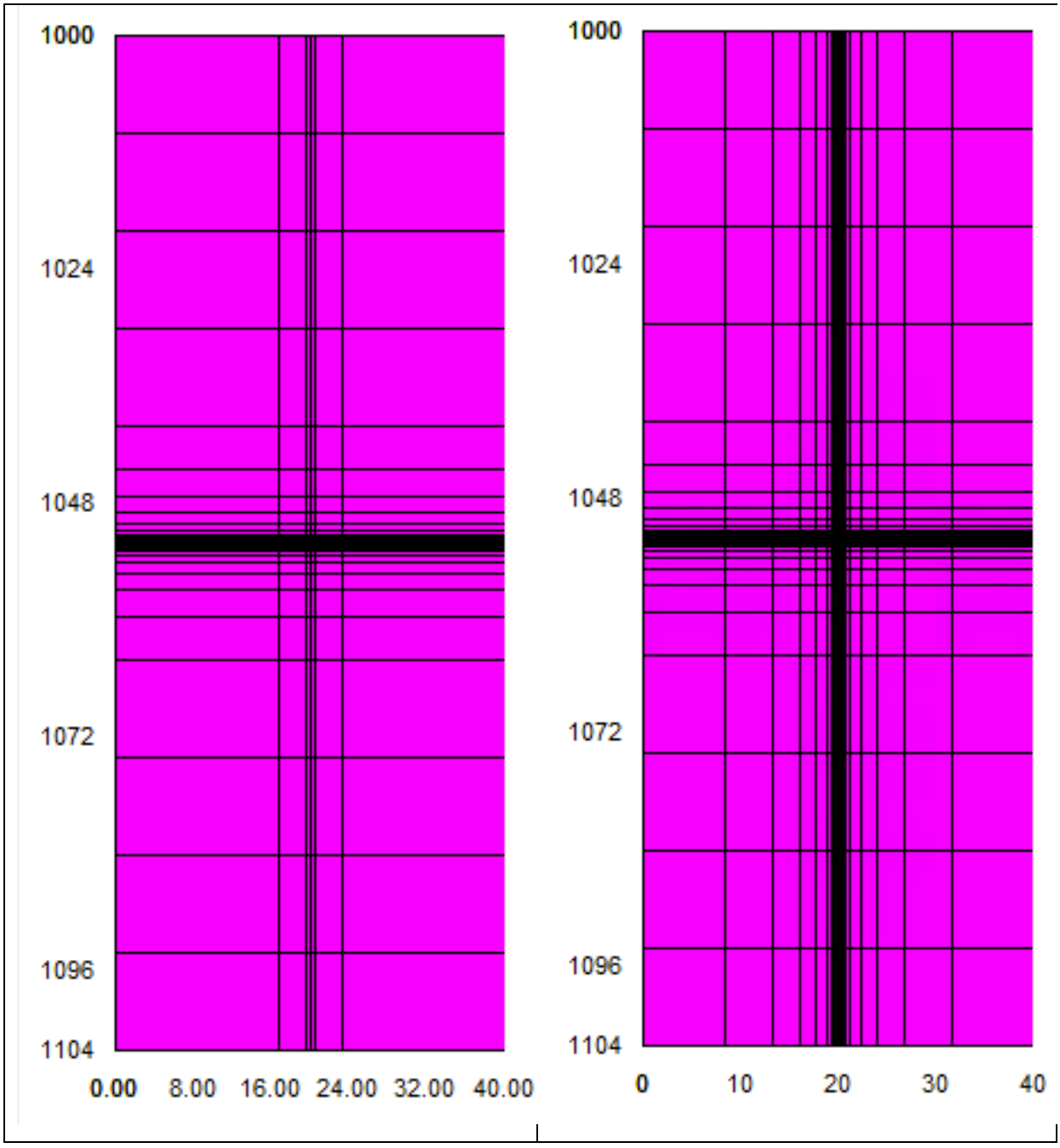

Figure 2.12 – Illustration of grid refinements due to variations in n_y. Left: n_y = 9, right: n_y = 25. Many of the grid blocks become so narrow that they are impossible to separate from each other.

The simulated oil rates are shown in Figure 2.13. As the figure shows the simulations are much less affected by the grid refinement in the y-direction than by the grid refinement in the area between the FBLs. The difference in steady state oil rate for n_y = 9 and n_y = 25 is less than 1%.

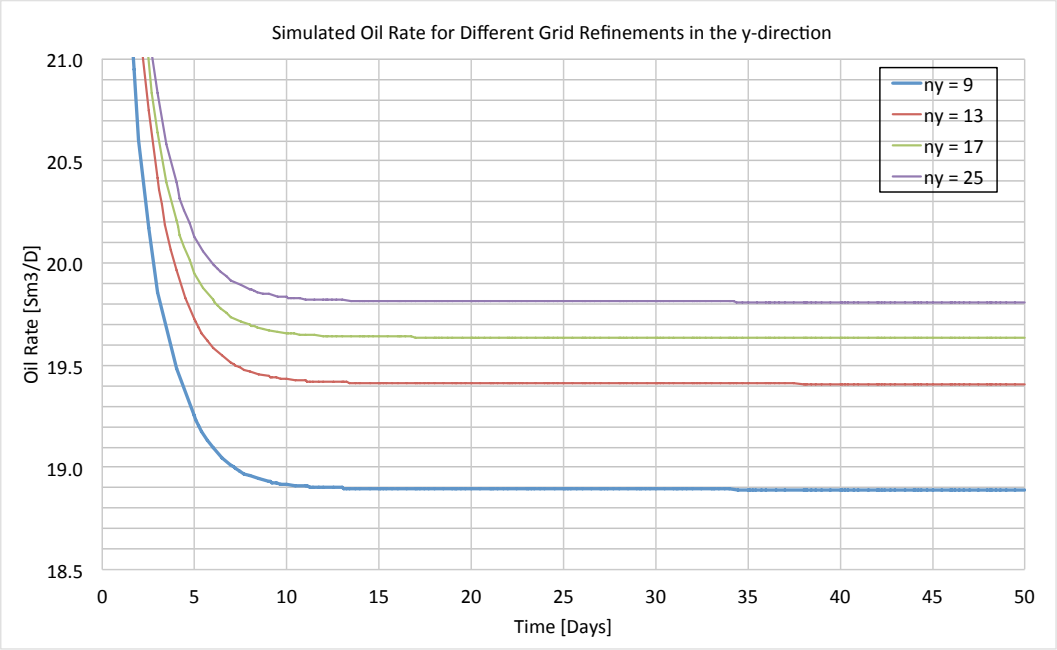

Figure 2.13 – Simulated oil rates for different grid refinement in the y-direction.

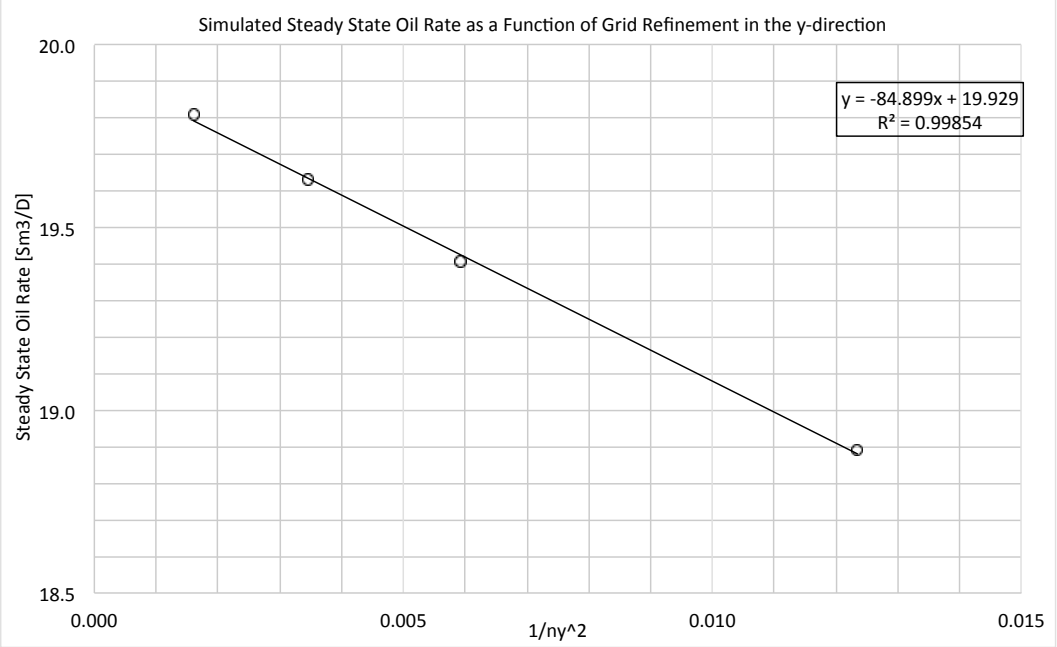

Figure 2.14 – Simulated steady state oil rates for different grid refinements in the y-direction. A linear curve fit is included for extrapolation to $1/n_y^2 = 0$.

Figure 2.14 shows the simulated steady states oil rates for the four different grid refinements as a function of the inverse square of n_y, which gave the most linear like curve. A linear trend line fits the data nicely and the exptrapolation suggests that the steady state oil rate for an infinitely large grid refinement in the y-direction is 19.9 Sm^3/D, which is less than 1% higher than the steady state rate resulting from a $n_y = 25$. The points have a slightly upwards curving

trend compared to the linear trend line, but this should not affect the value of the extrapolated steady state rate significantly.

Figure 2.15 shows the pressure profile from the well to the edge of the reservoir. There are no significant differences between the pressure profiles for the different refinements in the y-direction. What is noticeable however is that the pressure profile is quite different from the pressure profiles seen in sections 2.1.1 and 2.1.2. In Figure 2.6 and Figure 2.9 the pressure deviated upwards from the radial straight line, but then dropped down again close to the well. The pressures in Figure 2.15 also deviates upward, but this is a smooth upcurving deviation all the way to the well. The difference is probably caused by the addition of a well. Figure 2.6 and Figure 2.9 only contain a single well completion to enable production from the needles and thus the flow in the y-direction will converge into the completion, creating a pressure drop close to the well. When a well is added there will not be as much flow perpendicular to the plane containing the FBLs because fluid far away from the FBLs will rather flow into the well than to the FBLs.

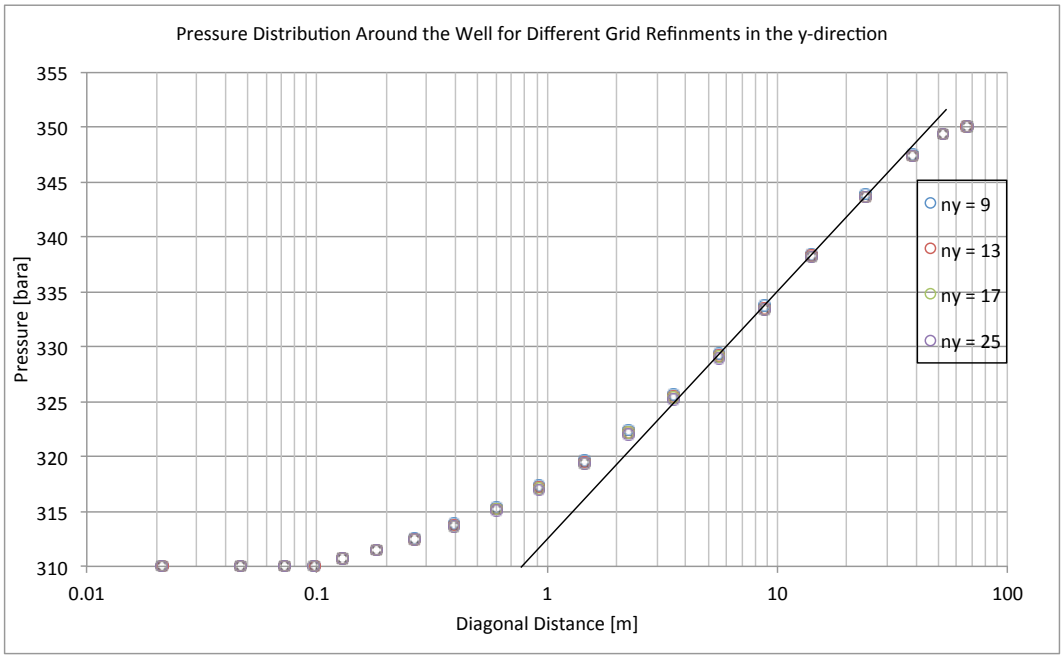

Figure 2.15 – Pressure profiles for different grid refinements in the y-direction. A hydrostatic correction has been made. The pressure in the block containing the well completion is not included. The distance is measured from the center of the well.

2.2 Modeling Fishbones Laterals as Laterals

Section 2 discussed how the Fishbones laterals can be modeled as laterals by using completions with a 0.014 m diameter in 12 m long blocks (lateral blocks). In order to reduce

the error associated with having many well completions closely spaced together the grid around the lateral blocks should be refined. This is discussed in section 2.2.1.

It is desirable to have the CSA of the lateral block as small as possible. The lower theoretical limit is of course determined by the peaceman equation, but the actual lower limit is larger than this. This is because a well requires a blocks with larger CSA since it has a larger diameter. Because of this the CSA of the lateral blocks will be larger than what would be considered ideal. The effect of this is discussed in section 2.2.2. Section 2.2.3 combines the Fishbones laterals and a horizontal well and discuss an appropriate grid refinement in the y-direction.

The completions within the laterals act as mass sinks and thus there is no need to place a well completion in the block between the needles. In fact placing another completion here would increase the expected negative effects of closely spaced completions discussed. Without a completion in the block it will act as a normal grid block and drain into the needles or the well from the inside, which is also wrong. To eliminate this the porosity in the grid was set to zero. This was only done to the center block in the plane containing the needles. All the other planes contained normal grid blocks in the center. This is illustrated in Figure 2.16.

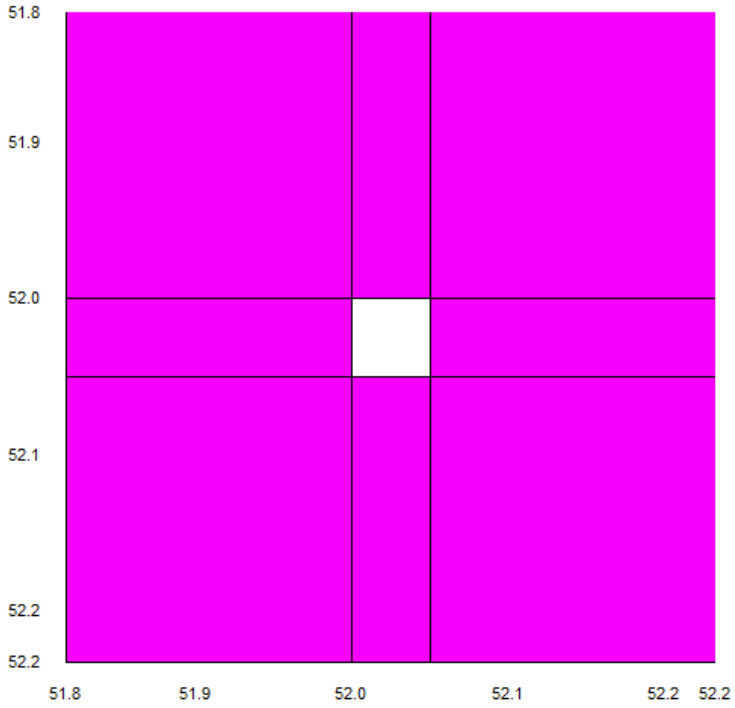

Figure 2.16 – Close up illustration of the well and lateral blocks. The white grid block has porosity set to 0. The lateral blocks extend further out from the illustration.

2.2.1 The Effect of Grid Refinement around the Lateral Blocks

The same procedure as in section 2.1.1 is used in this section to see the effect of grid refinement around the lateral blocks. Four different cases with an n_{GR} varying between two, four, eight and 12 were run. The lateral blocks had a square CSA with 0.05 m sides, which resulted in a C_{GR} of 15, 3.6, 1.8 and 1.4 the grid in the near area will behave the same as in Figure 2.3. The same gridding was used in the y-direction.

Simulated oil rates are shown in Figure 2.17. The figure shows the simulated steady state oil rates are clearly affected by the grid refinement. The difference in simulated oil rate between a $n_{GR} = 2$ and a $n_{GR} = 12$ is 132%. Increasing n_{GR} does however have a positive effect as the difference in steady state oil rate between a $n_{GR} = 8$ and a $n_{GR} = 12$ is only 3%. Compared to the grid refinements in section 0 the steady state rates for the two coarsest grid refinements are pretty similar, but the two finer grids give a slightly higher steady state rate. The difference in steady state rate between a $n_{GR} = 8$ and a $n_{GR} = 12$ is also higher than in section 2.1.1.

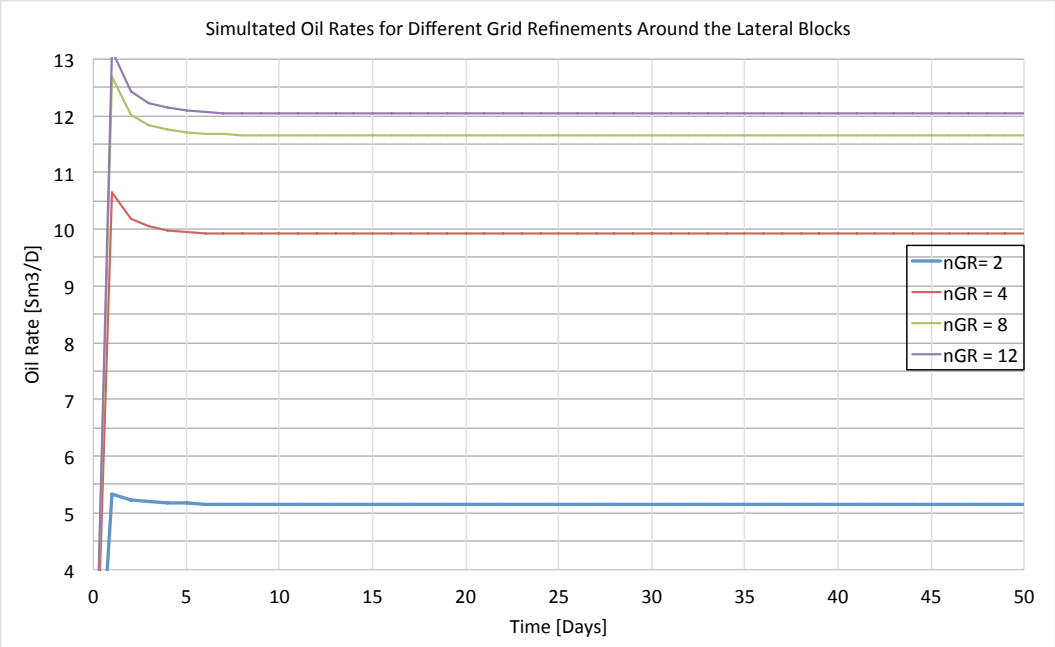

Figure 2.17 – Simulated oil rates for different grid refinements around the Lateral Blocks.

Figure 2.18 shows a plot of the simulated steady state rates against the inverse square of n_{GR}, which gave the most linear trend. An exponential trend line shows a good match with the data points. Extrapolating the trend line to $1/n_{GR}^2 = 0$ gives a steady state rate of 12.2 Sm^3/D, which is a 2% higher steady state rate than with $n_{GR} = 12$. The extrapolated steady state rate is 8% higher than the extrapolated steady state rate in section 2.1.1.

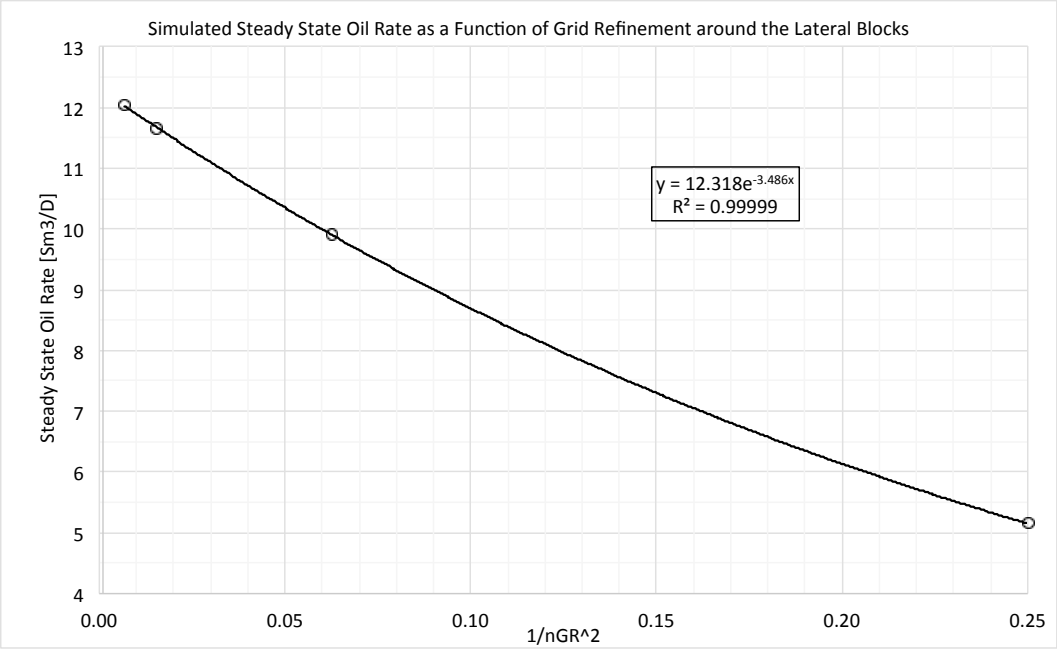

Figure 2.18 – Simulated steady state oil rates for different grid refinements around the Fishbones laterals. An exponential curve fit is included for extrapolation to $1/n_{GR}^2 = 0$.

Figure 2.19 shows the pressure distribution from the well to the edge of the reservoir. The pressure profile for $n_{GR} = 2$ clearly deviates from the other, while the pressure profile for $n_{GR} = 4$ deviates slightly. The pressure profiles for the two finest grid refinements are more or less equal. The effect of the stimulation is seen from the deviation from the radial straight line roughly two meters away from the well for the three finest grid refinements. This is very similar to the pressure profile in section 2.1.1, but the pressure profiles do not show the same downward curving trend very close to the well. When the Fishbones laterals were modeled as fractures in section 2.1.1 there was only added a single well completion between the Fishbones laterals. This single completion then acted as a point mass sink for the entire reservoir volume as was discussed in section 2.1.1. When the Fishbones laterals were modeled as laterals there were a lot more completions. This gave the fluid a larger area to flow into and thus less converging flow occurred.

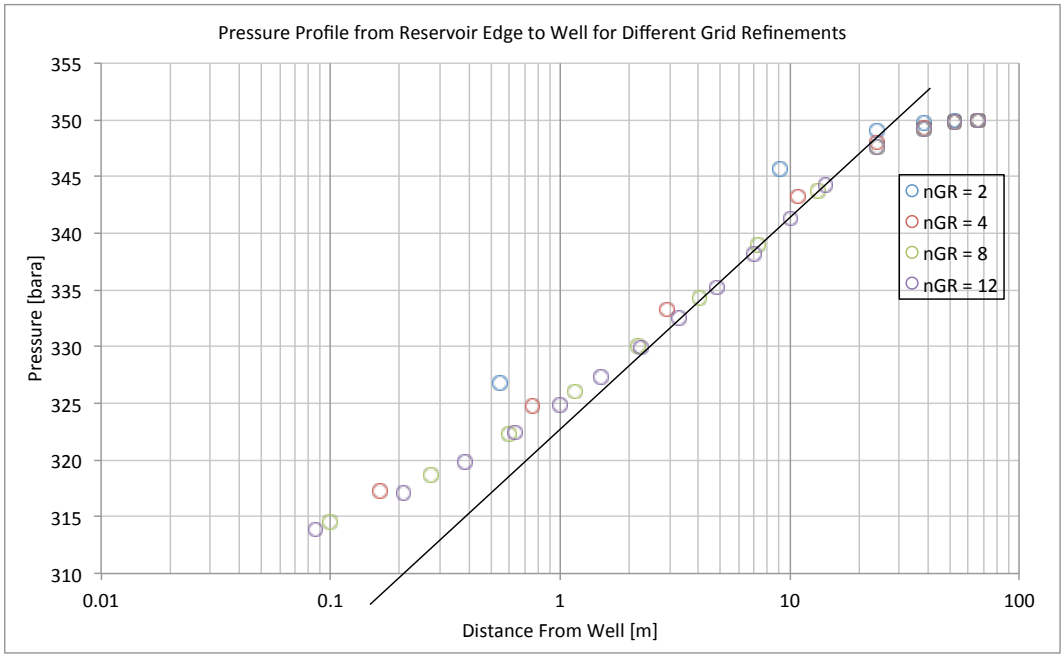

Figure 2.19 – Pressure profiles for different grid refinements around the lateral blocks. A hydrostatic correction has been made. The pressure in the center block is not included. The distance is measured from the center of the well.

2.2.2 The Effect of the Size of the Cross Sectional Area of the Lateral Blocks

Four cases were run to see the effect of the CSA of the lateral blocks. The CSA of the lateral blocks had sides that varied between 0.05 m, 0.1 m, 0.2 m and 0.5 m. Lateral blocks with a CSA with 0.5 m sides were the only ones that allowed the placement of a 0.175 m diameter well. Gridding is the same in the y-direction as in x- and z- and a grid refinement with n_{GR} = 12 was used. Because the size of the lateral blocks varied the C_{GR} for each case was 1.43, 1.33, 1.23 and 1.10.

Figure 2.20 shows the simulated production rates for the different CSAs. The CSA of the lateral block clearly affects the simulated steady state rate. The difference in steady state rate between a lateral block with 0.05 m and a 0.5 m sides is 4 %. There also does not seem to be a good converging trend when the CSA is decreased. It is to be expected that the difference between two steady state rates should decrease when the CSA is decreased. The figure shows that this is the case when the length of the sides is reduced from 0.5 m to 0.2 m and from 0.2 m to 0.1 m, but when the length of the sides is reduced from 0.1 m to 0.05 m the difference increases again. The different sizes of the CSAs caused a slight difference in how far out the lateral blocks extended in the reservoir.

Figure 2.21 shows the pressure profiles from the well to the reservoir edge. The pressure profiles are equal for all the cases, but there is a difference in how close to the well the pressure can be recorded. This is due to the different CSA for each case.

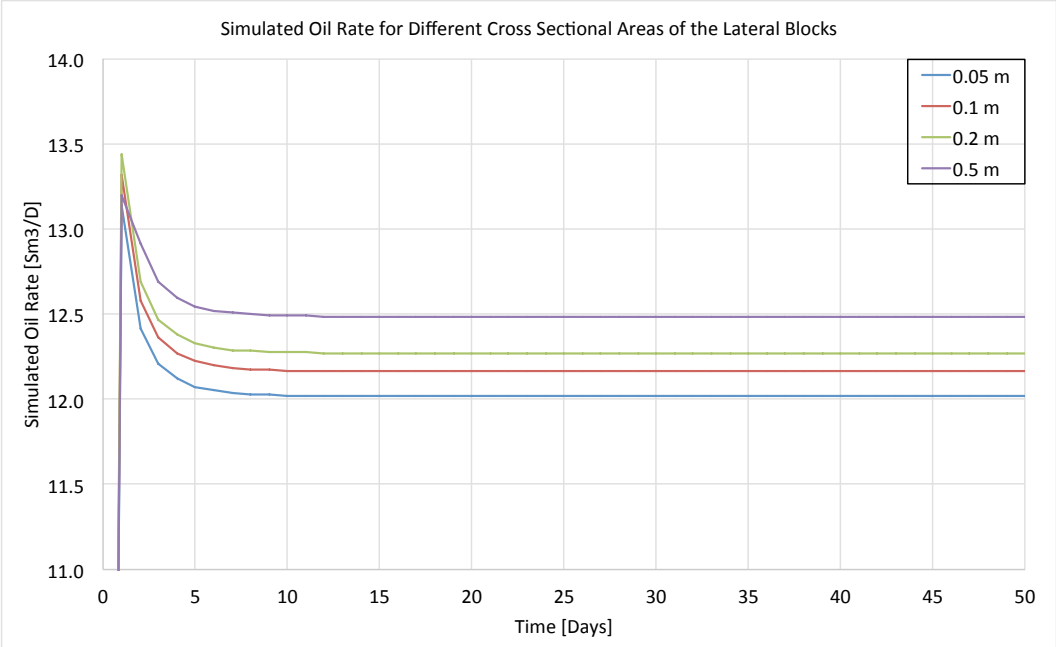

Figure 2.20 – Simulated oil rates for different CSAs of the lateral blocks.

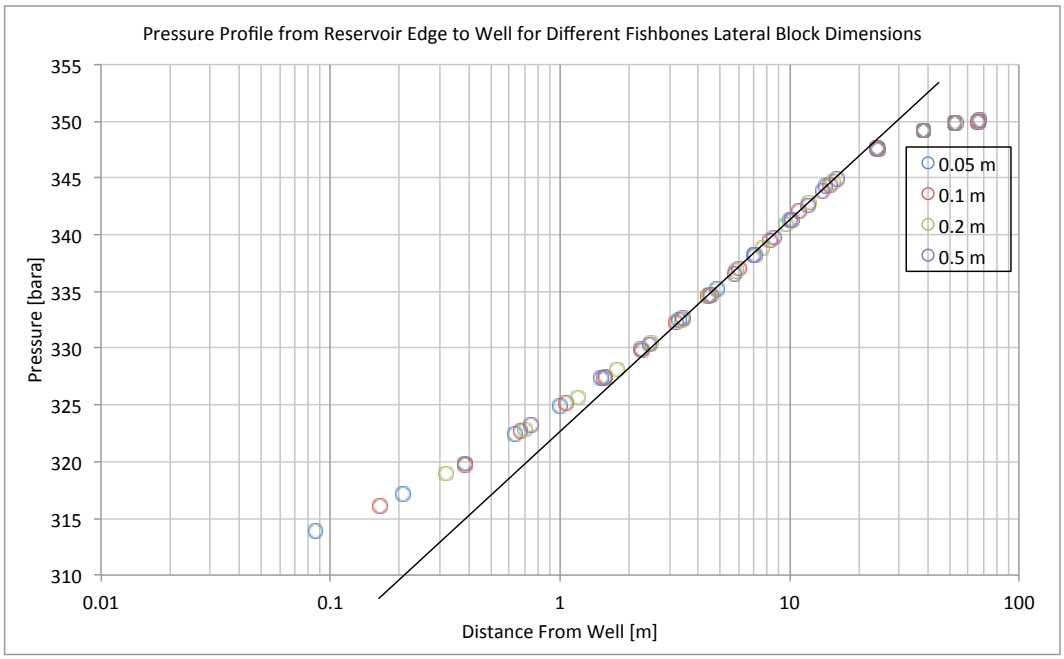

Figure 2.21 – Pressure profiles for different CSAs of the lateral blocks. A hydrostatic correction has been made. The pressure in the center block is not included. The distance is measured from the center of the well.

2.2.3 Combining Well and Fishbones Laterals

This section combines the results from sections 2.2.1 and 2.2.2 into a horizontal well with four FBLs. The well and reservoir was 40 m long in the y-direction with the lateral blocks located in the middle xz-plane. The grid around the lateral blocks was refined using a n_{GR} = 12. The sides in the square CSA of the lateral blocks were set to 0.5 m to enable a well to be included and the pore volume in the grid block in the middle of the Fishbones laterals was set to zero.

In order to find the optimal gridding in the y-direction, four cases were run with the length in the y-direction being divided into nine, 13, 17 and 25 blocks. The Δy in the center xz-plane was 0.5 m for all cases and logarithmic gridding was used to get a total reservoir length of 40 m. This corresponded to a C_{GR} of 2.2, 1.6, 1.4 and 1.2. The grid refinement will affect the grid in the same way as in Figure 2.12.

The simulated rates for each case are shown in Figure 2.22. As the figure shows there is very little difference between the coarsest and the finest y-refinement with the difference being only 1%. Figure 2.23 shows the simulated steady state rate plotted against the inverse square of ny, which gave the most linear trend. A linear trend line fit the data nicely and extrapolation to $1/n_y^2 = 0$ gave a 20.47 Sm3/D steady state rate, which is less than a 1% difference compared to the rate with $n_y = 25$. The data points do not follow a nice trend however and they seem to have a slight s-shape. It is unknown what is causing this effect.

The steady state pressure profile from the upper corner diagonally towards the well is shown in Figure 2.24. Because the profile is read along a downward sloping diagonal the pressure has been hydrostatically corrected to the same datum as the well. The pressure profiles show that there is no significant difference between the different grid refinements in the y-direction.

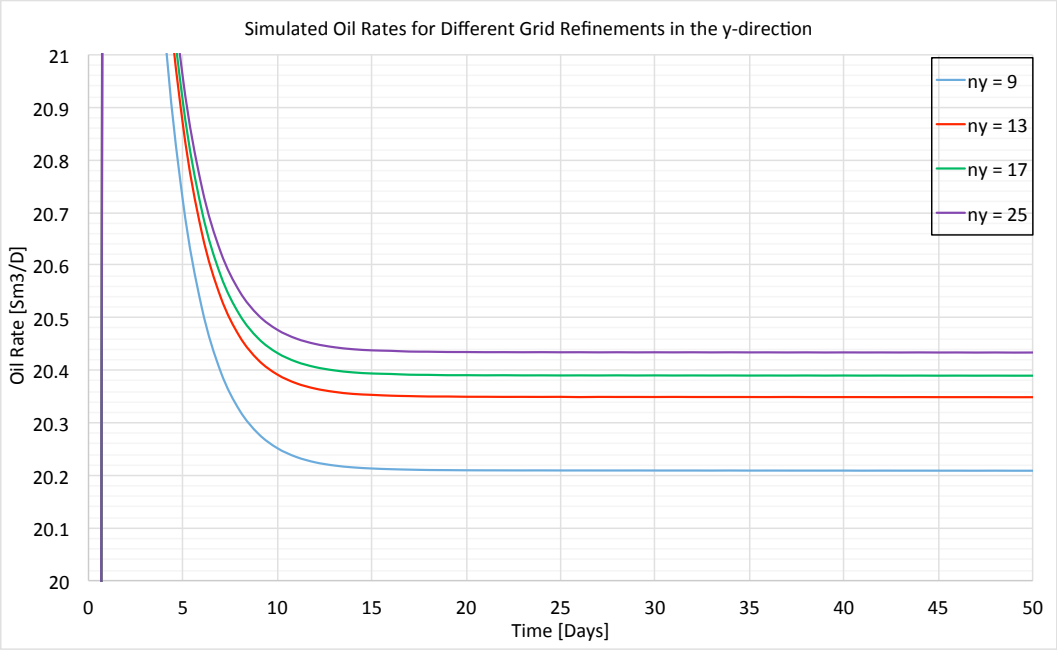

Figure 2.22 – Simulated oil rates for different grid refinements in the y-direction.

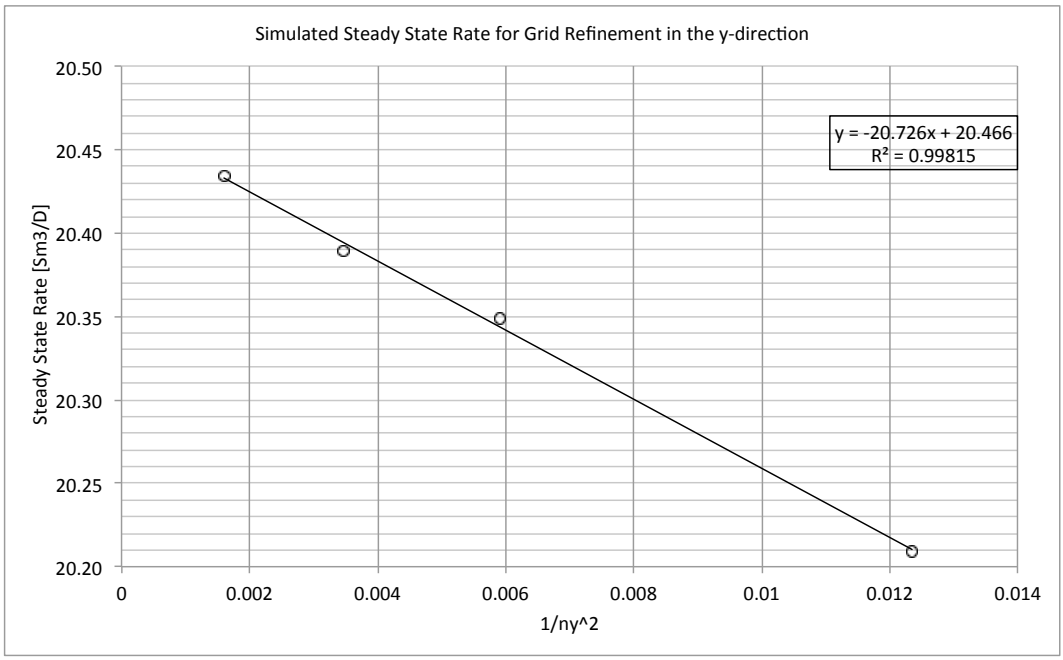

Figure 2.23 – Simulated steady state rate plotted against $1/n_y^2$. A linear curve fit is included for extrapolation to $1/n_y^2 = 0$.

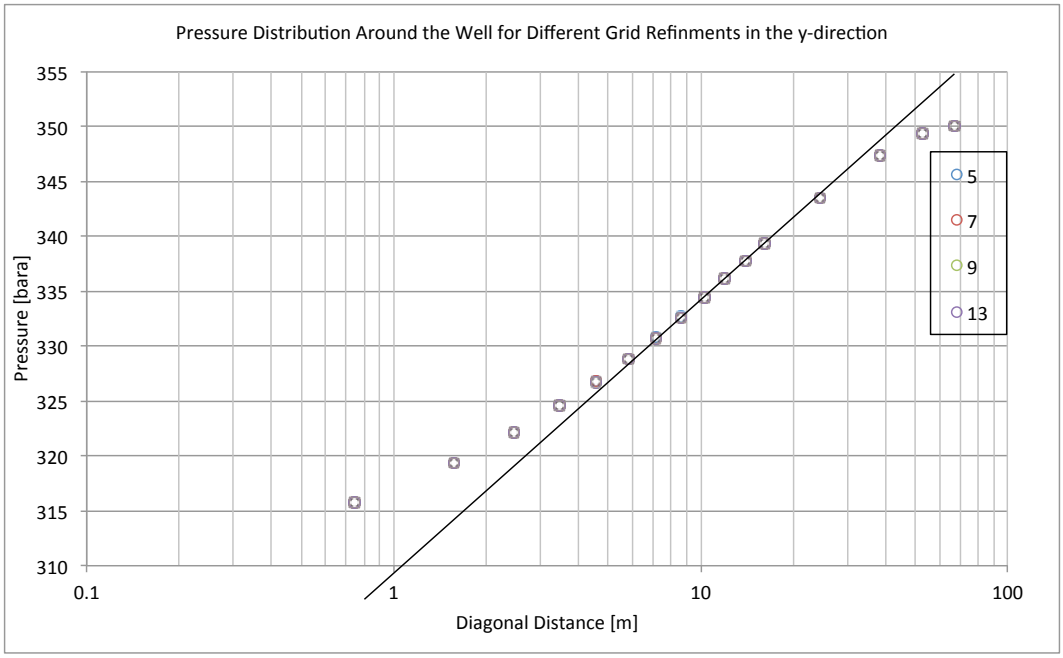

Figure 2.24 – Pressure profiles for different refinements in the y-direction. A hydrostatic correction has been made. The pressure in the center block is not included. The distance is measured from the center of the well.

2.3 Comparing the Two Models

In order to determine which method should be used to analyze the effect of a Fishbones stimulation the results from section 2.1.4 and 2.2.3 were compared. Simulated rate and pressure profile from the well to the reservoir edge with a $n_y = 17$ was used in the comparison, as this showed to be a sufficient refinement for both models. Both models used a grid refinement with $n_{GR} = 12$.

Figure 2.25 shows the simulated oil rate for the two different FBL models. The steady state rate from the lateral model is roughly 4% higher than the steady state rate from the fracture model. The figure also shows that the lateral model had a faster run time since it does not need to chop time steps, while the fracture model ran on chopped time steps during the entire simulation. The difference in run time was 6 seconds for the lateral model and 126 seconds for the fracture model. The many small grid blocks that had to be used to create the modified well is probably the main reason for the big difference in run time.

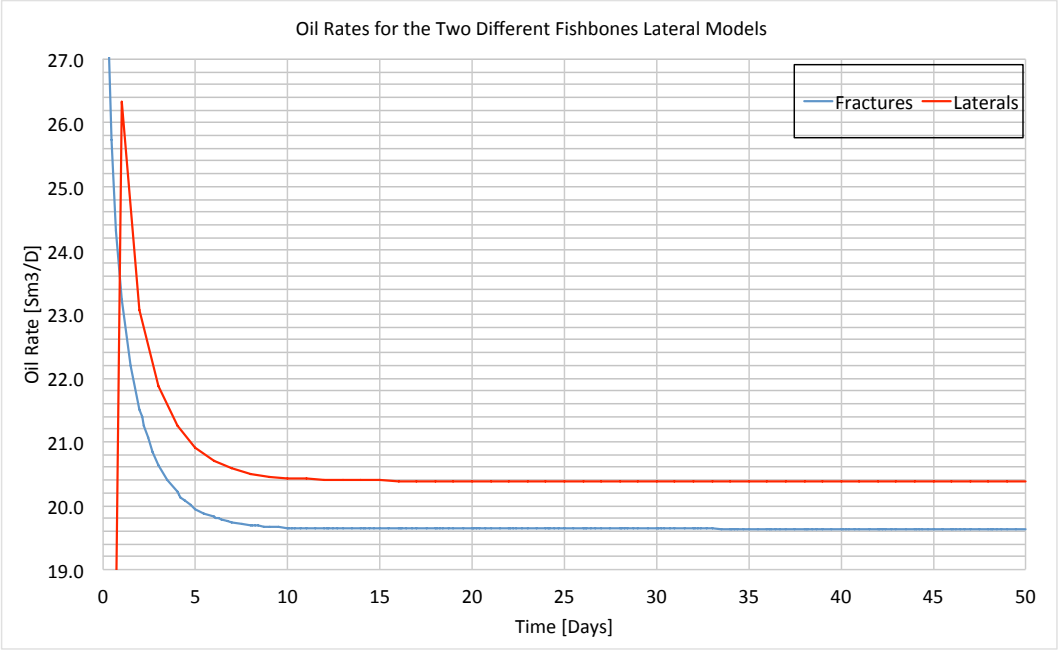

Figure 2.25 – Simulated oil rates for the two different FBL models.

Figure 2.26 shows the pressure profile from the well to the edge of the reservoir. There is a small difference between the two profiles. The pressure profile for the lateral model has a slightly steeper radial straight line and the deviation also happens further away from the well. This gives a higher r_{wa} and thus a better stimulating effect, just as Figure 2.25 shows.

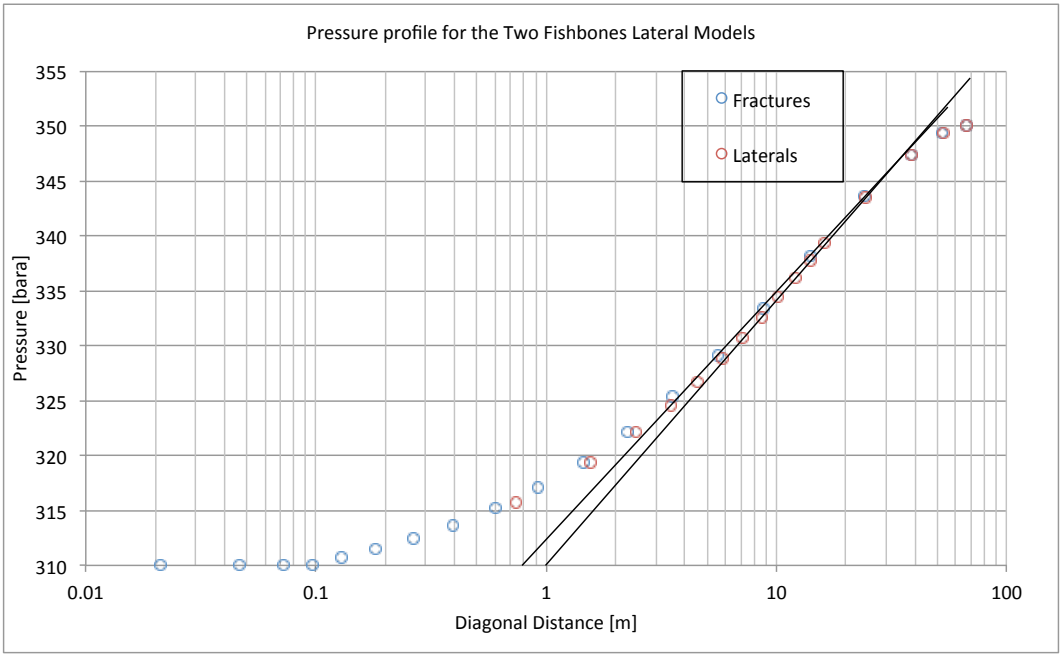

Figure 2.26 – Pressure profiles two different FBL models. A hydrostatic correction has been made. The pressure in the center block is not included. The distance is measured from the center of the well.

As Figure 2.25 and Figure 2.26 show the difference in steady state rate between the two FBL models is not dramatically large, but it is significant. It us unknown what is causing this

difference. It may be because there are so many completions close together and that the FBLs only partially penetrate the reservoir. As (Shu, 2005) showed this will give an error in the simulations. It may also be because the grid blocks containing the FBLs had to have a large CSA because a well was added. Figure 2.20 showed that this caused a 4% increase in steady state rate. Figure 2.20 and Figure 2.23 also showed that the lateral model behaved weirdly in some cases. The fracture model also have some inaccuracies because the grid refinements and k_f were nor as fine as they could have been as shown in sections 2.1.1 – 2.1.4. The inaccuracy was not more than 5% however. Because of this the fracture model was considered the best model to be used in further studies.

3 The Effect of Fishbones on Well Performance

The previous chapter presented two different ways of modeling the FBLs on a fine scale and found the fracture model to be most accurate. This chapter will therefore use the fracture model to investigate the effect that Fishbones has on the productivity in a well. Sections 3.1, 3.2 and 3.3 will discuss how the sub spacing and the FBL length affect steady state production. Sections 3.4 and 3.5 discuss how Fishbones affect steady state production in damaged wells and wells in isotropic formations. The effect that Fishbones has in a layered reservoir is discussed in section 3.7.

As chapter 2 showed the fracture model did require quite long run times due to the many small blocks in the model. In a small model like the ones considered in this thesis this will not be a problem, but for large-scale full field or sector models the large run time will become a problem. To mitigate this Fishbones can be up scaled to large large-scale simulations using an r_{wa} instead of the fine scale grid. Sections 3.1 and 3.6 also discuss' how simulations with an r_{wa} compare to simulations with a fine scale grid in different flow regimes.

A reservoir with dimensions 284 m x 20 m x 284 m, 1 mD homogeneous and isotropic permeability and 30% porosity was used in all the simulations, except in section 3.1 where the length in y-direction varied. The reservoir was made larger than in chapter 2 to have a longer region with radial flow outside the needles and also to get a larger pore volume. The well was placed in the y-direction and spanned the entire reservoir length in all the cases. The needles were placed in the middle xz-plane and were 12 m long unless specified otherwise. A n_{GR} = 12 was used to refine the grid around the needles and a C_{GR} = 2.4 was used to refine the grid in the y-direction. The refinement in the outer area of the xz-plane was divided into one 10 m long block and six 20 m long blocks. The center xz-plane had a Δy length of 0.012 m. k_f was 10^8 mD and k_w was 10^5 mD. Steady state conditions were created by multiplying the pore volumes in all the grid blocks in the first and last xy- and xz-plane by 1000. The reservoir pressure was kept at 350 bara and a 310 FBHP was used for all the steady state cases. The pseudo steady state cases were all run with constraints ensuring a reservoir pressure above the bubble point pressure.

3.1 The Effect of Sub Spacing on Steady State Production Rate

To see the effect that spacing between the subs containing the FBLs has on steady state production rate, nine different cases where run. The spacing between the subs was varied between 0 m to 60 m. Because the minimum spacing between the subs is limited by the needle length a 12 m spacing can be considered the smallest possible sub spacing with 12 m long needles. The shorter spacings included thus only have theoretical purposes.

Figure 3.1 shows the relative increase in steady state rate from a well with Fishbones compared to an unstimulated well for varying sub spacing. The points follow an upward curving trend that indicates that the relative increase becomes larger for shorter sub spacing. This indicates that the FBLs affect the entire drainage area to a much larger degree for short spacing compared to larger spacing. It is to be expected that the shorter the sub spacing is the better the productivity of the well is going to be. If one considers the limit where the spacing between the subs is zero the well would essentially have four parallell hydraulic fractures extending 12 m out from the well.

Figure 3.2 and Figure 3.3 show the simulated rate for a well with Fishbones and an unstimulated well with 15 m and 60 m sub spacing. The figures also show the total rate from the well with Fishbones split into the contributions from the FBLs and the well using regions in ECLIPSE. The production rate into the FBLs is much larger for the 15 m spacing than for the 60 m spacing and it is actually larger than the total production into the unstimulated well. For the well with 60 m spacing the production rate directly into the well is much larger than the production rate directly into the FBLs.

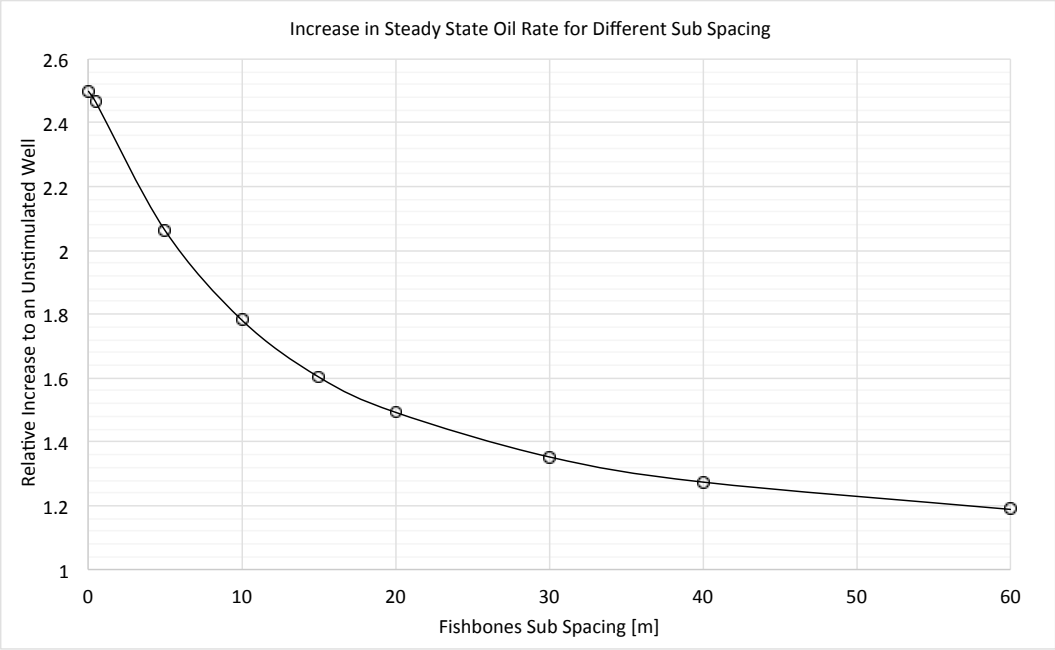

Figure 3.1 – Relative increase in steady state oil rate for different sub spacing.

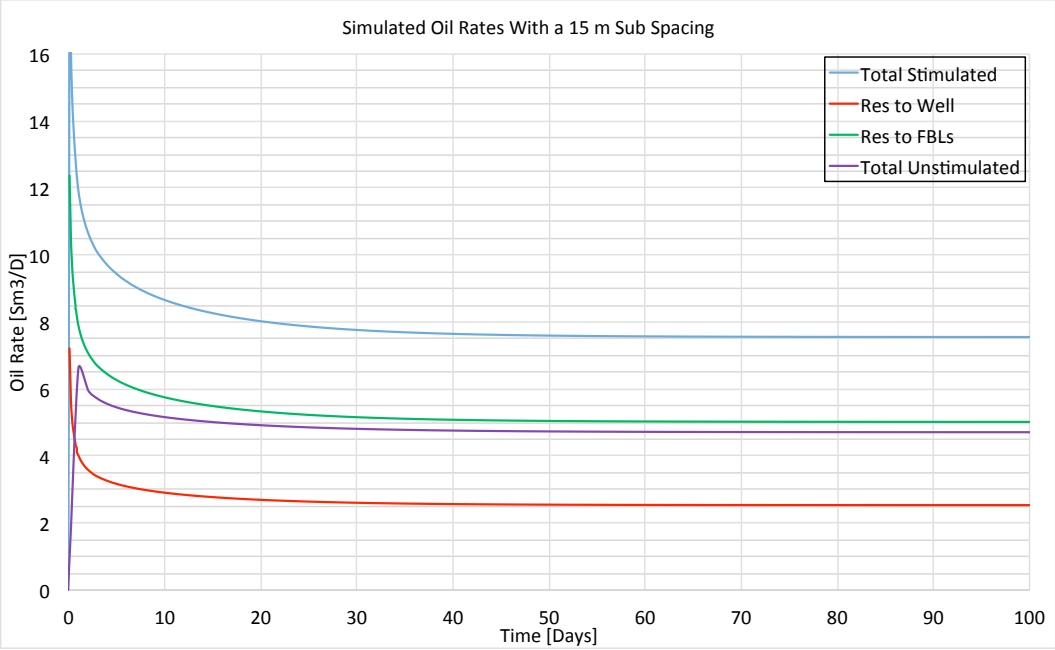

Figure 3.2 – Simulated oil rates for a 15 m sub spacing. In addition the green and red lines show the oil rates corresponding to flow from the reservoir into the FBLs and the reservoir directly into the well.

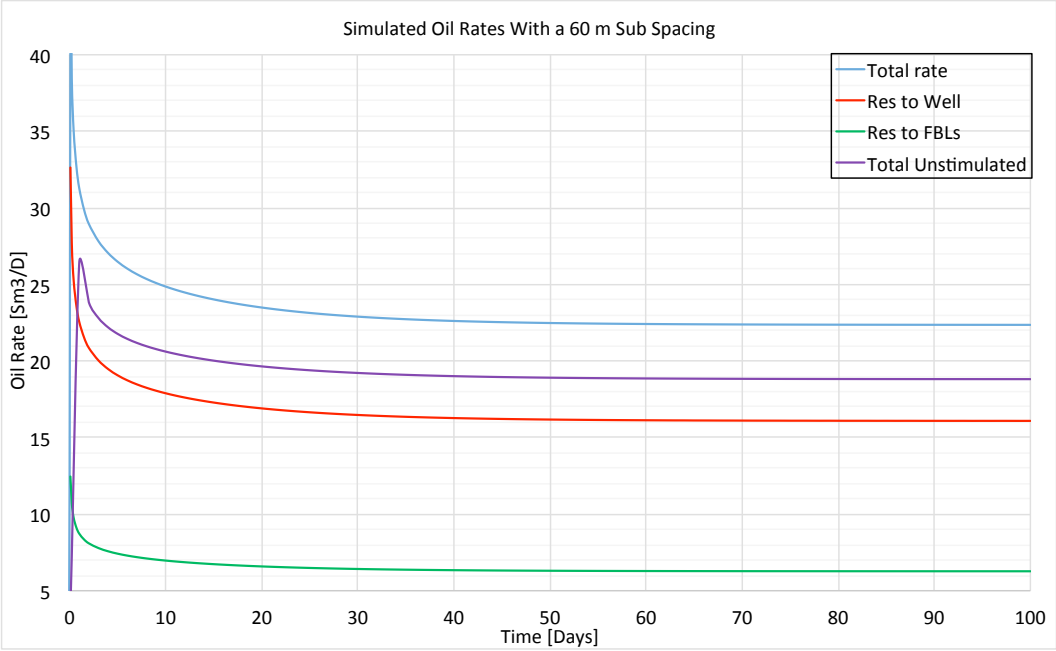

Figure 3.3 – Simulated oil rates for a 60 m sub spacing. In addition the green and red lines show the oil rates corresponding to flow from the reservoir into the FBLs and the reservoir directly into the well.

Figure 3.1 indicates that the closer the subs are spaced the more efficient the stimulation is. This is quite opposite from the results in Figure 1.3, which indicates that a higher FBLs (perforation) density, the less efficient the stimulation becomes. Figure 1.3 is plotted against another parameter however, and this is what is causing the apparent difference. FBLs density is calculated by dividing the number of FBLs per sub on the sub spacing, in this case four divided by the spacing. Figure 3.4 shows the same results as Figure 3.1, but now plotted against FBL density. Some more points are added by interpolation of points with a spacing between 0.5 m and 5 m in Figure 3.1 (the curve fit had an $R^2 = 1$ in excel) to better show the transition of the curve. While Figure 3.4 have a different scale on the x-axis than Figure 1.3, it shows the same trend with a rapidly increasing relative increase in steady state rate for low FBL densities that flattens out for larger needle densities. The reason that Figure 3.1 and Figure 3.4 seem to give opposite impressions of the efficiency of spacing the FBLs closer is because they relate to different things. Figure 3.1 relates to the efficiency of the stimulation, but Figure 3.4 relates to the efficiency of each FBL. Thus spacing the Fishbones subs closer together will increase the efficiency of the stimulation as a whole, but each FBL will become less efficient, i.e. for decreasing spacing each FBL will produce a decreasing rate.

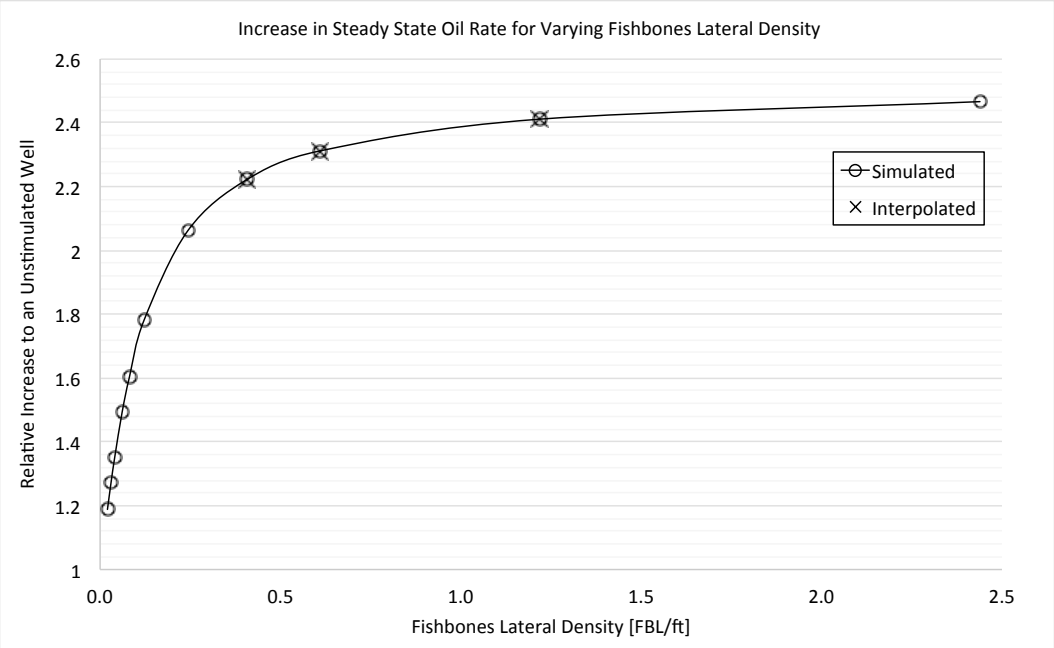

Figure 3.4 – Relative increase in steady state rate for different FBLs density. The relative increase is plotted against needles/ft to be more comparable to Figure 1.3. Points marked with a cross have been interpolated using Figure 3.1 to better show the trend in the area where the curve flattens.

Figure 3.5 and Figure 3.6 show the pressure profiles from the well to the edge of the reservoir in the center and outer xz-plane for the variable sub spacing. The distances to the mid point of the outer xz-plane where the pressure is recorded are 5.5 m, 7.6 m, 11.7 m, 14.2 m and 27.5 m in the y-direction. The pressure profiles in the middle xz-plane are similar for each spacing and show a clear upward deviation for the radial straight line near the well. In the outer xz-plane the pressure profile for the well with 60 m spacing is close to a straight line, while the pressure profile for the well with 15 m have pretty much the same pressure profile as in the center xz-plane.

There is no doubt that Fishbones improves the flow in a well compared to an unstimulated well. How closely spaced the subs can be depends on several factors. The first is the length of the needles as mentioned. However, close spacing will also improve operational risk as there are more laterals to jet. In addition there is cost of the stimulation to be considered. Even though the liners have cost, the major cost connected with oil and gas operations are that of renting the rig. This means that even though more liners make the liner string more expensive, all the laterals can be jetted simultaneously, which should save much time working on the rig.

3.1.1 Apparent Wellbore Radius

Table 3.1 shows calculated skin, calculated apparent wellbore radius (r_{wac}), graphically determined r_{wag} and r_{was} from simulations. The skin was calculated by using Eq. (2) with an

equivalent r_e according to Eq. (6). r_{wac} was calculated using Eq. (7) based on the calculated skin. r_{wag} was found by extrapolating the radial straight line from the pressure profile between the needles down to the 310 bara line. This is illustrated in Figure 3.5. r_{was} was found by matching the steady state rate from an open hole well with a r_{was} to the steady state rate from the Fishbones stimulated well through trial and error. For convenience a conventional open hole well definition was used to determine r_{was}, but section 2.1.3 showed that the two well models were equal.

It is to be expected that there is a difference between r_{wac} and r_{was} as r_{wac} uses an approximated r_{ea} in the calculations. The pressure profile plots have shown the boundary effects from the square reservoir cleary affect the production and the approximated r_{ea} is not able to capture these effects. r_{wac} is however a good initial guess to be input into the simulations to make the trial and error process when determining r_{was} quicker.

The r_{wag} seems to work well for the cases with short sub spacing, but show large deviations from the simulated r_{wa} for the cases with large spacing. This is because the FBLs have a stimulating effect along the entire well for the short spacings, while the long spacings loose parts of the stimulation effect far away from the FBLs. Figure 3.5 and Figure 3.6 clearly show that the effect of the FBLs are felt along the entire length of the well for a 15 m sub spacing, while the pressure profile for a 60 m spacing is almost radial. How the wells with an r_{wa} behave during the transient and decline periods is discussed further in section 3.6.

Skin and Apparent Wellbore Radius for Varying Sub Spacing				
Sub Spacing	**Calculated Skin**	**Calculated r_{wa}**	**Graphical r_{wa}**	**Simulated r_{wa}**
m	**-**	**m**	**m**	**m**
15	-2.8	1.48	1.04	1.12
20	-2.5	1.04	1.00	0.79
30	-2.0	0.62	0.90	0.48
40	-1.6	0.44	0.80	0.38
60	-1.2	0.29	0.70	0.25

Table 3.1 – Skin and apparent wellbore radius for varying sub spacing. Actual r_w is 0.0825 m.

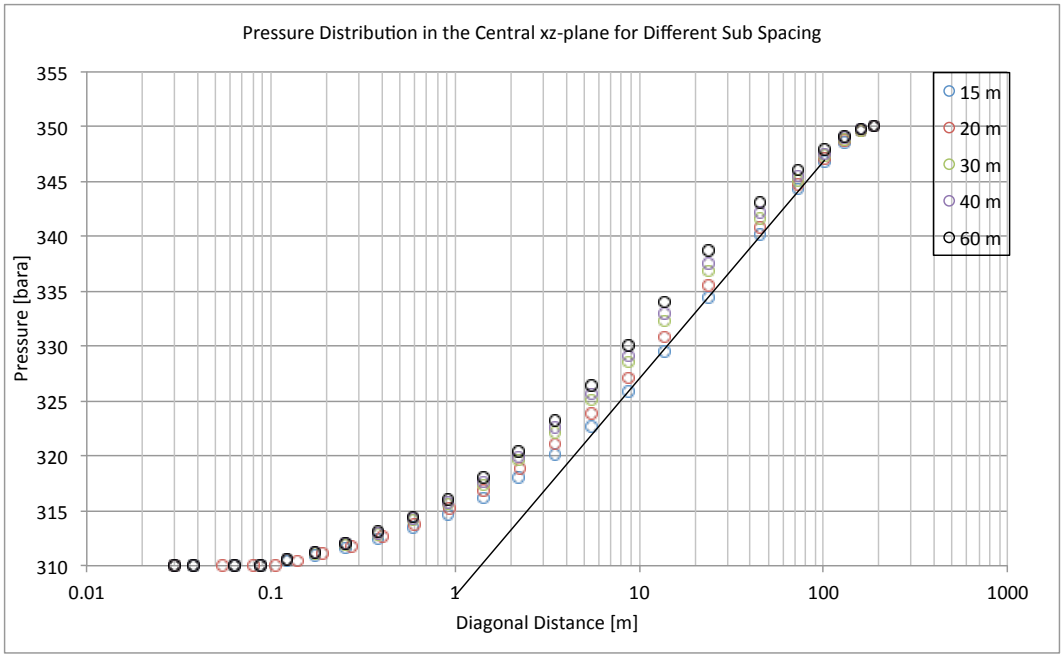

Figure 3.5 – Pressure profiles different sub spacing in the central xz-plane. A hydrostatic correction has been made. The pressure in the center block is not included. The distance is measured from the center of the well. The straight line shows the extrapolation method used to determine the graphical r_{wa}.

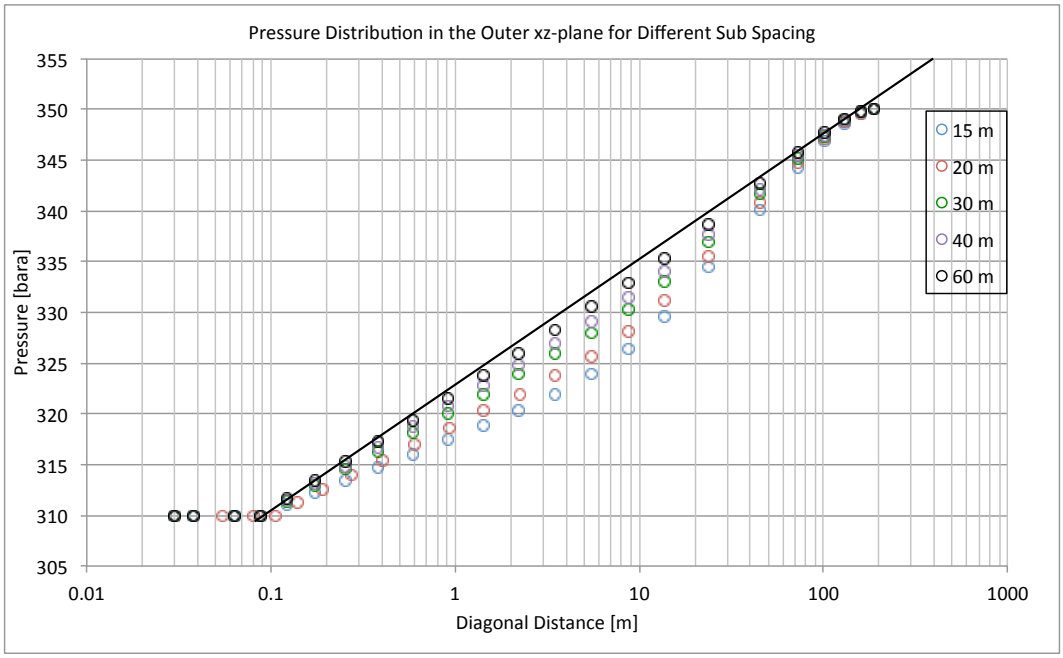

Figure 3.6 – Pressure profiles different sub spacing in the outer xz-plane. A hydrostatic correction has been made. The pressure in the center block is not included. The distance is measured from the center of the well. The straight line shows the extrapolation method used to determine the graphical r_{wa}.

Even though the simulated flow rate may be matched using an apparent wellbore radius there may still be a big difference in the pressure profile along the well. This could have a large impact on the multi phase behavior of a well as different pressure profiles can cause water or gas breakthrough at different times for different parts of the well.

Figure 3.7 and Figure 3.8 compare the pressure profiles from the well to the reservoir edge for a well with Fishbones and a well with r_{was} for a 20 m and 60 m sub spacing. Both spacings show that Fishbones affects the pressure profile in the near wellbore area quite differently than the radial flow that is resulting from the case with r_{was}. Far away from the needles the flow is radial for both cases and the profiles are quite similar. There is a slight difference between the profile recorded in the needle plane and the profile recorded in the outer plane for the case with 20 m spacing, but it is minor. The difference is larger for the case with 60 m spacing however, but significant deviations between the different points happens close to the well and this is not likely to have a great effect on the simulations.

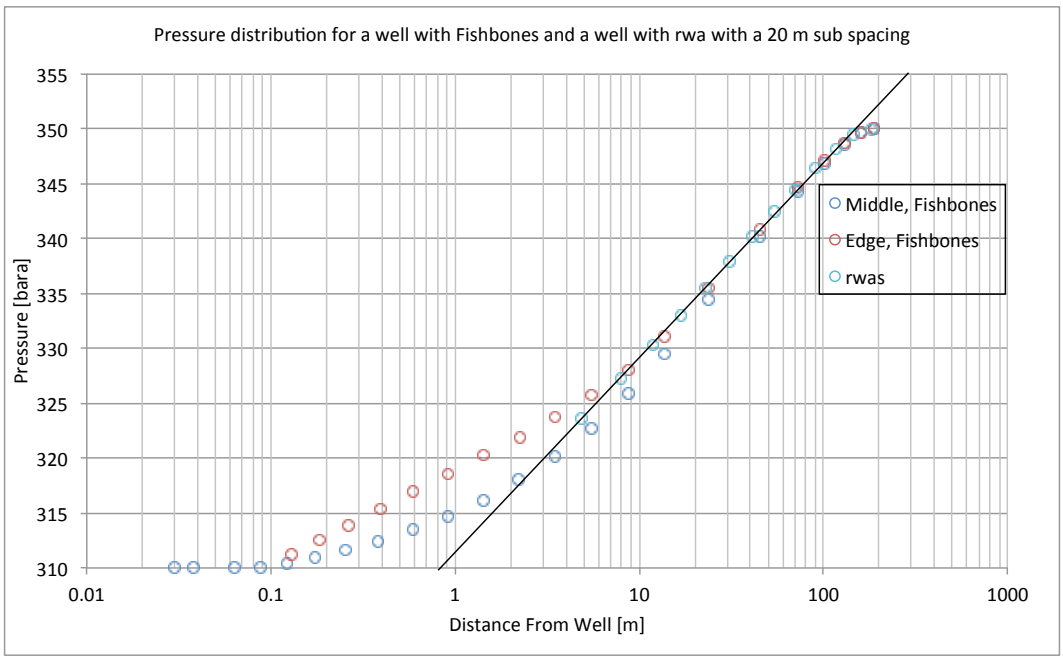

Figure 3.7 – Pressure profiless for a well with Fishbones and a well with r_{wa} with a 20 m sub spacing. A hydrostatic correction has been made. The pressure in the center block is not included. The distance is measured from the center of the well.

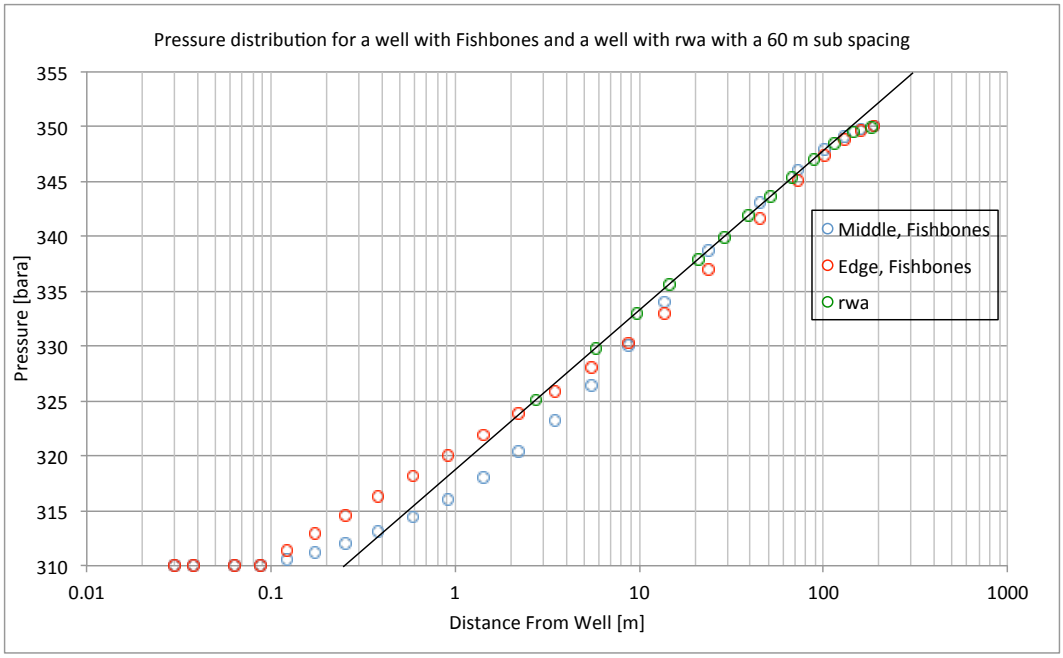

Figure 3.8 – Pressure profiles for a well with Fishbones and a well with r_{wa} with a 60 m sub spacing. A hydrostatic correction has been made. The pressure in the center block is not included. The distance is measured from the center of the well.

3.2 The Effect of Fishbones Lateral Length

Figure 1.4 shows that there may be an upper limit for the FBL length upon which further increasing the length will not increase productivity much. The perforation density in Figure 1.4 is much greater than the FBL density in a well with Fishbones however. To see how the FBL length affected the steady state production rate in a well five cases with varying FBL length were run. The length varied between 2.1 m, 3.2 m 4,9 m 7.67 m, 12 m and 22 m. A 22 m needle length is physically impossible with 20 m needle spacing, but is included for theoretical purposes. The reason for the awkward lengths was because of the logarithmic gridding.

Figure 3.9 shows the relative increase in steady state production rate compared to an unstimulated well for the different FBL lengths. The relative increase follow a slightly upward curving trend for small FBL lengths and transform into a more linearly increasing trend for longer lengths. The curve between the 12 m and 22 m point is actually slightly downward curving. This is according to Figure 1.4 that shows that increasing perforation density has reduced effect for large perforation densities. However, the spacing between the FBL in the case considered is 0.2 FBL per meter (0.06 needles per feet), which is much lower than the cases shown in Figure 1.4 where the lowest density is 3.3 per meter (one needle per feet). Figure 1.4 also shows that decreasing the perforation density results in a larger downward curvature so it is to be expected that the Fishbones case show very little downward curvature.

By using numerical differentiation on the data points it was found that the second derivative of the relative increase with respect to needle length change from being positive to being negative somewhere in between a 12 m and 22 m needle length. This means that the curve for relative increase as a function of needle length shifts from an upward curving to a downward curving trend for somewhere between 12 m and 22 m long needles. The upward curving trend is not seen in any of the lines in Figure 1.4, but this may be because very low perforation densities were not investigated.

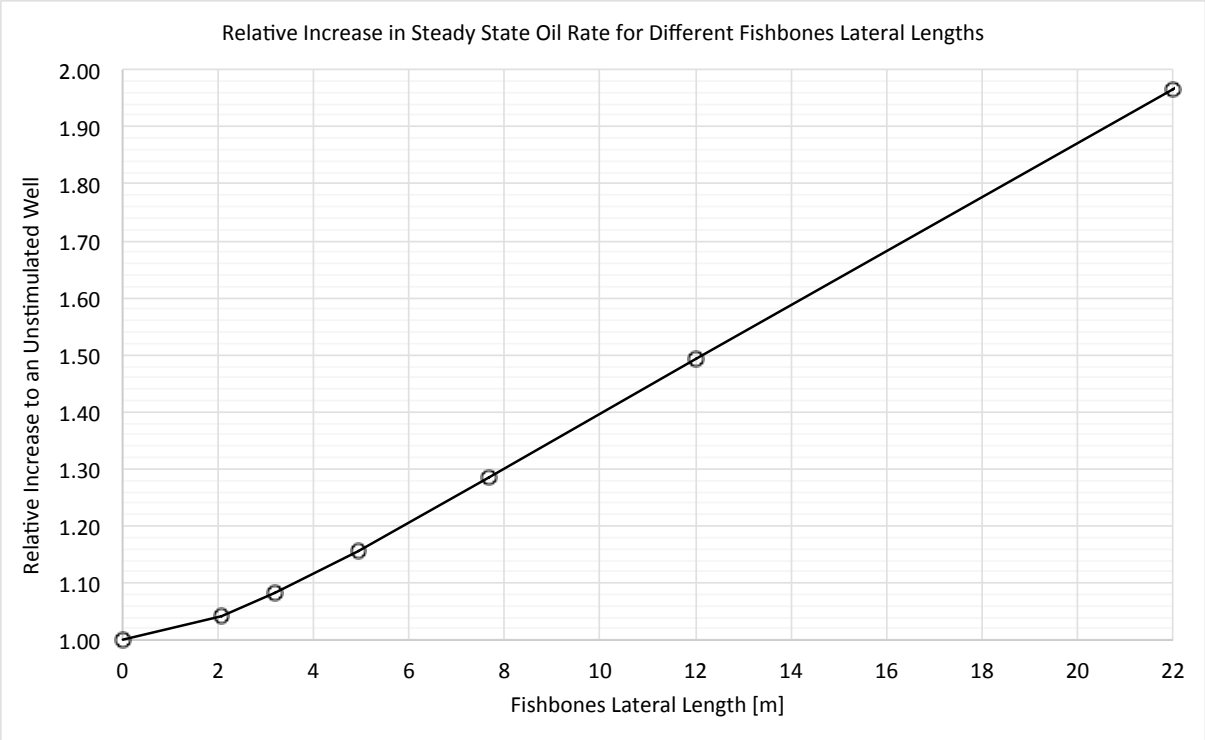

Figure 3.9 – Relative increase in steady state oil rate compared to an unstimulated well for different FBLs lengths.

3.3 The Effect of Variable Spacing and Fishbones Lateral Lengths

As section 3.1 showed decreasing sub spacing increased the steady state production rate. However, the FBLs themselves are a limit to how closely the subs can be spaced. This is because the spacing between the subs must be larger than the length of the FBLs so there is room to store the FBLs within the liner when the liner is run. In order to get a closer spacing the FBL length would have to be reduced, but section 3.2 showed that reducing FBL length also reduced the steady state production rate. In order to see which of the effects that dominated the change in steady state rate five cases were run with different sub spacing and FBL lengths.

Figure 3.10 shows the relative increase in steady state production rate compared to an unstimulated well for the five cases with different sub spacing and FBL lengths. It is clearly more effective to use large sub spacing and long FBLs compared to a short spacing and short needles.

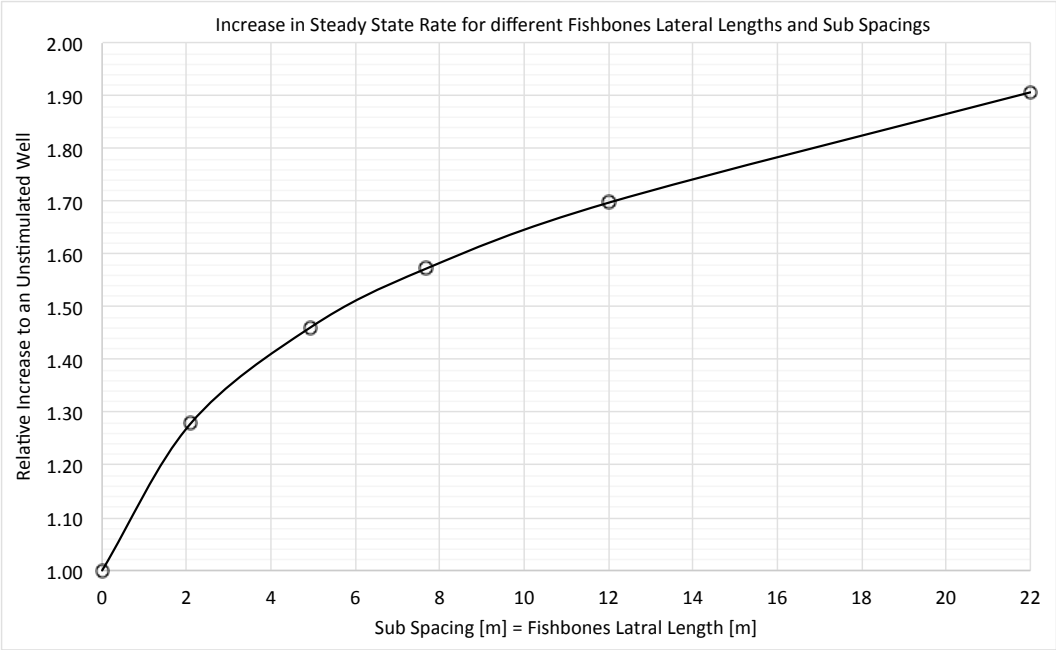

Figure 3.10 – The relative increase in simulated steady state oil rate for different FBLs lengths and spacing compared to an unstimulated well.

A couple of things need to be taken into consideration regarding Figure 3.10 however. First of all it is assumed that it is possible to use a sub spacing that equals the FBL length. This is probably not the case in reality. Pictures of the subs (Rice et al., 2014) seem to indicate that the spacing will be roughly 0.5 m – 1 m longer than the FBLs. Even though it is possible to have a well that is almost twice as productive as an unstimulated well by using even larger

spacing and longer FBLs this will probably increase the risk of an unsuccessful operation. The larger the FBLs get the harder it will be to jet them to full extension and avoid bending in the process. Failing to jet the needles could have a big negative impact on productivity as the last sections showed that large spacing and short needles give a small productivity using Fishbones. Figure 3.1 Figure 3.10 also shows that increasing spacing and FBL length reduced increase (downward curving trend) per meter of increased spacing and FBL length. Shorter spacing and FBL may also increase operational complexity as more FBLs needs to be jetted in the same interval.

3.4 The Effect of Fishbones in Wells with Damage in the Near Well Region

Horizontal wells are often damaged by mud invasiong during the drilling of the well because they are exposed to very long mud circulation times due to long reservoir sections. This could lead to a serious damage in the near well area due to mud infiltration. Because the Fishbones FBLs penetrate deep into the formation relative to the diameter of a well with Fishbones they may therefore penetrate the damaged zone and reduce or remove the effect of the damage.

In order to see how Fishbones affects a well with damage in the near well area two different cases with a 1.15 m and 4.76 m damaged zone were run. The permeability in the damaged zone, k_s, was varied between 0.1 mD, 0.01 mD and 0.001 mD. This approximately equaled a skin factor equal to 24 for the best case and 4113 for the worst case according to Eq. (4). A skin factor equal to 24 indicates a significantly damaged well and a skin factor equal to 4113 and unproducible well. The reason for the awkward depths of the damaged zone is because of the grid around the well resulting from the logarithmic grid refinement.

Figure 3.11 and Figure 3.12 show the simulated oil rates for the different damages around a well with Fishbones compared to an unstimulated well. The production from the unstimulated well is heavily impacted by the damage for both depths of the damaged zone and the wells are not likely to be economical. When the well has Fishbones however, it is much less affected by the damage. For a 1.15 m damage depth the needles actually still improve the rate compared to an unstimulated and undamaged well. The production rate is approximately the same in a well with a 4.76 m deep damaged zone and Fishbones, as for an unstimulated, undamaged well.

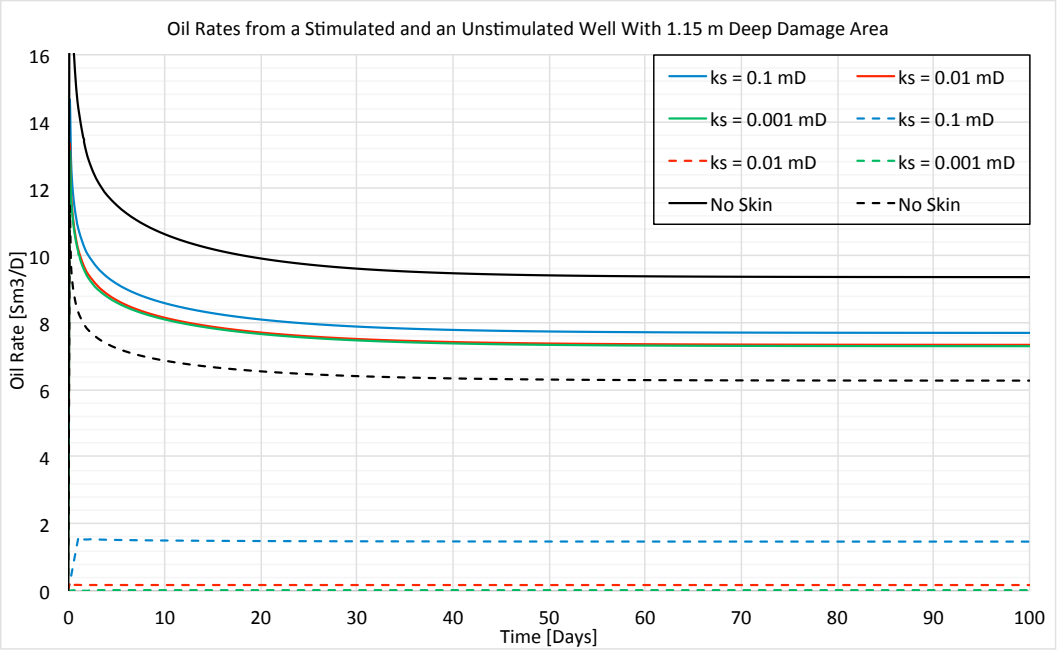

Figure 3.11 – Simulated oil rates for a well stimulated with Fishbones (continuous line) and an unstimulated well (dashed line). Both wells have an area with reduced permeability extending 1.15 m into the formation. The simulated rates without the reduced permeability area is also shown.

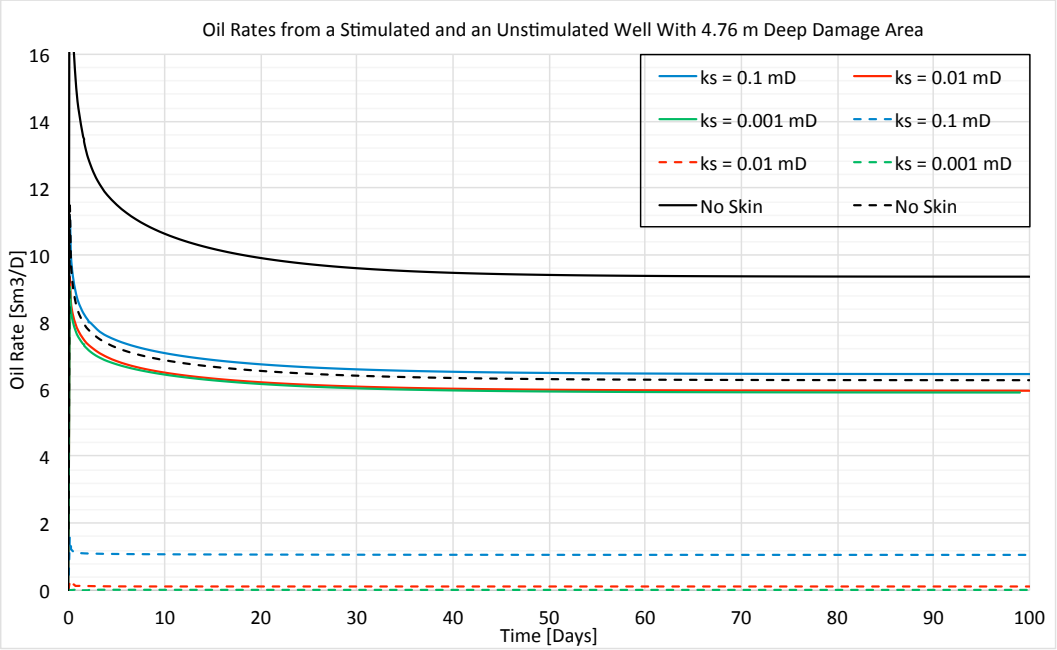

Figure 3.12 – Simulated oil rates for a well stimulated with Fishbones (continuous line) and an unstimulated well (dashed line). Both wells have an area with reduced permeability extending 4.76 m into the formation. The simulated rates without the reduced permeability area are also shown.

Figure 3.13 and Figure 3.14 show the production rates for the least damaged and the most damaged well with and without Fishbones. In addition the total rate for the well with Fishbones is split into contribution from the FBLs and well. The well is contributing slightly in the least damaged case, but the majority of the production goes through the FBLs. For the

worst damaged case the well is not contributing at all and all production is coming from the FBLs.

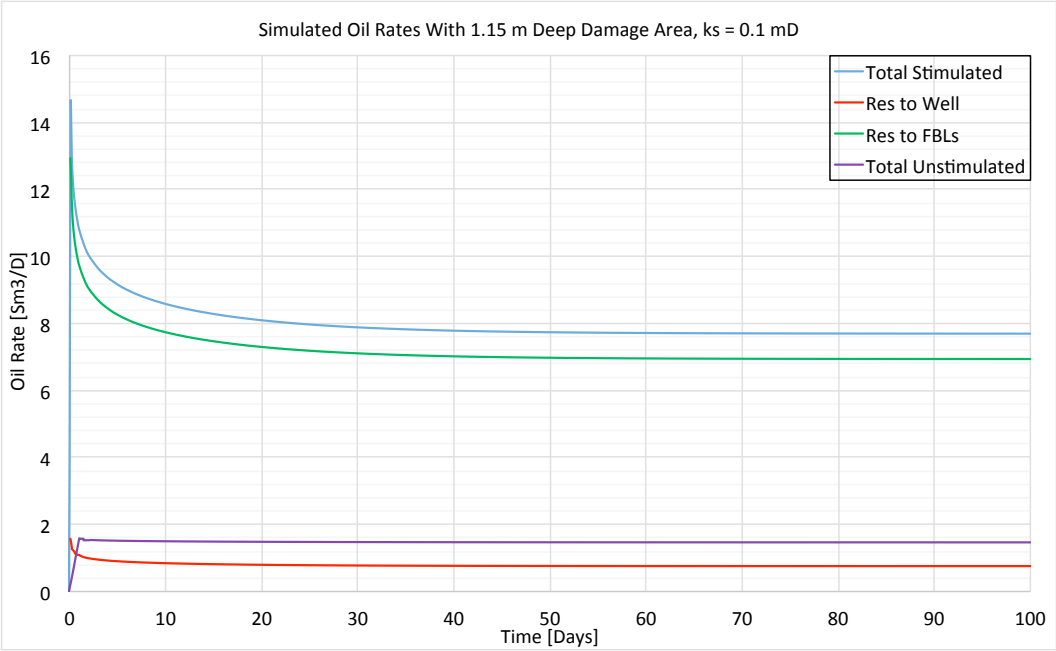

Figure 3.13 – Total oil rate for a well with Fishbones compared to an unstimulated well for a well with a 1.15 m deep damaged zone with k_s = 0.1 mD. In addition the green and red lines show the oil rates corresponding to flow from the reservoir into the needles and the reservoir directly into the well.

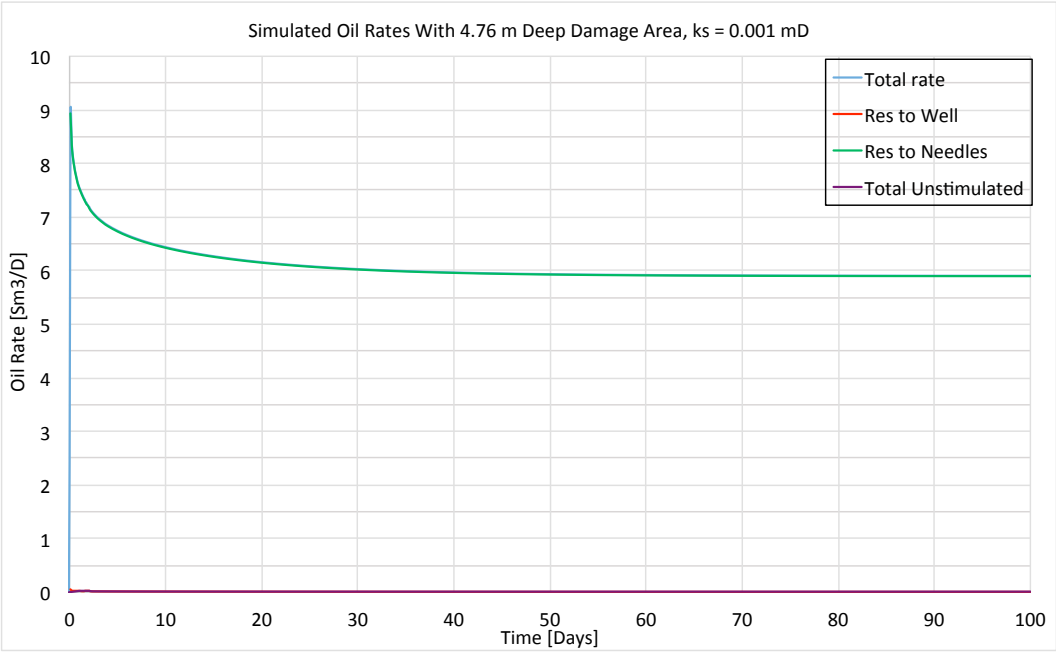

Figure 3.14 – Total oil rate for a well with Fishbones compared to an unstimulated well for a well with a 4.76 m deep damaged zone with k_s = 0.001 mD. In addition the green and red lines show the oil rates corresponding to flow from the reservoir into the needles and the reservoir directly into the well.

Figure 3.11 to Figure 3.14 show that Fishbones may remove the effect of damage in the near wellbore region and in some cases also increase production a little compared to an

unstimulated and undamaged well. Only one sub spacing has been considered in this section though. Section 3.1 showed that the FBLs were able to have a good stimulating effect along the entire drainage area for a 20 m spacing. This explains why the FBLs are able to significantly improve the flow, even for unrealistic damages that completely stop flow into an unstimulated well. Section 3.1 did however show that the FBLs had a much smaller stimulating effect when the spacing was increased to 60 m and the majority of the fluid was produced directly into the well. There is thus reason to believe that a well with the same damage as the cases above, but with a 60 m spacing, will not be more affected by the damage.

3.5 The Effect of Fishbones in Formations with varying k_v/k_h

A challenge with horizontal wells is that they are heavily affected by horizontal layers within the reservoir with low or zero permeability. This is because it is unable to the layers, like a vertical well can, and vertical communication through the reservoir may therefore be poor. A normal method of modeling layered reservoirs is to use a k_v/k_h below one. The FBLs should improve productivity in reservoirs with low k_v/k_h because they will allow a larger portion of the fluids to produce horizontally into the extending FBLs instead of vertically into the well. In order to see how Fishbones affects the production in an anisotropic reservoir three cases three cases were run. The k_v/k_h was varied between 0.1, 0.01 and 0.001.

Figure 3.15 shows the production rates from a well with Fishbones compared to an unstimulated well for the different cases. Both the well with Fishbones and the unstimulated well are heavily affected by the anisotropy. The reduction in rate due to the anisotropy is 55%, 72% and 77% for the well with Fishbones and 66%, 89% and 95% for the unstimulated well. Even for the case with lowest anisotropy the production rate from the well with Fishbones is lower than the production rate from an unstimulated well in an isotropic reservoir.

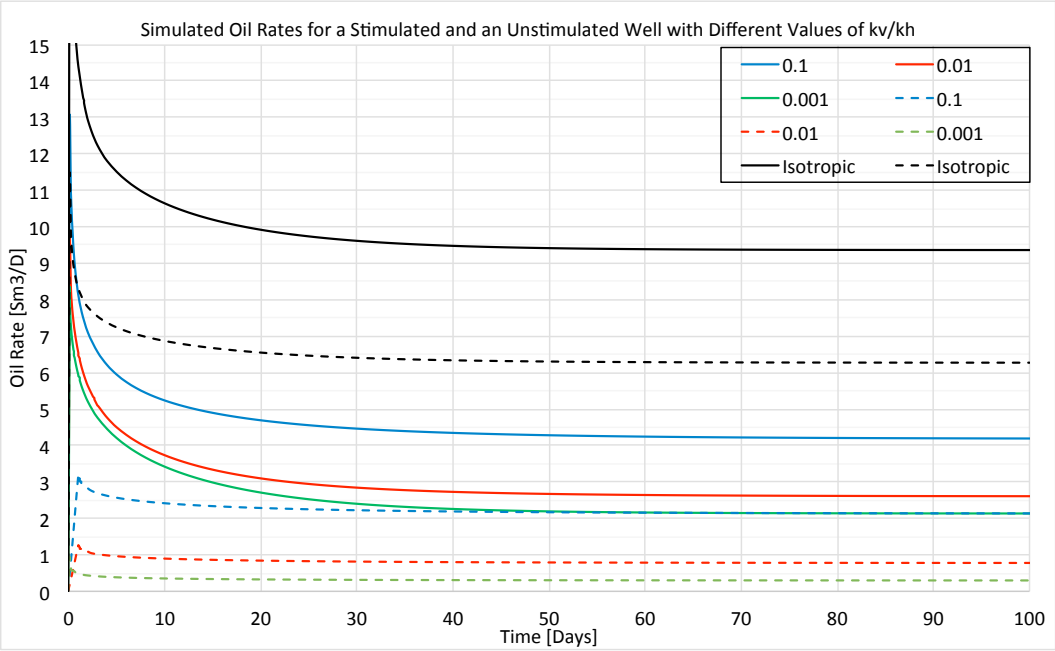

Figure 3.15 – Simulated oil rates for a well stimulated with Fishbones (continuous line) and an Unstimulated well (dashed line) for different k_v/k_h. The simulated oil rates in an isotropic reservoir from a well with Fishbones and an unstimulated well are also included.

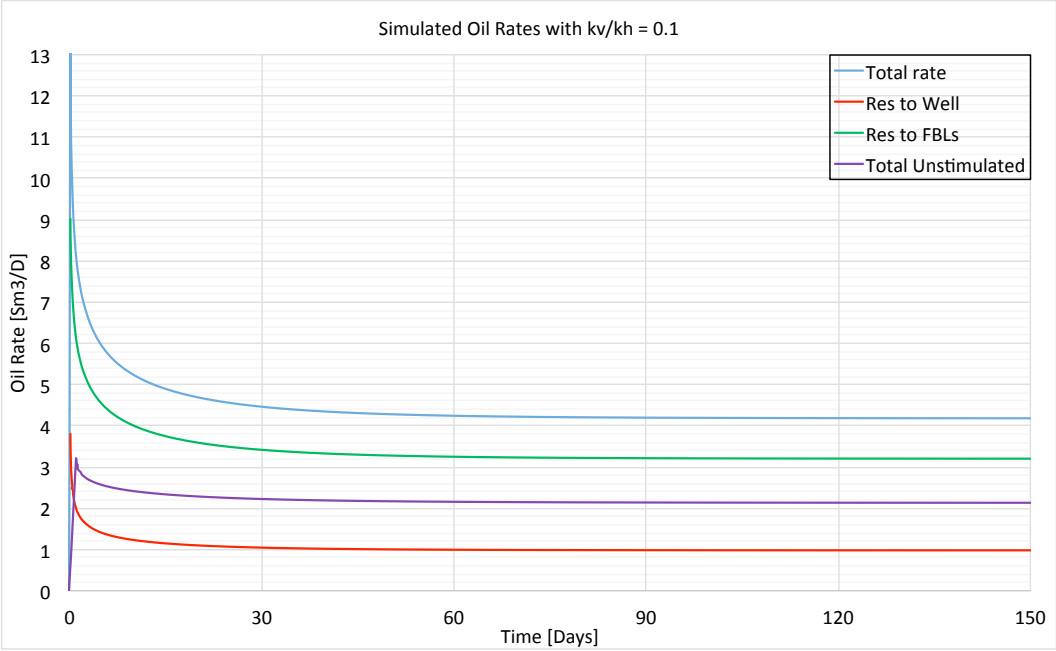

Figure 3.16 – Simulated oil rates for a well with Fishbones compared to an unstimulated well in an anisotropic formation with k_v/k_h = 0.1. In addition the green and red lines show the oil rates corresponding to flow from the reservoir into the FBLs and the reservoir directly into the well.

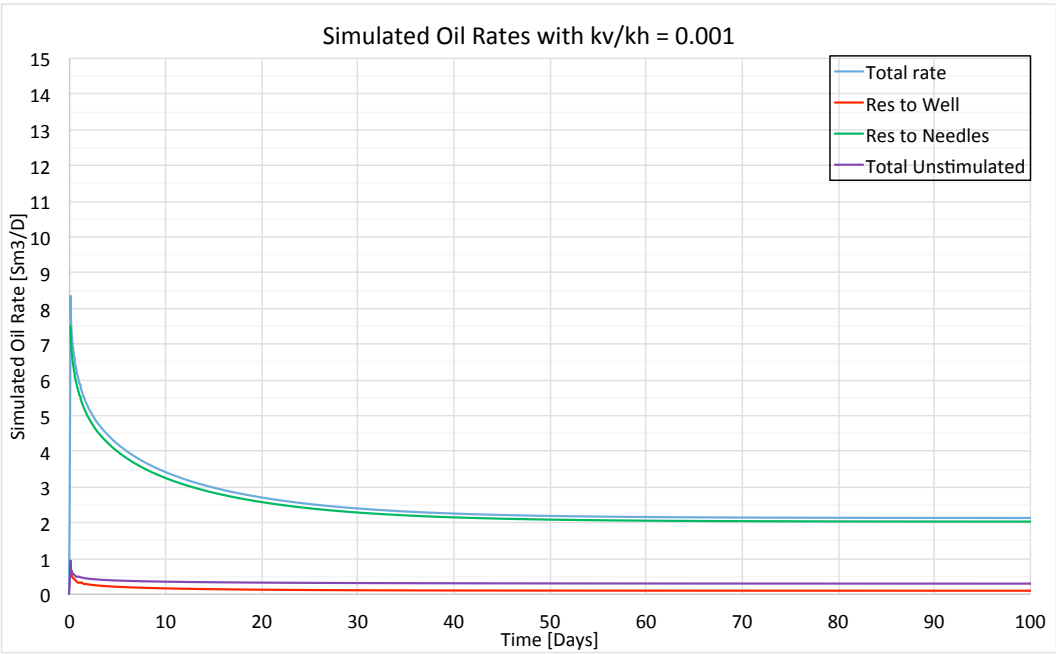

Figure 3.17 – Total oil rate for a well with Fishbones compared to an unstimulated well for a well in an anisotropic formation with k_v/k_h = 0.001. In addition the green and red lines show the oil rates corresponding to flow from the reservoir into the FBLs and the reservoir directly into the well.

Figure 3.16 and Figure 3.17 show the total production rate from a well with Fishbones and an unstimulated well for k_v/k_h = 0.1 and k_v/k_h = 0.001. The contribution from the FBLs and the well in the well with Fishbones is also shown. Both the well and FBLs contribute to the production when k_v/k_h = 0.1, but the production rate into the FBLs is more than 300% higher than into the well. The production rate into the FBLs alone is roughly 45% higher than into an

unstimulated well. When k_v/k_h = 0.001 the production into the well is no longer significant and all the production is due to the needles.

Modeling an anisotropic formation with a k_v/k_h less than one does not accurately represent the actual flow within the reservoir. It is a technique that is used to upscale anisotropy in reservoir simulator when the low permeability layers are so thin that they cannot be modeled on the scale used in the reservoir model. When using a k_v/k_h less than one, the flow velocity in the vertical direction will be small throughout the entire reservoir height. For a layered reservoir with interchanging high and low permeability layers the flow velocity in the vertical direction can be high throughout the height of the high permeability layers and low through the low permeability layers. This difference is not a problem for a vertical well that penetrates all the layers, as the flow will be purely horizontal and the effect of the anisotropy is not felt[8]. For a horizontal well or a partially penetrating FBL this will be a big problem however. When a FBL only partially penetrates one of the high permeability layers, the case with reduced k_v/k_h will then limit the vertical flow into the FBL despite it being in a high permeability layer. The layered reservoir case will be able to properly model the flow within the high permeability layer, while also maintaining barriers between the layers. Layers within 12 m of the well should therefore be modeled with detail when FBLs are modeled on a fine scale. A well with an impermeable layer close to the well with Fishbones is simulated in section 3.7.

[8] If one neglects the effects of uneven depletion of layers that can result to cross flow.

3.6 Upscaling using an r_{wa} in non Steady State Conditions

The r_{was} determined in section 3.1 was based on a steady state flow regime. Most reservoirs do not produce under steady state, but are experiencing either a PSS period, a decline period or they may still be in the infinite acting flow IAF period depending on permeability. In order to see how the determined r_{was} from section 3.1 behaves in different flow regimes four cases were run. Two cases were run with a constant FBHP and two cases were run with a constant flow rate. The cases were run both with the detailed Fishbones grid and with an r_{was}, which was found to be 0.79 m for a 20 m sub spacing.

For the two well controls both the IAF period and the decline or PSS periods were investigated. The IAF period was investigated by running the cases with a 0.001 days time step to a total time of two days. The decline/PSS[9] period was investigated by running the model for 1500 days. The well controlled on FBHP had a 310 bara FBHP and the well controlled on constant flow rate had a 1 Sm3/D rate. The reason for the very low flow rate was because the model required very small time steps to ensure convergence for larger flow rates.

Figure 3.18 to Figure 3.19 show the simulated production rate and cumulative production during the IAF and decline period for the wells controlled on FBHP. There is a small deviance for the very early IAF period where well with r_{wa} simulates a slightly higher rate. This difference disappears quickly however and after approximately 0.1 days and onwards the two simulations are equal. The decline period shows that the well with r_{wa} has a slightly higher simulated rate during the middle time, but the difference is minor. The r_{wa} determined from the steady state simulations is sufficient to model a well controlled on constant FBHP for all flow regimes

[9] Depending on well control

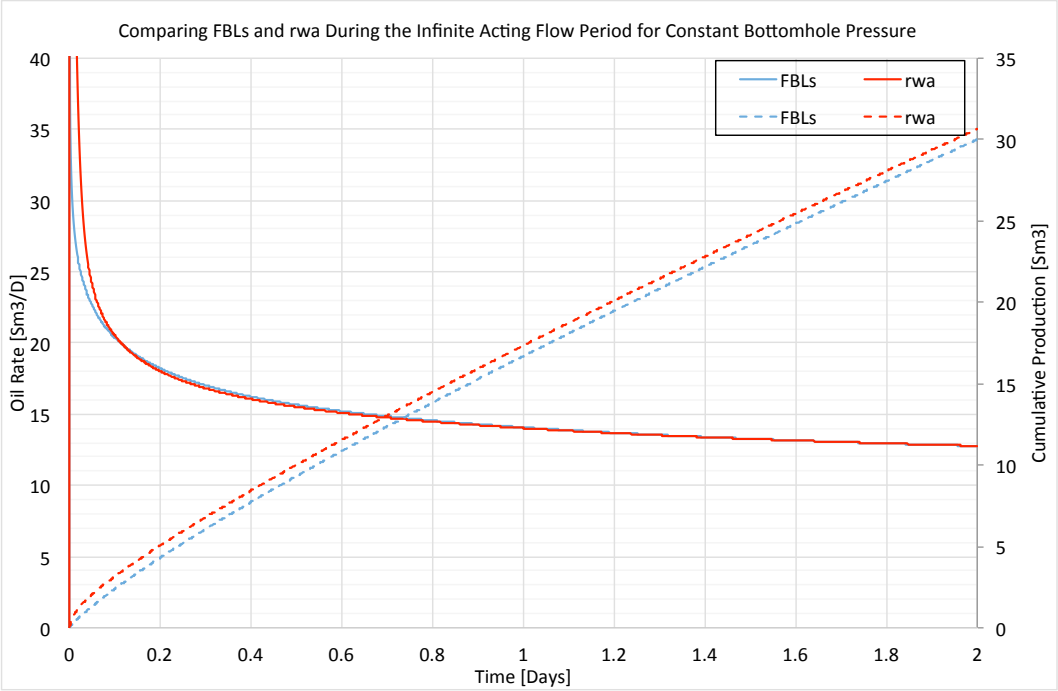

Figure 3.18 – Simulated production rate (countinous line) and cumulative production (dashed line) for a well with Fishbones compared to a well with an r_{wa}. The well is producing under an IAF regime with a constant FBHP.

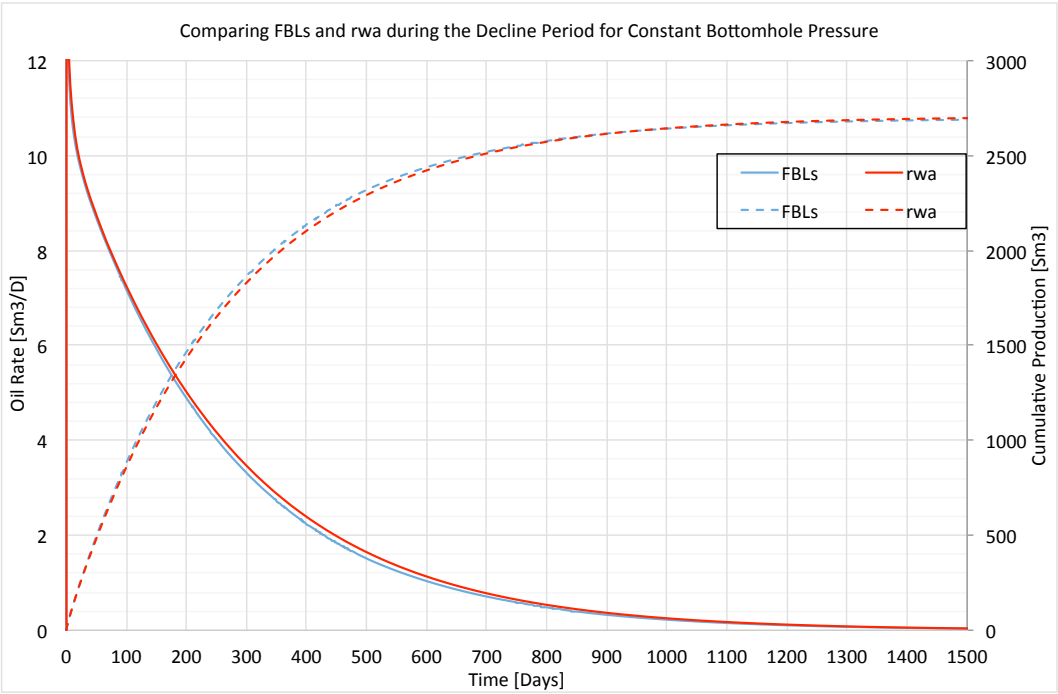

Figure 3.19 – Simulated production rate (countinous line) and cumulative production (dashed line) for a well with Fishbones compared to a well with an r_{wa}. The well is declining with a constant FBHP.

Figure 3.20 and Figure 3.21 show the simulated FBHP during the IAF and PSS periods for the wells controlled on a constant production rate. The well with and r_{wa} has a higher FBHP than the well with Fishbones during the first day of IAF. This is similar to the case controlled on

constant FBHP, but it takes longer time until the two solutions become equal. The two simulated FBHPs are equal for the entire PSS period. The r_{wa} determined from the steady state simulations is sufficient to model a well controlled on constant production rate for all flow regimes.

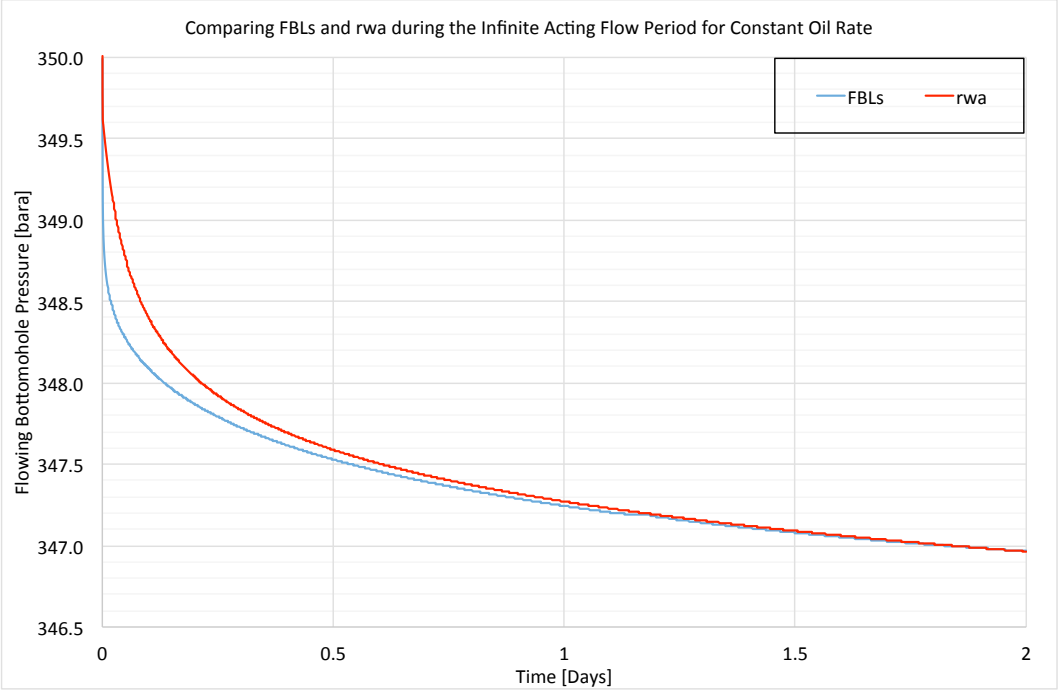

Figure 3.20 – Simulated FBHP for a well with Fishbones needles compared to a well with a r_{was} determined in section 3.1. The well is producing under an IAF regime with a constant flow rate well control.

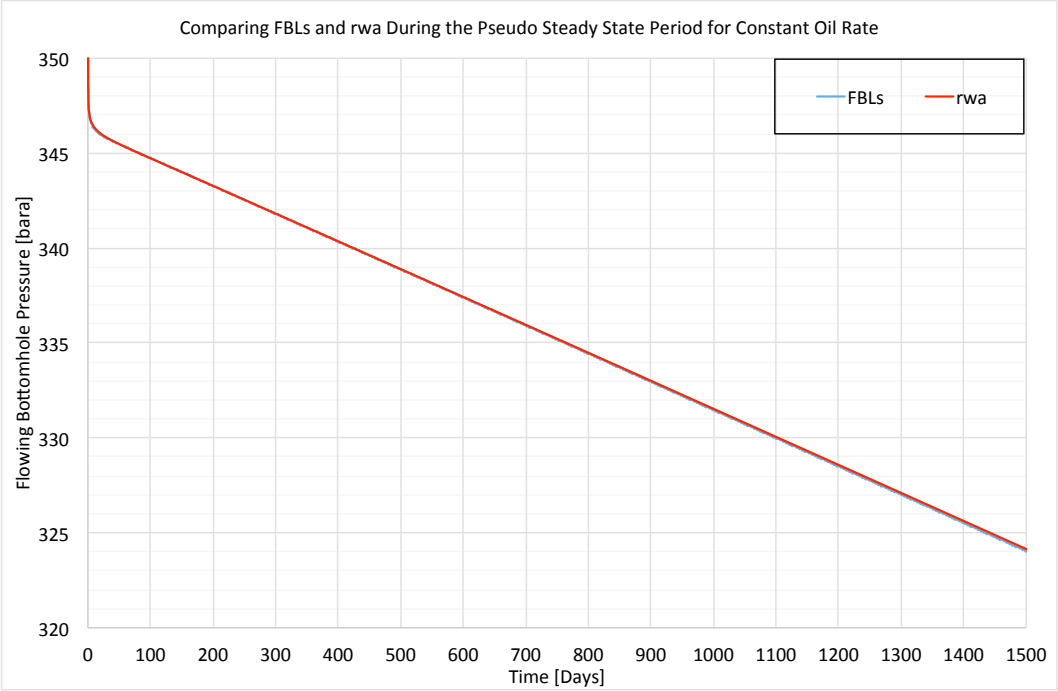

Figure 3.21 – Simulated FBHP for a well with Fishbones compared to a well with a r_{was} determined in section 3.1. The well is producing under pseudo steady state conditions with a constant rate well control.

3.7 The Effect of Fishbones in a Layered Reservoir

One of the major benefits with Fishbones is to improve vertical communication in a layered reservoir. This is done by penetrating impermeable layers close to the well and produce overlying or underlying layers through the FBLs. In order to see the effect of Fishbones in a layered reservoir, two cases with a layered reservoir were run. A 7 cm thick, impermeable layer was placed above or below the well in the two cases. The layers were placed close enough to be penetrated by the FBLs and they reduced the hydrocarbon pore volume (HCPV) in communication with an unstimulated well to approximately half the original volume. The well was run on a constant 310 bara FBHP, but without pore volume modification so after a quick transient period the well started to decline.

Figure 3.22 and Figure 3.23 show the production rates from a stimulated and an unstimulated well with the impearmeable layer above and below the well. The wells with Fishbones clearly have a higher production rate during the lifetime compared to the unstimulated wells and production into the FBLs is dominating. This is to be expected as one FBL penetrating the impermeable layer drains approximately half the HCPV.

Figure 3.24 shows the cumulative production for a well with Fishbones compared to an unstimulated well. It clearly shows that the well with Fishbones communicates with a reservoir that is roughly twice the size of that for an unstimulated well. As Figure 3.24 shows weather the impermeable layer is placed above or below the well does not matter in terms of recovery. Figure 3.23 does however show that the case with the impermeable layer below the well have signs of fluctuations in the simulations, which are not seen in Figure 2.22. The case with the impermeable layer below the well also required significantly shorter, and thus more, time steps to run the simulations. This indicates that gravity may have an affect on the simulations, but this is not seen on the production.

Figure 3.25 compares the production rate and cumulative production from a well with Fishbones in a reservoir with and without layers. It shows that the FBLs enable the well above or below an impermeable layer to produce the same cumulative production as a well in an isotropic formation. The only difference between the two cases is the time it takes to produce the fluid. As expected the well in the isotropic formation is able to produce a higher flow rate in the beginning than the well in the layered reservoir. This is naturally because the well and other FBLs are able to aid the drainage of the entire reservoir, while a single FBL in the anisotropic case drains half the HCPV alone.

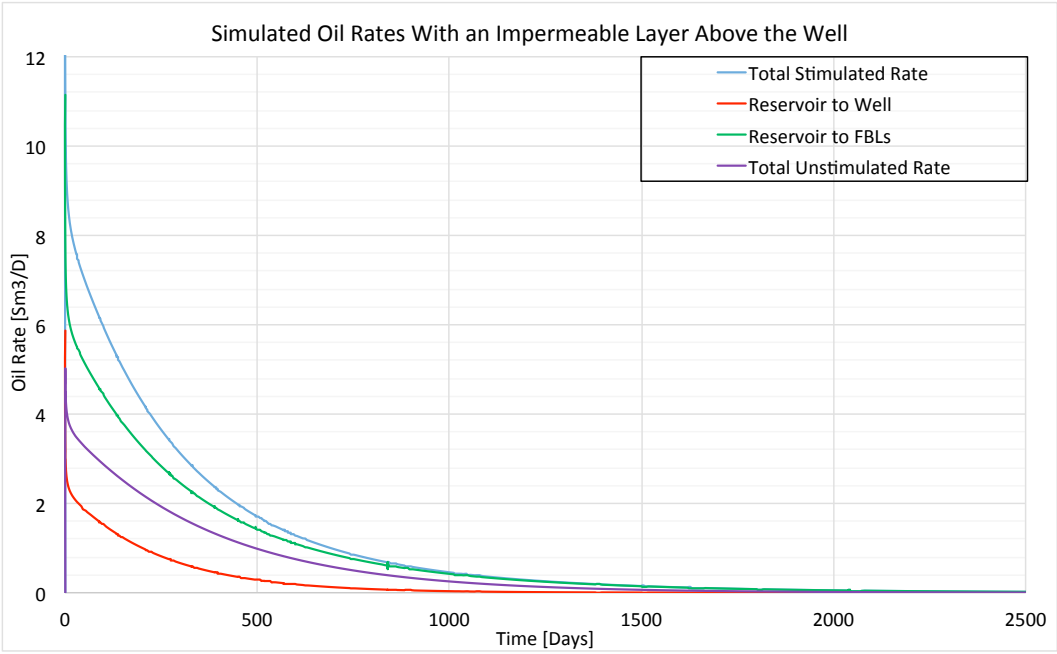

Figure 3.22 – Simulated oil rates with an impermeable layer above the well for a well with and without Fishbones. Flow rate from the reservoir into the well and from the reservoir into the FBLs are included for the well with FBLs.

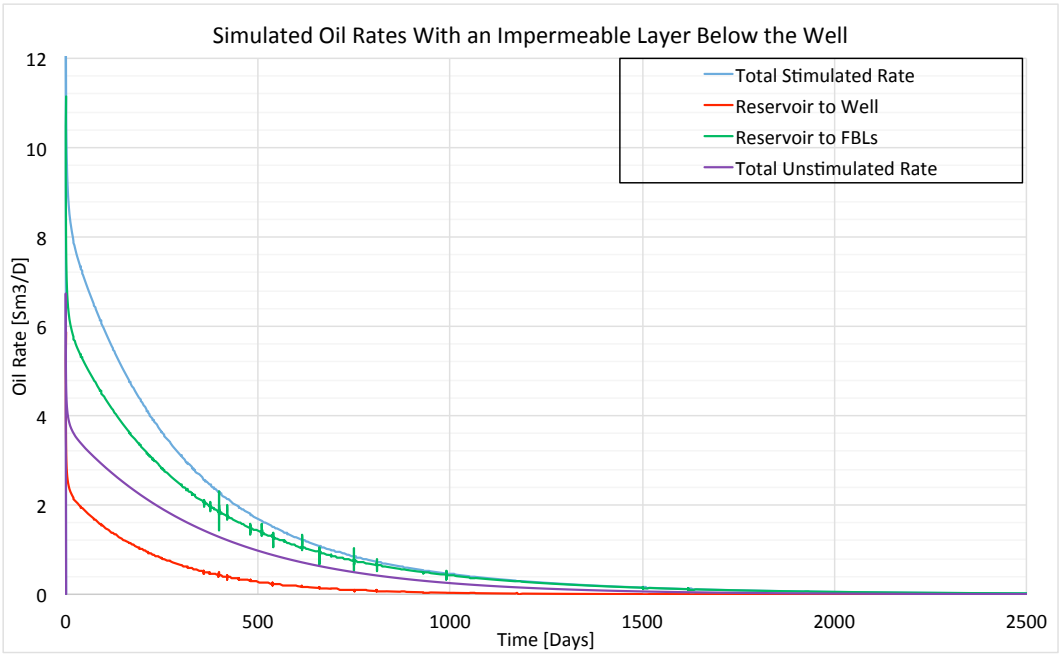

Figure 3.23 – Simulated oil rates with an impermeable layer below the well for a well with and without Fishbones. Flow rate from the reservoir into the well and from the reservoir into the FBL are included for the well with FBLs.

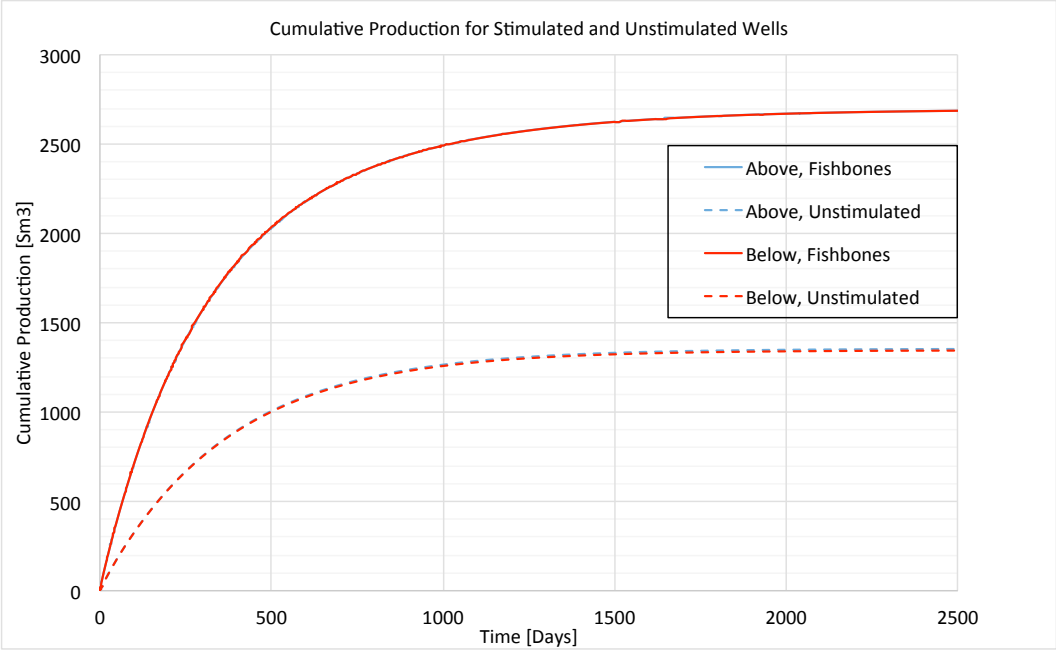

Figure 3.24 – Simulated cumulative Production for a well with Fishbones (continuous line) and an unstimulated well (dashed line). Both the case with an impermeable layer above the well and the case with an impermeable layer below the well are shown.

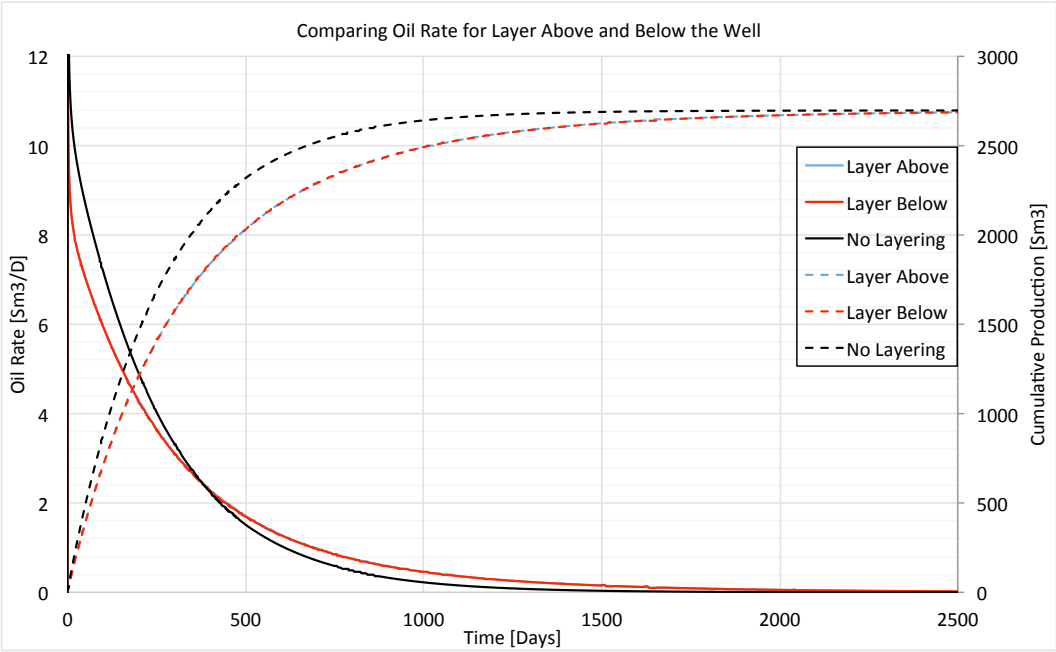

Figure 3.25 – Simulated oil rate rate (continuous line) and cumulative production (dashed line) for a well with Fishbones and an impearmeable layer either above or below the well. The decline rate and cumulative production for a reservoir without any layering is also included.

It is clear that Fishbones will have a big advantage over an unstimulated well in layered formations with poor vertical communication as it is able to greatly improve the communication within the reservoir. This agrees well with the results of (Freyer and Shaoul, 2011). Even though the well in the layered reservoir is able to produce the same fluid volume as a well in an equal, but isotropic formation, it can still not be considered equally good. This

is because the fluid volume is produced over a longer time span, thus stretching the income from the oil over a longer period compared to a case with an isotropic reservoir. This means that the net present value of the fluid in place is lower for the anisotropic case, even though the same fluid volume is ultimately produced.

The case considered in this section only has one impermeable, horizontal layer close to the well. Because of the limited extent of the FBLs they will not penetrate any layers that are more than 12 m away from the well. It could also be that laterals are unable to reach full extension due to very hard rocks within the reservoir or because they are not jetted out ortogonally to the well. Fishbones may therefore be able to improve communication through layers that are a maximum of 12 m away to the well as a maximum upside case. Developing a system with longer FBLs will of course further improve the communication in the reservoir, but it will also increase the operational challenges.

4 Discussion

This is a discussion of the overall results and effects affecting many of the sections. Individual discussions are done in the respective sections.

Based on results from chapter 3 there is no doubt that Fishbones has the potential of being a very good stimulation method. A 60% increase in production rate is significant, especially if one considers the control the operator has on the stimulation process. Equally important is the fact that Fishbones may completely remove the effect of damage around a well and penetrate horizontal barriers. This could mean that if a drilling operation fails and the well is seriously damaged, Fishbones can be run into the well to salvage it and potentially saving several 100 million NOKs. The fact that it can penetrate layers also means that it will make well placement more forgiving since the driller essentially gets a 24 m big target to hit instead of a 30 cm.

Because of the very detailed model required there may be some uncertainty towards if ECLIPSE is able to model Fishbones correctly. Fishbones is a new technology and there are neither many wells currently completed with it nor has there been published very much work on how to accurately model it. The author therefore lacks reliable sources of information that can be used to verify the results. (Priskila, 2014) did do simulations in a CFD simulator that was assumed to be able to accurately model Fishbones. An attempt to compare the fracture model discussed in section 2.1 with the results of (Priskila, 2014) was made, but the information provided was unfortunately not sufficient to replicate the results accurately.

Figure 3.1 and Figure 3.4 follow the same trends as Figure 1.3 and Figure 1.4 from (McDowell and Muskat, 1950), but they are not directly comparable. It was unfortunately not possible to replicate these results in ECLIPSE as they were conducted in a cylindrical reservoir. (Freyer and Shaoul, 2011) showed that the productivity may be increased by 20-30%, but they do not give any details about needle spacing and well length. 20-30% is however within the range of the results shown in section 3.1.

The coal bed methane and carbonate field tests showed that the increase in production rate from Fishbones was significant, but they do not provide enough information to be used as comparison to the simulations in this thesis. The CFD simulations done on the tight sandstone pilot indicated a 20% increase in production for a 41 m sub spacing compared to an unstimulated well. Figure 3.1 shows that a 40 m spacing gives around 27% increased steady

state rate. The tight sandstone pilot only contained three needles per sub and the needles are 1.2 m shorter however and this could explain the seven percentage points lower increase in production. Unfortunately, too little info is given in (Torvund et al., 2016) so a proper comparison cannot be done.

The fracture model did require a much longer run time than the lateral model, which was most likely caused by the small grid blocks in the model. This was not a problem for models considered in this thesis, as they were both small and short simulation times. In a full field model large run times may become a problem though, but this can be avoided by using an r_{wa} instead of the explicit Fishbones modeling. Sections 3.1 and 3.6 showed that this gave sufficient accuracy. The up scaling with an r_{wa} has unfortunately not been done for layered reservoirs. Because of the ability of Fishbones to connect the well through horizontal layers this is perhaps the most a crucial part of the up scaling process. This is recommended as a future work.

There are some inaccuracies in the simulations that could not be removed. They were caused both by grid effects due to insufficient grid refinement and because the grid needed to be modified to accommodate the well with the laterals as shown in chapter 2. These inaccuracies were very small (less than 5%) however and they caused under predictions of the results. They should therefore have minimal impact on the results. In a real reservoir there are also a lot of uncertainties connected to inhomogeneity and anisotropy and these will far outweigh the small inaccuracy caused by the grid. The results in thesis should therefore be considered more on a "order of magnitude scale" rather than absolute results.

All the wells considered in this thesis have been completed along the entire length of the reservoir. In a real reservoir this is very rarely the case because of the large dimensions of a regular reservoir. The reason that no cases with the well completed along a shorter distance was run was because the work of (Shu, 2005) showed that modeling a well with the peaceman connection factor in wells that do not completely penetrate the drainage area lead to large errors. Despite this the results should give a good indication of the effect that Fishbones will have on a "long" horizontal well, i.e. a well that penetrates so much of the drainage area that flow into the tips can be neglected. The results will not be accurate for a "short" horizontal well however, as the flow into the tips will be significant. To model short wells the well index in the tip of the well could be modified according to (Wolfsteiner et al., 2003) or similar.

The simulations were assumed to be completely frictionless in all parts of the well. Results in section 2.1.2 indicate that if pressure happens in the system it may have a big impact. There are three regions in the well that may be affected by frictional pressure drop; the needles, the well annulus and the through the liner ports. (Freyer and Shaoul, 2011) reported that pressure drop inside the needles are not a problem according to CFD simulations, but no mention of the flow rates considered were given. Appendix A presents "back of the envelope" calculations for all three parts of the system. It shows that there are no significant pressure losses within any of the three mentioned parts of the system. There may of course become a significant pressure drop within the liner if the well is long and produces at a high rate. The frictionless system also indicates that the fracture model in ECLIPSE have good accuracy.

Wells stimulated with Dreamliner instead of Fishbones will be much harder to model in ECLIPSE. This is because the Dreamliner only contains three needles per sub that have a 120° phasing. The reason Fishbones can be modeled in ECLIPSE is because the needles have a 90° phasing, which can be represented by a cross in Cartesian grids. The same cannot be done when the laterals have a 120° phasing. As sections 3.1 and 3.6 showed modeling Fishbones with an r_{wa} is accurate and there are no reasons to believe that this should not work for laterals with 120° phasing as well. A well stimulated with Dreamliner can then be modeled in a CFD simulator that can build the geometry (or in ECLIPSE with corner point geometry) and an r_{wa} can be determined. This can then be used in the ECLIPSE simulations.

Multi phase flow simulations have not been done in this thesis. Most reservoir reach conditions during their lifetime that creates multi phase flow in the reservoir so this is important to consider. The small scale on the grid blocks used in the fracture model may cause convergence problems and instabilities when two or more phases are introduced however. It will be possible to model several phases using an r_{wa}, but it is uncertain of the r_{wa} determined in section 3.1.1 can be used.

5 Conclusions

- It is possible to simulate a well stimulated with Fishbones on a fine scale in ECLIPSE by defining the needles as fractures. This requires a detailed grid around the needles and a modified way of defining the well.
- A Fishbones stimulation may increase the steady state production rate in a well by up to 60% depending on sub spacing.
- Fishbones is capable of almost completely removing the effect of mud invasion skin, given that the invasion does not go past the length of the FBLs.
- Fishbones will improve the steady state production rate in a reservoir with a low vertical to horizontal permeability ratio compared to an unstimulated well. It will penetrate impermeable layers close to the well and improve reservoir communication.
- Single-phase production rate during transient, steady state, pseudo steady state and decline period from a well stimulated with Fishbones can be matched in a reservoir without layers using an equivalent wellbore radius.

6 Further Work

- Investigate how the effect of Fishbones layered reservoir can be up scaled without using a fine detailed model.
- Investigate the effect of Fishbones in multi phase flow.

7 References

BJØRSVIK, B. T. 2013. *Oljeverdenens ti på topp, petro, 18 October 2013* [Online]. http://petro.no/oljeverdenens-ti-pa-topp/10897. [Accessed 07.06 2016].

FISHBONES AS. 2016. *Technology in brief* [Online]. http://fishbones.as/technology-in-brief/. Available: http://fishbones.as [Accessed 07.06 2016].

FREYER, R. & SHAOUL, J. 2011. Laterals Stimulation Method. *Presented at Brasil Offshore Conference and Exhibition* Macaé, Brazil, 14-17 June 2011 SPE 143381-MS http://dx.doi.org/10.2118/143381-MS.

GOLAN, M. & WHITSON, C. H. 1996. *Well Performance, Second Edition,* Trondheim: Tapir.

HORN INTERNATIONAL AS. 2015. *Fishbones, hornonline* [Online]. http://hornonline.com/fishbones/. [Accessed 07.06 2016].

KLEPPE, J. 2016. Review of basic Steps in Derivation of Flow Equations, Lecture Notes, Norwegian University of Science and Technology, Trondheim, Norway.

KLOVNING, C.-I. 2015. *A Study of Simulation of Fishbones Performance and Reservoir Simulation in Brilliant.* Atumn Project, Norwegian University of Science and Technology, Trondheim, Norway.

MCDOWELL, J. M. & MUSKAT, M. 1950. The effect on well productivity of formation penetration beyond perforated casing. *JPT,* 2 (11) SPE 950309-G http://dx.doi.org/10.2118/950309-G.

PEACEMAN, D. W. 1978. Interpretation of Well-Block Pressures in Numerical Reservoir Simulation With Nonsquare Grid Blocks and Anisotropic Permeability. *SPE j.,* 23 (03) SPE 10528-PA http://dx.doi.org/10.2118/10528-PA.

PRISKILA, L. M. 2014. *Evaluation of Fishbones Lateral Stimulation - A simulation study.* M.Sc, Norwegian University of Science and Technology, Trondheim, Norway.

QVALE, P. 2015. *Dette var verdens største olje- og gassprodusenter i 2016, tu, 8 April 2015* [Online]. http://www.tu.no/artikler/dette-var-verdens-storste-olje-og-gassprodusenter-i-2014/222332. [Accessed 07.06 2016].

RICE, K., JØRGENSEN, T. & WATERS, J. 2014. First Installation of Efficient and Accurate Multilaterals Stimulation Technology in Carbonate Reservoir. *Presented at the SPE Regional Meeting.* Charleston, West Virginia, 21-23 October. SPE 171021-MS http://dx.doi.org/10.2118/171021-MS.

SCHLUMBERGER. 2016. *fishbone wells, slb* [Online]. http://www.glossary.oilfield.slb.com/Terms/f/fishbone_wells.aspx. [Accessed 04.06 2016].

SHAOUL, J. 2013. Modeling fishbones completion in 3D reservoir simulation models.

SHU, J. 2005. *Comparison of Various Techniques for Computing Well Index.* M.Sc, Stanford University, California, USA.

TORVUND, S., STENE, K., JENSAAS, H., RENLI, E., RICE, J. K. & JORGENSEN, T. 2016. First Installation of Multilateral Drilling Stimulation Technology in Tight Sandstone Formation. *Presentated at the SPE Western Regional Meeting.* Anchorage, AK, 23-26 May SPE 180390 http://dx.doi.org/10.2118/180390-MS.

WOLFSTEINER, C., DURLOFSKY, L. J. & AZIZ, K. 2003. Calculation of well index for nonconventional wells on arbitrary grids. *Computational Geosciences,* 7 (1): 61-82, https://earthsci.stanford.edu/ERE/research/suprihw/publications/pub-docs/wi_comp_geo_version_03.pdf.

Appendix A

As mentioned in chapter 2 the well with Fishbones was modeled under the assumption that all parts of the well were frictionless. Section 2.1.2 showed that pressure drop within the laterals will have a significant effect on the steady state rate. In order to investigate the pressure drop in the different parts of a well with Fishbones simulation results from a well with 20 m sub spacing from section 3.1 were used. They showed that 20 m sub spacing resulted in a 9.36 Sm^3/D total steady state rate with 5.46 Sm^3/D being produced into the needles and 3.90 Sm^3/D being produced directly into the well. Pressure drop in the needles, annulus between the Fishbones liner and the wellbore wall and through the liner ports are calculated using the equations shown below.

$$\Delta p = f \frac{L}{d} \frac{\rho}{2} v^2, \quad \text{(A.9)}$$

$$f = \frac{64}{\mathrm{Re}}, \quad \text{(A.10)}$$

$$\mathrm{Re} = \frac{vd\rho}{\mu}, \quad \text{(A.11)}$$

$$\Delta p = f \frac{L}{d_o - d_i} \frac{\rho}{2} v^2, \quad \text{(A.12)}$$

$$\Delta p = 0.5 \rho v^2, \quad \text{(A.13)}$$

Eq. (A.9) gives pressure drop in a circular pipe that is completely filled by a single-phase fluid for different flow regime. The expression for the friction factor, f, varies depending on which flow regime that is present. The Reynolds number, Re, is a good indication to determine the flow regime in the pipe. As a rule of thumb laminar flow will exist for Re < 2500 the flow is laminar and f is calculated by **Eq. (A.10)**. For Re > 2500 the flow will be turbulent and Eq. (A.10) is replaced by an expression for a turbulent friction factor. This is not of interest in this appendix, as laminar flow is assumed due to low flow rate. **Eq. (A.12)** is

a modification of Eq. (A.9) to account for pressure drop in the annulus instead of within a pipe. **Eq. (A.5)** models pressure drop through a circular liner port.

Pressure Drop in the Fishbones Laterals for 20 m Sub Spacing				
Total Prod Into FBL	Prod per FBL	Reynolds Number	Pressure Drop	Equivalent k_f
Sm^3/D	Sm^3/D	-	bara	mD
2.25	0.56	1131	0.0007	6.13E+09
5.50	1.38	2765	0.0018	6.13E+09
11.00	2.75	5530	0.0036	6.13E+09

Table A.1 - Pressure drop in the Fishbones laterals. The equivalent permeability that match the pressure drop according to the fracture model shown in section 2.1 is also shown.

Table A.1 shows the calculated pressure drop in the needle for three different flow rates. The laterals were 12 m long with a 0.014 m diameter. Viscosity and formation volume factor was calculated from tables in Appendix B using linear interpolation with a 310 bara FBHP. Oil density was calculated to be 600 kg/m^3 using the PVT data. As the Reynolds number show the two higher flow rates could be experiencing turbulent flow or be in a transition area between laminar and turbulent flow. As such the calculated pressure drops would probably be a little higher because of the turbulent flow. The pressure drop is however so small that it is not significant.

The equivalent k_f that would give the same pressure drop in the fracture blocks in the fracture model (section 2.1) is also shown. It shows that the permeability used in the fracture model is roughly one order of magnitude too small. Pressure drop in the fracture blocks for 20 m sub spacing was 0.07 bara, which is also small enough to not effect the simulations. A $k_f = 10^8$ mD is therefore sufficient to model the FBLs as was indicated in section 2.1.2.

Pressure Drop in the Annulus for 20 m Sub Spacing		
Total Prod Into Annulus	**Reynolds Number**	**Pressure Drop**
Sm^3/D	**-**	**bara**
2.00	1108	0.00003
4.00	2217	0.00005
8.00	4433	0.00010

Table A.2 – Pressure drop in the annulus between a 4.5 in Fishbones liner and a 6.5 in well.

Table A.2 shows the pressure drop in the annulus between a 4.5 in Fishbones liner and a 6.5 in well. This is the liner and well diameter that was used in the carbonate pilot well rice (Rice et al., 2014). Based of the short distance between the FBLs and the liner port seen in Figure 1.2 it was assumed that the fluid produced into the FBLs would not cause a large pressure drop and that all the fluid that was produced directly into the annulus traveled for 20 m before flowing into the liner through the liner ports. The pressure drop is so small that it is undoubtedly negligible.

Pressure Drop Across the Liner Ports for 20 m Sub Spacing		
Total Prod Through Ports Sm^3/D	**Prod per Port Sm^3/D**	**Pressure Drop bara**
4.25	2.13	0.003
9.50	4.75	0.017
19.00	9.50	0.069

Table A.3 – Pressure drop across the Fishbones liner ports.

Table A.3 shows the pressure drop through the ports in the Fishbones liner. Each sub has two ports with a 7 mm diameter and the pressure drop is calculated using Eq. (A.13). The calculations have been performed using the simulated rate with 20 m spacing and compared to a halved and doubled rate. None of the rates give a significant pressure drop.

Appendix B

Relative Permeability for Water and Capillary Pressure		
S_w	k_{rw}	P_{cow} bara
0.12	0	0
1	0.00001	0

Table B.1 – Relative permeability and oil-water capillary pressure.

Relative Permeability for Gas and Capillary Pressure		
S_g	k_{rg}	P_{cog} bara
0	0	0
0.02	0	0
0.05	0.005	0
0.12	0.025	0
0.2	0.075	0
0.25	0.125	0
0.3	0.19	0
0.4	0.41	0
0.45	0.6	0
0.5	0.72	0
0.6	0.87	0
0.7	0.94	0
0.85	0.98	0
1	1	0

Table B.2 – Relative permeability and oil-gas capillary pressure

Relative Permeability for Oil-Water and Oil-Gas		
S_o	k_{row}	kr_{og}
0	0	0
0.18	0	0
0.28	0.0001	0.0001
0.38	0.001	0.001
0.43	0.01	0.01
0.48	0.021	0.021
0.58	0.09	0.09
0.63	0.2	0.2
0.68	0.35	0.35
0.76	0.7	0.7
0.83	0.98	0.98
0.86	0.997	0.997
0.879	1	1
0.88	1	1

Table B.3 – Relative permeability for oil.

Surface Densities		
Oil kg/m^3	Water kg/m3	Gas $kg/^{m3}$
786.1	1037.3	0.9692

Table B.4 – Fluid surface densities.

PVT-properties Water			
Ref Pressure bara	Ref FVF Sm3/Sm3	Compressibility 1/bara	Viscosity cP
276.9	1.029	4.54E-05	0.31

Table B.5 – PVT properties of water.

Dry Gas PVT-data		
pg	**Bg**	**myg**
bara	**Sm3/Sm3**	**cP**
1.01	93.583	0.008
18.26	6.79	0.0096
35.5	3.523	0.0112
69.98	1.795	0.014
138.94	0.906	0.0189
173.43	0.727	0.0208
207.91	0.606	0.0228
276.88	0.455	0.0268
345.84	0.364	0.0309
621.7	0.217	0.047

Table B.6 – PVT properties dry gas.

Oil PVT-data			
Rs	**po**	**Bo**	**myo**
Sm3/Sm3	**bara**	**Sm3/Sm3**	**cP**
0.2	1.01	1.062	1.04
16.1	18.26	1.15	0.975
32.1	35.5	1.207	0.91
66.1	69.98	1.295	0.83
113.3	138.94	1.435	0.695
138	173.43	1.5	0.641
165.6	207.91	1.565	0.594
226.2	276.88	1.695	0.51
	345.84	1.671	0.549
	621.7	1.579	0.74
288.2	345.84	1.827	0.449
	621.7	1.726	0.605

Table B.7 – PVT properties oil.